VYSOKÉ UČENÍ TECHNICKÉ V BRNĚ

BRNO UNIVERSITY OF TECHNOLOGY

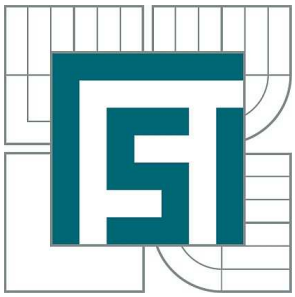

FAKULTA STROJNÍHO INŽENÝRSTVÍ

ÚSTAV PROCESNÍHO A EKOLOGICKÉHO INŽENÝRSTVÍ

FACULTY OF MECHANICAL ENGINEERING

INSTITUTE OF PROCESS AND ENVIRONMENTAL ENGINEERING

EFFERVESCENT BREAKUP AND COMBUSTION OF LIQUID FUELS: EXPERIMENT AND MODELLING

EFFERVESCENTNÍ ROZPRAŠOVÁNÍ A SPALOVÁNÍ KAPALNÝCH PALIV: EXPERIMENT A MODELOVÁNÍ

DIZERTAČNÍ PRÁCE

DOCTORAL THESIS

AUTOR PRÁCE — Ing. JAKUB BROUKAL

AUTHOR

VEDOUCÍ PRÁCE — doc. Ing. JIŘÍ HÁJEK, Ph.D.

SUPERVISOR

BRNO 2014

Abstract

This thesis presents an investigation of effervescent sprays and their application to spray combustion with emphasis on large-scale combustors. Both aspects – modelling and experiment – are addressed.

The thesis contains a general introductory part, where underlying phenomena of spray forming and turbulent combustion are explained and effervescent atomization is presented. Then, adopted experimental approaches are described both for the spray measurement and for the measurement of wall heat fluxes during combustion experiments. In the following chapter numerical models and their philosophy is discussed. Models for spray formation, turbulence and combustion adopted during the research are introduced and explained.

The actual results of the thesis are presented in form of separate papers (published or accepted for publication) with an additional section devoted to unpublished relevant results. It is found that standard spray models can to some extent represent effervescent sprays. However, in order to predict a spray flame more detailed spray models are needed in order to describe accurately radial and axial variations of drop sizes. Numerous experimental measurements of effervescent sprays are performed using a proposed methodology. Drop size data are analysed with emphasis on radial and axial drop size evolutions and some new phenomena are described. The inverse relationship between gas-liquid-ratio and mean diameter has been confirmed. Moreover a complete reversal in radial mean diameter trends for various axial locations has been described. Finally, a result summary is put forward that recapitulates the main accomplishments and conclusions. In the closing remarks possible future research is outlined. Experimental data for future effervescent model validations are disclosed.

Keywords

Effervescent atomization, spray combustion, computational fluid dynamics, experiment, mean drop size, drop size distribution

Abstrakt

Tato práce se zaměřuje na oblast effervescentních sprejů a jejich aplikace na kapalné spalování s důrazem na průmyslové spalovací komory. Oba aspekty – modelování a experiment – jsou řešeny.

Práce obsahuje obecný úvod, ve kterém jsou vysvětleny základní jevy rozpadu kapaliny a vířivého spalování a dále je představena effervescentní atomizace. Poté jsou popsány použité experimentální postupy jak pro měření spreje, tak pro měření tepelných toků do stěn při spalování. V následující kapitole jsou popsány numerické modely a jejich podstata je vysvětlena. Jsou zde uvedeny modely pro rozpad spreje, turbulenci a spalování použité během výzkumu.

Vlastní výsledky práce jsou uvedeny formou samostatných článků (vydaných nebo přijatých) s dodatečnou částí věnovanou nepublikovaným relevantním výsledkům. Bylo zjištěno, že standardní modely sprejů jsou do jisté míry schopny popsat effervescentní spreje. Nicméně aby bylo možné predikovat plamen kapalného spreje, jsou zapotřebí detailnější modely sprejů, které dokáží přesně zachytit změnu průměrů kapek v radiálním a axiálním směru. Experimentální měření effervescentních sprejů bylo provedeno pomocí navrhnuté metodiky. Výsledky měření byly analyzovány s důrazem na radiální a axiální vývoj průměrů kapek a některé nové jevy byly popsány. Nepřímá úměrnost mezi gas-liquid-ratio a středním průměrem kapek byla potvrzena. Dále by popsán jev, kdy pro různé axiální vzdálenosti které dojde k úplnému převrácení závislosti středního průměru na axiální vzdálenosti. V závěru je uvedeno shrnutí, které rekapituluje hlavní výsledků a závěry. V závěrečných poznámkách je nastíněn možný budoucí postup. Experimentální data pro ověřování budoucích effervescentních modelů jsou poskytnuta.

Klíčová slova

Effervescentní atomizace, kapalné spalování, výpočtová dynamika tekutin, experiment, střední velikost kapek, velikostní rozložení kapek

BROUKAL, J., Effervescent breakup and combustion of liquid fuels: experiment and modelling. Brno: Vysoké Učení Technické v Brně, Fakulta strojního inženýrství, 2014. 123 s. Vedoucí disertační práce doc. Ing. Jiří Hájek, Ph.D.

Prohlášení o původnosti práce

Prohlašuji, že disertační práci jsem vypracoval samostatně pod vedením doc. Ing. Jiřího Hájka, Ph.D. a s použitím uvedené literatury.

V Brně 23. 5. 2014

Ing. Jakub Broukal

Acknowledgement

First and foremost I would like to thank my supervisor doc. Ing. Jiří Hájek, Ph.D. for his guidance, support and endless encouragement. I would also like to express my gratitude to Prof. Paul E. Sojka for allowing me to spend a wonderful year at Purdue University and to prof. Ing. Petr Stehlík, CSc. for giving me the opportunity to study and work at the Institute of Process and Environmental Engineering.

A great thank you goes to my family and my girlfriend, whose support and patience helped me overcome all encountered obstacles.

Poděkování

Především bych rád poděkoval svému vedoucímu doc. Ing. Jiřímu Hájkovi, Ph.D. za jeho vedení, podporu a neutuchající povzbuzování. Dále bych rád vyjádřil svoji vděčnost Prof. Paulu E. Sojkovi za to, že mi umožnil strávit nádherný rok na Purdue University, a prof. Ing. Petru Stehlíkovi, CSc. za to, že mi dal možnost studovat a pracovat na Ústavu Procesního a Ekologického Inženýrství.

Velký dík patří mé rodině a přítelkyni, jejichž podpora a trpělivost mi pomohla překonat veškeré překážky.

Ing. Jakub Broukal

Contents

1 Introduction 1

1.1 Objectives and Thesis Overview 1

1.2 Thesis Structure 2

2 Underlying Phenomena 3

2.1 Factors Influencing Atomization 3

2.1.1 Liquid Properties 3

2.1.2 Ambient Conditions 3

2.2 Primary Atomization 3

2.2.1 Jet Breakup 4

2.2.2 Sheet Breakup 7

2.3 Secondary Atomization 8

2.3.1 Drop Breakup 8

2.3.2 Drop Collisions 8

2.4 Turbulence 9

2.5 Combustion 9

2.6 Effervescent Atomization 9

References 10

3 Experimental Methods 13

3.1 Spray Measurements 13

3.1.1 Phase Doppler Anemometry 13

3.1.2 Other Measurement Techniques 14

3.1.3 Methodology of Spray Characterization 14

3.2 Combustion Experiments 15

References 17

4 Numerical Methods 19

4.1 Governing Equations of the Fluid Flow 19

4.2 Turbulence 20

4.3 Spray Representation 20

4.3.1 Particle Tracking 21

4.3.2 Primary Breakup Models 21

4.3.3 Secondary Breakup Models 22

4.3.4 Drop Collision Models 23

4.3.5 Drop Drag Models 23

4.4 Combustion 24

4.4.1 Drop Evaporation 24

References 24

5 Results 27

5.1 Effervescent Atomization of Extra-light Fuel-oil: Experiment and Statistical Evaluation of Spray Characteristics 29

Abstract 29

5.1.1 Introduction 29

5.1.2 Measurement and Data Processing 30

5.1.3 Modelling 33

5.1.4 Results and Discussion 36

5.1.5 Future Work 38

5.1.6 Conclusion 39

Acknowledgement 39

References 39

5.2 Validation of an Effervescent Spray Model with Secondary Atomization and its Application to Modeling of a Large-scale Furnace 43

Abstract 43

5.2.1 Introduction 43

5.2.2 Experiments 47

5.2.3 Modelling 48

5.2.4 Results and Discussion 52

5.2.5 Conclusions 55

Acknowledgement 55

References 56

Figures 59

Tables 64

5.3 Experimental and Numerical Investigation of Wall Heat Fluxes in a Gas Fired Furnace: Practicable Models for Swirling Non-premixed Combustion 65

Abstract 65

5.3.1 Introduction 65

5.3.2 Experimental Measurement 66

5.3.3 Modelling 67

5.3.4 Results and Discussion 67

5.3.5 Conclusion and Future work 69

Acknowledgement 70

References 70

5.4 Review on Validation of CFD Models of Swirling Flows by Experimental Data 73

Abstract 73

5.4.1 Introduction 73

5.4.2 Structure and Classification 74
5.4.3 Isothermal Flows 74
5.4.4 Reacting Flows 76
5.4.5 Conclusion 77
Acknowledgement 78
References 78
5.5 Drop Size Distributions in Effervescent Sprays: An Experimental Study Using PDA Technique 83
Abstract 83
5.5.1 Introduction 83
5.5.2 Current Measurement Approaches 84
5.5.3 Measurement Techniques 85
5.5.4 Methodology of Spray Characterization 86
5.5.5 Results and Discussion 88
5.5.6 Conclusions 89
Acknowledgement 89
References 89
5.6 Experimental Analysis of Spatial Evolution of Mean Droplet Diameters in Effervescent Sprays 93
Abstract 93
5.6.1 Introduction 93
5.6.2 Experimental Setup 94
5.6.3 Results and Discussion 95
5.6.4 Conclusions 98
Acknowledgement 98
References 98
5.7 An Experimental Study of Effervescent Sprays: Axial Evolution of Mean Drop Diameter 101
5.7.1 Introduction 101
5.7.2 Experimental Apparatus and Data Analysis 102
5.7.3 Results and Discussion 103
5.7.4 Conclusions 106
Acknowledgment 106
References 107
5.8 Miscellaneous Unpublished Results 109
5.8.1 Mean and Representative Diameters of Effervescent Sprays 109
5.8.2 Drop Size Distribution Functions 109
References 110

6 Summary and Conclusions.....111

6.1 Results Summary 111

6.2 Conclusions and Future Work..... 112

Nomenclature and Acronyms 113

Appendix I - List of Author's Publications.....115

Appendix II – Experimental Drop Diameters 117

Appendix III – Experimental Drop Data.....123

1 Introduction

Liquid breakup, or atomization, is a complex process that transforms bulk liquid into a spray and thus increases its surface area. It is a key ingredient in many industrial applications ranging from pharmaceutics, fire suppression, spray coating and spray cooling to diesel engines and – significantly for the present thesis – liquid (spray) combustion. Liquid fuels have been, and still are, one of the main resources in the process and power industries. Spray combustion is therefore a crucial and essential process in achieving the final product - heat. A great deal of effort is constantly being put into understanding the fundamental phenomena and processes governing spray formation. In many industrial burners, spray combustion is accompanied by another complex phenomenon: swirling flow. The swirling aspect of combustion is essential as it enhances the mixing of reactants and stabilizes the flame. These efforts are motivated by the need to achieve better performance, lower emissions and longer lifetime of furnaces and combustors in various industrial applications.

In the last few decades Computational Fluid Dynamics (CFD) tools have been employed to facilitate the designs of combustors and furnaces. However, the modelling of an atomization process presents a formidable challenge. Since for the majority of industrial applications it is prohibitively expensive to model these problems using state-of-art approaches, careful compromises must be made and appropriate models need to be applied for various stages of the atomization process as well as turbulence, chemistry, or radiative heat transfer.

Despite the importance of liquid breakup (or atomization), its principles are not yet fully understood. Moreover, the behaviour and local properties of sprays are not always fully known, specifically in the case of effervescent atomization. The deficiencies of published experimental spray characteristics are aggravated in CFD spray combustion simulations by additional assumptions and simplifications. In order to enhance our ability to model swirling spray combustion it is therefore necessary to address an array of problems. And the purpose of this work is to help in this effort.

1.1 Objectives and Thesis Overview

This dissertation thesis aims to investigate a novel spray forming approach - effervescent atomization, with emphasis on atmospheric spray combustion. The long term goal toward which this research is aimed is to improve the predictability of swirling spray combustion, with focus on the distribution of heat loading (wall heat fluxes) in the combustion chamber of a fired heater. In order to contribute to the accomplishment of this goal many partial tasks were carried out.

- Literature review of the current state of the art in the area of effervescent sprays
- Experimental investigation of effervescent spray combustion
- Validation of current spray models against available drop size data
- Evaluation of effervescent spray combustion simulation and comparison to experimental data
- Detailed experimental investigation of multiple effervescent sprays

The subject of the research is very broad and the research was occasionally strayed into unexpected directions. Firstly, current spray models were tested and compared to available experimental data of effervescent sprays (5.1). At this point the first shortcomings of current spray models have been discovered, but their effect was underestimated. It was only after the model's

application to the large-scale combustion simulation and comparison with experimental data (5.2) that these shortcomings were fully recognized. In order to make sure the cause of the discrepancies lied in the spray model as opposed to other aspects of the simulation (mainly turbulence, chemistry and radiation) a comparative study on gas combustion has been performed (5.3). Moreover a review on swirling flow modelling and its validation has been performed (5.4). The focus of the research has therefore been shifted into better understanding the effervescent spray formation, which of course necessitates experimental data. According to the methodology presented in chapter 5.5 extensive experimental measurements of effervescent sprays have been performed. Analysis of the results presented in chapters 5.6 and 5.7 shows dependencies that, to the author's knowledge, have not yet been published. Chapter 5.8 contains additional experimental results that were not published yet, but are deemed useful to fellow researchers.

1.2 Thesis Structure

The presented thesis is written in a form of an annotated collection of research articles. The text is composed of 6 chapters. Chapters 1-4 form an introductory and unifying part which aims to provide a description of the phenomena involved in spray combustion, as well as methods and tools that were used in the course of this work. Chapter 5 contains the collection of published articles and represents a mapping of the author's research findings. Finally, summary and conclusions are provided in chapter 6.

Chapter 2 first covers the underlying phenomena taking place during spray combustion, namely factors influencing atomization (2.1), primary (2.2) and secondary (2.3) atomization principles and basic ideas behind turbulence (2.4) and combustion (2.5). In the section (2.6) the reader can familiarize himself with the notion of effervescent atomization. Experimental methods both for spray and combustion measurement are described in chapter 3 and the numerical approaches to the problem are explained in chapter 4. The results in the form of research articles are presented in chapter 5 and an overview and synthesis of all results is presented in chapter 6 along with a discussion and future work proposals. The experimental data obtained during the research of effervescent atomization are disclosed in the thesis' appendixes in full detail in order to facilitate future research and provide validation data for spray models.

2 Underlying Phenomena

Spray combustion is a very complex process where several physical and chemical phenomena occur simultaneously. Moreover it is quite sensitive to physical properties of the fluids involved. The scope of the following sections is to describe and explain the phenomena involved and to clarify the impact of physical properties.

2.1 Factors Influencing Atomization

The outcome of the atomization process depends on the size and geometry of the used atomizer and on the physical properties of the atomized liquid and the fluid in which the resulting spray is issued (usually gas, i.e. air). An overview of atomizer types and their dimensions can be found in (Lefebvre, 1989), the physical properties of the atomized liquid and ambient conditions are discussed in the following sections.

2.1.1 Liquid Properties

The atomization process of most atomizers is strongly influenced by the liquid density, viscosity and surface tension. The significance of density is diminished due to the fact that most of the atomized liquids have more or less similar value of density. Moreover, a great amount of experimental data indicates, that the influence of density is quite small (Lefebvre, 1989).

On the other hand, the effect of surface tension is significant. It represents the force that resists formation of a new surface area. Whenever atomization occurs under conditions where surface tension forces are important, the Weber number, which is the ratio of the inertial force to the surface tension force, is a useful dimensionless parameter for correlating drop size data. For most pure liquids in contact with air the surface tension decreases with the increase of temperature (Bayvel and Orzechowski, 1993).

Viscosity is also a very important liquid property since it does not only affect the size of the drops, but also the flow regime in the atomizer and the resulting spray pattern. The effect of viscosity on the nozzle flow is very complex and strongly depends on the type of atomizer in question. In general, viscosity increases the drop size and delays jet disintegration (Lefebvre, 1989). The viscosity of liquids generally decreases with increasing temperature (unlike gas viscosity, which exhibits the opposite effect).

2.1.2 Ambient Conditions

Sprays usually issue into a gaseous environment, most typically air. However, the state of the gas can vary immensely in terms of temperature and pressure. This is especially the case of spray combustion systems. In gas turbines the fuel spray is often injected into highly turbulent swirling flows and in recirculating flue gases. Moreover, supercritical gas conditions can be encountered during internal combustion processes. The influence of ambient conditions vary according to the specific type of atomizer in use; more details can be found in (Lefebvre, 1989).

2.2 Primary Atomization

The primary atomization is a process in which the bulk liquid disintegrates into drops (ligaments, filament usually appear as intermediate products of the disintegration process). This process can be understood as a disruption of the consolidating influence of the surface tension by the action of internal and external forces. In the absence of such disruptive forces the surface

tension tends to pull the liquid into the form of a sphere, since it has minimal surface energy. The liquid viscosity acts as a damping force trying to prevent deformations of the system geometry, while the aerodynamic forces promote the disruptive process by distorting the bulk liquid. Breakup occurs when the disruptive forces exceed the consolidating surface tension forces (Lefebvre, 1989).

Different mechanisms are responsible for the disintegration depending on the nature and also shape of the flow of the bulk liquid. In the following sections mechanisms for jet breakup and sheet breakup will be described.

2.2.1 Jet Breakup

When liquid emerges from a circular nozzle as a continuous body in cylindrical form, oscillations and perturbations occur as a result of the competition between disruptive aerodynamic forces and damping cohesive forces represented mainly by surface tension and liquid viscosity. Under certain favourable conditions the instabilities can resonate leading into the disintegration of the liquid body into drops (Lefebvre, 1989).

The phenomenon of jet breakup has been studied extensively in past decades and centuries, both theoretically and experimentally. A comprehensive review of jet flows has been performed by Krzywoblocki (1957). One of the first theoretical analyses was performed by Rayleigh (1878). His jet stability analysis employed the method of small disturbances to predict the conditions necessary to collapse a liquid jet discharging at small velocities (laminar flow of a non-viscous liquid). He compared the surface energy of the disturbed configuration with that of the undisturbed column and he stated that a liquid jet that is affected by surface tension forces only will become unstable to any axisymmetrical disturbance whose wavelength $\lambda > \pi d$, where d is the jet diameter. Furthermore, his results show that one class of disturbance will grow fastest and eventually control the breakup. Although Rayleigh's theory is based upon laminar and non-viscous flows that are not subjected to surrounding air influence, his conclusions are generally accepted and are often used as valid first approximations (Lefebvre, 1989). An example of Rayleigh's approximation can be seen in Figure 2-1.

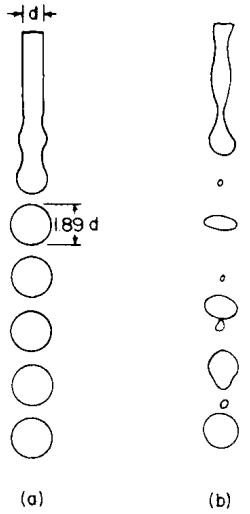

Figure 2-1 Comparison of (a) idealized and (b) actual jet breakup (Lefebvre, 1989)

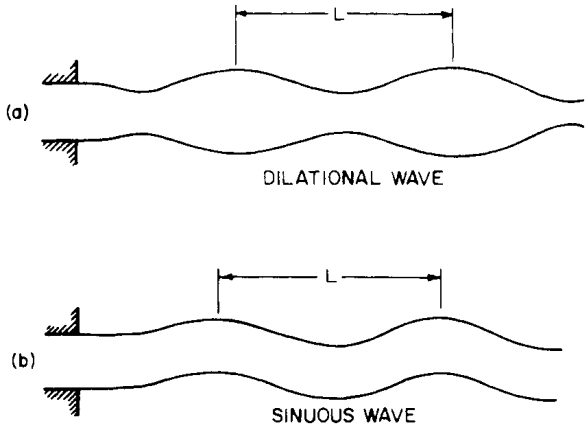

Figure 2-2 (a) Jet with rotationally symmetric disturbance, (b) Jet disturbance causing wave formation (Lefebvre, 1989)

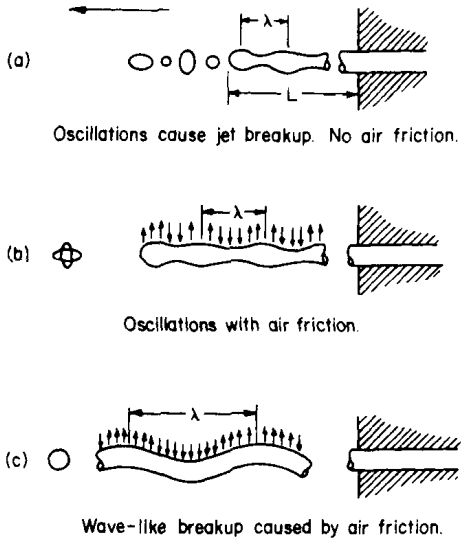

Figure 2-3 Mechanisms of drop formation (Haenlein, 1932)

Weber further extended Rayleigh's theory by taking into account viscous liquids (Weber, 1931). In his work he assumes that any disturbance causes rotationally symmetrical oscillations (see Figure 2-2a). If the wavelength of the initial disturbance is small, the surface tension forces will manage to damp out the disturbance. But when the wavelength exceeds a critical value, the surface tension forces will tend to increase the disturbance eventually leading to breakup and disintegration of the jet. The critical wavelength computed based on Weber's theory is very close to the value based on Rayleigh's approach. Weber further examined the influence of aerodynamic forces on the critical wavelength. He concluded that the effect of relative velocity between the liquid jet and surrounding air leads to decrease the critical wavelength. Weber also investigated the possibility of wave formation induced by air motion and showed this can occur only above a certain minimal value (Lefebvre, 1989). Haenlein (1932) consecutively presented an experimental validation of Weber's predictions and identified four distinct regimes of liquid jet disintegration.

- Drop formation without the influence of air. Radially symmetric waves, as seen in Figure 2-3a, are formed by interaction between primary disturbances in the liquid and surface tension forces.

- Drop formation with air influence (Figure 2-3b). As the jet velocity increases, the aerodynamic forces are no longer negligible and they tend to accentuate waves formed under regime 1.
- This regime is associated with the increasing influence of the aerodynamic forces in contrast to the less important surface tension (Figure 2-3c).
- Complete disintegration of the jet. The liquid is broken up at the nozzle in a chaotic and irregular manner

These four regimes can be easily identified, but there is no sharp border between them. Also, the fourth regime, which is the standard operating regime in industrial applications, is not easily described.

The most commonly quoted disintegration regimes were proposed by Ohnesorge (1936). His work was based on photographic records of jet disintegration where he focused on the relative importance of gravitational, inertial, surface tension and viscous forces. He expressed the breakup mechanism in three stages, each of which is characterized by Re and Oh, which is obtained as

$$\mathrm{Oh} = \frac{\sqrt{We}}{\mathrm{Re}} = \frac{\mu_l}{(\sigma \rho_l d_o)^{0.5}}. \tag{2.1}$$

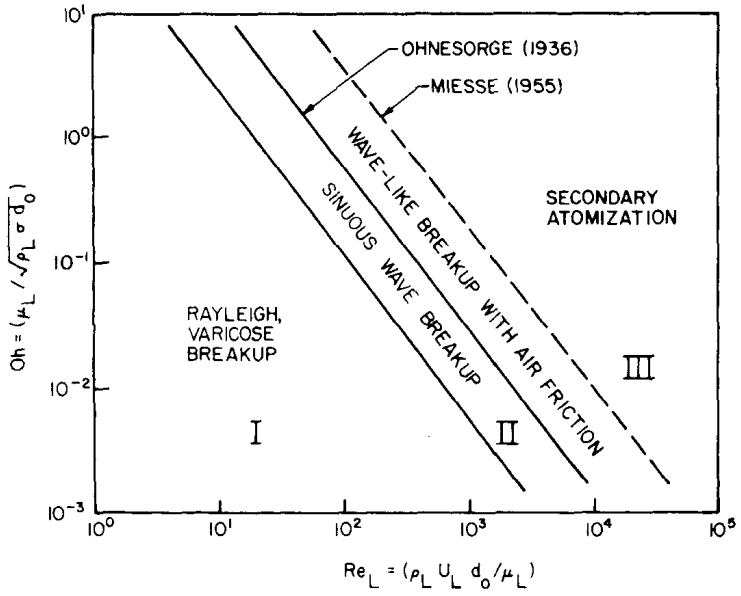

Figure 2-4 Classification of breakup modes, courtesy of (Ohnesorge, 1936)

Ohnesorge managed to show, that the various jet breakup mechanisms can be divided into three regions (Figure 2-4) according to the rapidity of drop formation (Lefebvre, 1989).

- At low Reynolds numbers, the jet disintegrates into large drops o fairly uniform size. This is the Rayleigh mechanism
- At intermediate Reynolds numbers, the breakup is caused by oscillations with respect to jet axis. A wide range of drop sizes is produced.
- At high Reynolds numbers, atomization is complete within a short distance from the discharge orifice.

There are many other classifications of jet disintegrations based on different criteria, but due to the very complex nature of the problem they are almost exclusively of empiric nature. For an overview see (Lefebrve, 1989; Bayvel and Orzechowski, 1993).

2.2.2 Sheet Breakup

Similarly to the jet breakup, disintegration of liquid sheets depends on liquid discharge velocity. Common to both processes is loss of jet stability, since the sheet disintegrates initially to jets and subsequently to drops (Bayvel and Orzechowski, 1993).

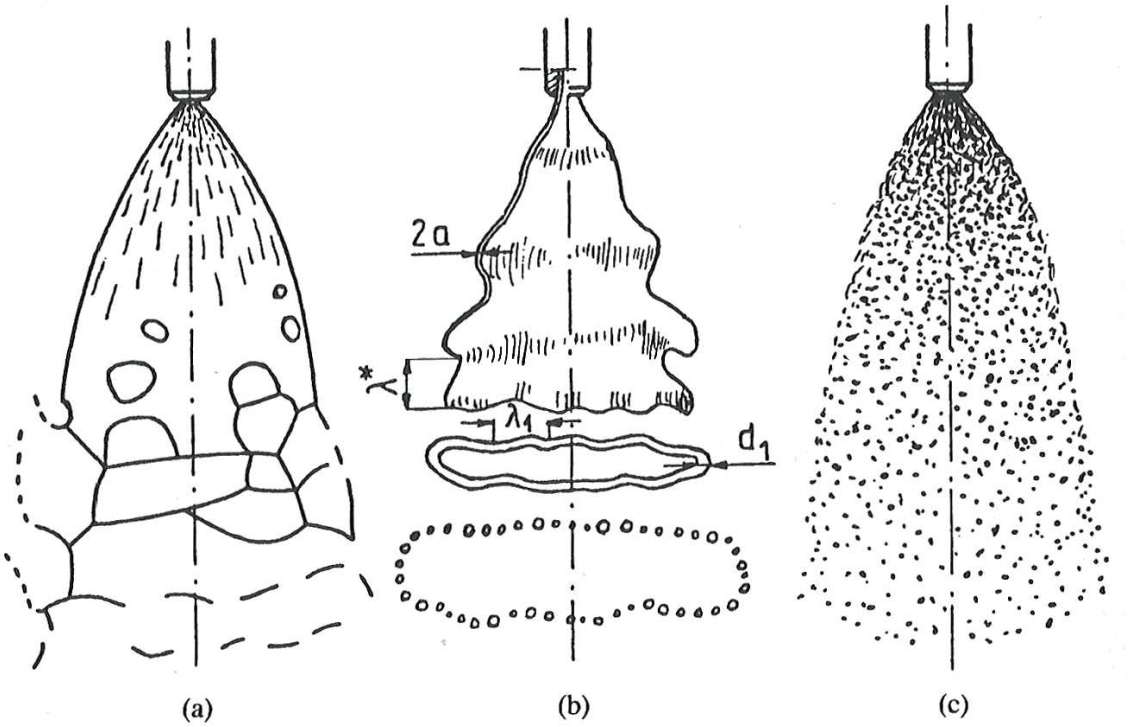

Figure 2-5 Drop development in swirl atomizer: (a) sheet disintegration due to perforation; (b) sheet disintegration due to wave phenomena; (c) liquid atomization, courtesy of (Bayvel and Orzechowski, 1993)

The two mostly encountered sheet types are flat and conical. Flat sheets can be a result of two impinging jets or specific types of atomizers. Conical sheets are more often encountered in industrial applications and produced by rotary or swirling atomizers. Three basic modes of disintegration are typically observed. Figure 2-5a displays a discharge with low velocity where with increasing distance from the nozzle, the sheet becomes thinner and perforations begin to appear. These perforations grow in size and when two neighbouring perforations meet a jet is formed, which subsequently disintegrates into droplets as it loses its stability. When the discharge velocity is increased wave disturbances begin to appear (Figure 2-5b). Circumferential waves dominate the disintegration and breakup the sheet into jet annuli, which further disintegrate into droplets. For the case of high discharge velocities only short waves develop and drops form before the annuli are separated from the waves. In case of very high discharge velocities the surrounding medium causes immense disturbances that do not even allow the waves to be formed and droplets are formed almost instantly (Figure 2-5c). This phenomenon is referred to as liquid atomization.

The theories behind sheet stability have been studied extensively with diverse degree of success. While stability theories for planar sheets have reached good agreement with experimental

measurements, theories for conical and cylindrical sheets still need further research effort (Sirignano and Mehring, 2000).

2.3 Secondary Atomization

When primary atomization occurs, a great variety of drops is produced. Some of them are still susceptible to further breakup depending on their size and the nature of the surrounding flow. The process during which these drops break up or disintegrate into smaller drops is called secondary atomization.

2.3.1 Drop Breakup

When drops are exposed to the surrounding flow it can lead to further atomization. A rigorous solution of the breakup result would demand exact knowledge of the aerodynamic pressure distribution on the drop. However, as soon as the drop is deformed by these pressures, the pressure distribution around the drop changes and either a state of equilibrium is reached or further deformation follows leading to possible breakup (Lefebrve, 1989).

The influence of pressure variations on the drop was examined extensively by Klüsener (1933). He assumes, that under equilibrium conditions the internal pressure of the drop at any point of the surface, p_I, is just sufficient to balance the external aerodynamic pressure p_A and the surface tension pressure p_σ so that

$$p_I = p_A + p_\sigma = \text{constant}. \tag{2.2}$$

Furthermore, for spherical drops the following holds

$$p_\sigma = \frac{4\sigma}{D}. \tag{2.3}$$

A drop will remain stable as long as p_σ is able to compensate changes in p_A so that p_I remains constant. However, when the change in p_A such that p_σ cannot compensate it to maintain p_I constant, the external pressure p_A can deform the drop to such extent, that breakup occurs. The newly formed drops have smaller diameters than the original one, therefore their p_σ increases. The breakup can occur further until p_σ is large enough to compensate for the changes in p_A.

In general, drop breakup in a flowing stream is controlled by the dynamic pressure, surface tension and viscous forces. In case of low viscosity, the deformation of the drop is determined by the ratio of aerodynamic forces and the surface tension forces. By opposing these two forces we get the Weber number.

$$We = \frac{\rho_g u_r^2 D}{\sigma}. \tag{2.4}$$

The larger the Weber number, the larger the deforming aerodynamic forces compared to the surface tension forces. The initial breakup condition for any liquid is achieved when the aerodynamic forces are equal to the surface tension forces. One can then define critical Weber numbers, drop diameters and velocities at which breakup will occur.

2.3.2 Drop Collisions

During primary atomization the drops are unlikely to collide with each other because of the different trajectories. However, further downstream the trajectories might intersect or faster-

moving drops can catch up with the slower ones and a collision takes place. Based on the size of the drops involved and on the nature of the collision several outcomes might arise: bouncing, coalescence, momentary coalescence or further breakup. The Weber number is generally acknowledged as the determining factor (Bayvel and Orzechowski, 1993; Pazhi and Galustov, 1979).

2.4 Turbulence

Turbulence is a physical phenomenon the fundamentals of which are not yet fully understood. It is a quasi-chaotic time dependent behaviour seen in many fluids that causes the formation of swirling eddies of different length scales. We can mathematically describe turbulence only in a phenomenological sense – we are not talking about causes but about consequences. Turbulent flow arises in all kinds of problems when the Reynolds number surpasses a certain critical value. Turbulent flows are characterized by fluctuating velocity fields. These fluctuations mix transported quantities such as momentum, energy, and species concentration, and cause the transported quantities to fluctuate as well. Since these fluctuations can be of small scale and high frequency, they are too computationally expensive to be simulated directly, at least in all practical engineering applications. Instead, the instantaneous (exact) governing equations are averaged, in order to remove the small scales, resulting in a modified set of equations that are computationally less expensive to solve. However, the modified equations contain additional unknown variables, and turbulence models are needed to determine these variables in terms of known quantities (Warnatz et al., 2001).

2.5 Combustion

Combustion is a chemical process, where a sequence of exothermal chemical reactions occurs between a fuel and an oxidant. The reactants (fuel and oxidizer) are conversed into products (flue gasses) and due to the exothermal nature of the process heat is released. The production of heat can result in a visible flame. The key process in combustion is mixing of the reactants and oxidizer. If the fuel and oxidizer are in a turbulent region of the flow, the mixing process is enormously enhanced. This in turn leads to quicker combustion, shorter and more controllable flames, minimization of pollutants that arise as a result of imperfect combustion. It is therefore evident that the vast majority of industrial combustion applications heavily rely on turbulent flow fields.

2.6 Effervescent Atomization

Sprays are produced in a variety of ways. There are a number of nozzles, in this context referred to as atomizers, which facilitate the atomization process using different mechanisms. Conventional atomizers disintegrate the liquid by creating high relative velocity between the liquid and gaseous phase. This can be achieved either by ejecting the liquid at high velocity into quiescent air (pneumatic or pressure atomizers, pressure-swirl atomizers) or by exposing the liquid to a high-velocity gas stream (airblast atomizers). Due to the need to fulfil specific industry requirements other atomizers using different mechanisms have been devised, such as electrostatic, ultrasonic or vibrating atomizers. One of the most recent spray formation mechanisms is effervescent atomization, which was pioneered by Lefebvre and his colleagues (Lefebvre et al., 1988) and is gaining popularity especially for combustion purposes ever since.

Effervescent atomization is often confused with flash atomization. Unlike flash atomization, where an atomizing gas is dissolved in the liquid inside the nozzle, effervescent atomization does

not require solubility of the atomizing gas. Instead, the principle of effervescent atomization is based on the formation of a two-phase flow inside the nozzle. A small amount of gas (usually air) is introduced in the liquid before it exits the atomizer and a two phase flow is formed (Figure 2-6). When the mixture exits through the nozzle, pressure suddenly drops. The pressure drop causes fast expansion of gas bubbles, which in turn leads to the disintegration of the atomized liquid into drops. The spray formation process in effervescent atomizers therefore does not rely solely on high liquid pressure and aerodynamic forces. This breakup mechanism allows the use of lower injection pressures and larger nozzle diameters without compromising the drop-size distribution and preventing clogging and fouling. In contrast to airblast atomizers the amount of atomizing air is minimal (Babinsky and Sojka, 2002). On the other hand the atomizer body is quite complicated and usually consists of multiple parts, whose structure, size and dimensions have an effect on the resulting spray (Jedelský et al., 2009a).

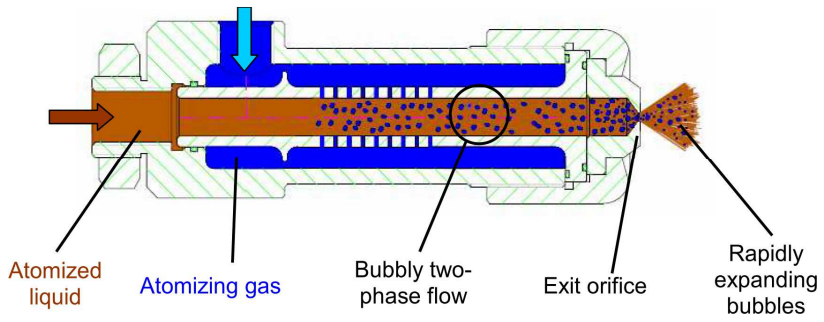

Figure 2-6 Schematics of the effervescent atomization process, courtesy of (Jedelský et al, 2007)

Effervescent sprays often suffer from unsteadiness; the involved spray forming process is after all inherently unsteady (Luong and Sojka, 1999). This phenomena has been thoroughly investigated in many research papers, such as (Jedelský et al., 2009b; Luong and Sojka, 1999; Gadgil et al., 2011; Liu et al., 2011). The most important conclusion in terms of industrial applications is that the unsteadiness can be minimized by carefully choosing the operating conditions.

References

Babinsky, E., Sojka, P.E., 2002. Modeling drop size distributions. Progress in Energy and Combustion Science 28, 303–329. doi:10.1016/S0360-1285(02)00004-7

Bayvel, L.P., Orzechowski, Z., 1993. Liquid atomization. Taylor & Francis.

Gadgil, H., Dolatabadi, A., Raghunandan, B.N., 2011. Mass Distribution Studies in Effervescent Sprays. Atomization and Sprays 21, 375–390. doi:10.1615/AtomizSpr.2011003661

Haenlein, A., 1932. Disintegration of a Liquid Jet. NACA TN 659.

Jedelský, J., Beinstein, Z., Jícha, M., 2009b. Unsteadiness in Effervescent Sprays: Influence of Operational Conditions and Atomizer Design, in: 11th Triennial International Annual Conference on Liquid Atomization and Spray Systems, Vail, Colorado USA.

Jedelský, J., Jícha, M., Otáhal, J., Katolický, J., Landsmann, M., 2007. Velocity field in spray of twin-fluid atomizers, in: 21st Sympozium on Anemometry, Proceedings. Presented at the 21st Sympozium on Anemometry, Prague, Czech Republic, pp. 67–74.

Jedelský, J., Jícha, M., Sláma, J., Otáhal, J., 2009a. Development of an Effervescent Atomizer for Industrial Burners. Energy & Fuels 23, 6121–6130.doi: 10.1021/ef900670g

Klüsener, O., 1933. The Injection Process in Compressorless Diesel Engines. VDI Z. 77.

Krzywoblocki, M.A., 1957. Jets-review of literature. Jet Propulsion 26, 760–779.

Lefebvre, A.H., 1989. Atomization and sprays. Hemisphere, New York.

Lefebvre, A., X. Wang, and C. Martin, 1988, Spray Characteristics of Aerated-Liquid Pressure Atomizers. Journal of Propulsion and Power, 4(4), 293-298.

Liu, M., Duan, Y., Zhang, T., Xu, Y., 2011. Evaluation of unsteadiness in effervescent sprays by analysis of droplet arrival statistics - The influence of fluids properties and atomizer internal design. Experimental Thermal and Fluid Science 35, 190–198. doi:10.1016/j.expthermflusci.2010.09.001

Luong, J.T.K., Sojka, P.E., 1999. Unsteadiness in effervescent sprays. Atomization and Sprays 9, 87–109.

Ohnesorge, W., 1936. Formation of Drops by Nozzles and the Breakup of Liquid Jets. Journal of Applied Mathematics and Mechanics 16, 355–358.

Pazhi, D.L., Galustov, V.S., 1979. Liquid Atomizers. Moscow.

Rayleigh, Lord, 1878. On the Instability of Jets. Proc. London Math. Soc. 10, 4–13.

Sirignano, W.A., Mehring, C., 2000. Review of theory of distortion and disintegration of liquid streams. Progress in Energy and Combustion Science 26, 609–655. doi:10.1016/S0360-1285(00)00014-9

Warnatz, J., Maas, U., Dibble, R.W., 2001. Combustion: Physical and Chemical Fundamentals, Modeling and Simulation, Experiments, Pollutant Formation. Springer.

Weber, C., 1931. Disintegration of Liquid Jets. Z. Angew Math. Mech. 11, 136–159.

3 Experimental Methods

Experimental measurements are arguably the most important part in the process of model development. Regardless of how carefully the model is developed, without proper validation it cannot be employed in industrial applications. Clearly the scope of measurement is to obtain as much relevant data as possible without compromising measurement accuracy and while minimizing measurement errors. Two types of experimental measurement are essential in case of spray combustion: measurement of the spray characteristics and measurement of the combustion characteristics. The present chapter provides an overview of experimental approaches employed within the dissertation.

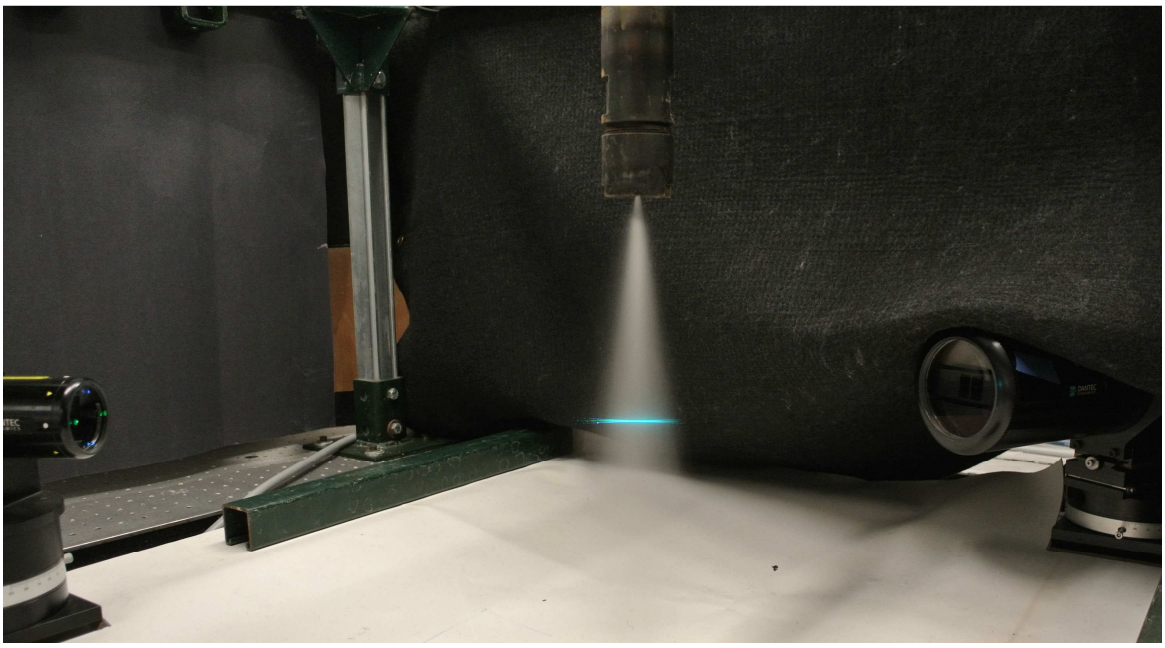

Figure 3-1 PDA setup

3.1 Spray Measurements

When setting up a spray measurement, the sought variables are usually drop size (drop diameter) and drop velocity. The following paragraphs provide the reader with an overview of the most used measurement with emphasis on the Phase/Doppler Particle Analyser (P/DPA) or sometimes also called Phase Doppler Anemometry (PDA).

3.1.1 Phase Doppler Anemometry

The Phase Doppler Anemometry is an extension of the Laser Doppler Anemometry used mainly to study local velocities (up to 3 components) in fluid flows. The extension lies in the ability to measure diameters of particles (both fluid and solid) present in the fluid flow (bubbles in liquid, droplets in gas, etc.). The PDA is a non-intrusive optical technique, on-line and in-situ (Albrecht, 2003) Due to the nature of the technique, optical access to the measurement area is needed, which can be sometimes limiting for on-site industrial measurements. Since the method requires particles to be spherical (or only slightly deformed), measurements must be taken at a sufficient distance from the discharge orifice. Also, the method is not suitable for very dense spray regions. The measurement device consists of a laser based optical transmitter, an optical

receiver, a signal processor and a software for data analysis. The two laser beams emitted by the transmitter intersect, creating a small sample volume. When a droplet passes through this laser intersection the scattered light forms a fringe pattern. As the drop moves, the scattered interference pattern is registered by the receiver at the Doppler difference frequency, which is proportional to the drop velocity. The droplet diameter is then inversely proportional to the spatial frequency of the fringe pattern. Due to the purely optical nature of the measurement process, no calibration is required and since the sampling volume is usually very small (1 mm^3) high spatial resolution can easily be achieved.

This technique is ideal for high precision measurements of liquid sprays and its results can be used to perform detailed validation of numerical models. Although it gives excellent qualitative representation of the spray (local drop size and velocity distributions), quantitative results, such as mass concentration, can be misleading as reported by (Babinsky and Sojka, 2002, Broukal et al., 2010). This is most probably the result of the trade-off for high spatial resolution and possibly also due to rejection of non-spherical droplets.

3.1.2 Other Measurement Techniques

An alternative to PDA is provided by the so called whole-flow-field techniques, like Particle/Droplet Imaging Analysis (PDIA) or Particle Image Velocimetry (PIV). These non-intrusive techniques were originally devised to measure velocity fields of seeded flows. The basic principle of these methods is to take two consecutive images of an illuminated cross-section of the flow and by comparing the displacement of the particles compute the velocity vector field. However, information about drop diameters can be gathered as well by employing advanced image processing algorithms (Avulapati and Ravikrishna, 2012; Wang et al., 2002).

To remedy the potential inaccuracy of mass concentration measurements in the PDA measurements, Planar Laser-Induced Fluorescence (PLIF) can be employed (Jedelský and Jícha, 2012). During the measurement, a spray cross-section is shortly illuminated by a laser sheet and after some time (in the order of nano or microseconds) the droplets de-excite and emit a portion of the light which is captured by a camera. The emitted light intensity is proportional to the liquid concentration.

3.1.3 Methodology of Spray Characterization

This section will aim at providing guidelines for gathering ideal experimental data of effervescent sprays to be used for validation of numerical spray models. From the previous section it is evident, that in order to get high resolution drop size and velocity measurement together with accurate mass concentration information, two measurement techniques need to be employed. However, in this part emphasis will be put on the PDA measurement technique.

For the purpose of model development and validation, the primary breakup region of the spray is the most important. Unfortunately, due to the limitations of the PDA technique we cannot measure the spray at its origin, since the droplets are far from being spherical and also the liquid density might be too high. The goal then is to get as close to the spray nozzle as possible. In (Li et al., 2012) it is demonstrated that PDA measurements can be taken at distance from the spray origin $x^* = x/d_0 = 3.3$ (where x is axial distance and d_0 is the discharge orifice diameter), which can still be regarded as area dominated by primary atomization. Data collected here can be a good starting point for the model validation and can even be used as boundary conditions for CFD simulation if needed. After the closest possible location to the spray nozzle has been identified, the set of measurement points should be then expanded in the radial direction to the spray edge

using at least two new locations. If the drop size distributions or SMD measurements vary substantially between these points, additional measurement locations should be introduced. To understand the axial evolution of the spray, this process should be repeated at least once more further downstream. The number of radial measurement points should be increased since the spray cone naturally widens. The radial measurements can be taken in multiple directions to check the symmetric behaviour of the spray.

For the current research, experimental measurements were performed at three axial locations – 5, 10 and 15 cm. Measurements performed at closer distances yielded no results (probably due to high spray density). At each axial distance, several radial measurements points were established. First, equidistant radial measurement points 1 cm apart were chosen – a total of 3, 5 and 6 radial measurement points for distances 5, 10 and 15 cm respectively. In order to increase the measurement resolution, at axial distance 5 cm the respective distance of radial points was lowered to 0.5 cm, which finally yielded 6 radial measurement points. This division proved to be adequate as it captured well the drop size variations and no major fluctuation between adjacent radial points was observed.

When performing a PDA measurement the user has to choose a receiver mask based on the expected range of drop diameters. If the range of generated droplets does not fall in the range specified by the mask, a part of the drop size distribution will be trimmed. It is therefore advisable to perform measurements with multiple masks and eventually merge resulting distributions. In such case the distributions must be weighted properly prior to merging and also, attention must be paid to whether the mask ranges overlap.

One of the parameters influencing the quality of measured data is the number of sampled droplets. It is reasonable to expect, that the actual drop size distributions are smooth, including the peripheries or so called tails, where the droplet fraction is small. To obtain such distribution it is important to sample a sufficient number of droplets. Various sampling numbers are adopted, form 2,000 (Li et al., 2012), 10,000 (Panchagnula and Sojka, 1999), 20,000 (Jedelský et al., 2009) up to 50,000 and 100,000 (Liu et al., 2010). There is no universal rule to determine this number, but it can be derived during the measurement itself by judging on the convergence of the drop size distribution. In some cases the smoothness of the drop size distribution might be also compromised by a wrong choice of mask, or by high noise. The latter case can be remedied by shielding the measurement area from any other light sources and/or by increasing the PDA lasers power.

During experimental drop size measurements performed in the current research (5.5, 5.6 and 5.7) the goal was to collect ideally 20,000 samples at each location. At certain operating conditions and spray locations it was not possible to reach this number due to local spray properties (spray density) and therefore less samples were collected. The average number of samples collected was 10,000. Seven measurements (out of 136) yielded less than 1,000 samples.

3.2 Combustion Experiments

Wall heat fluxes in combustion chambers, furnaces and boilers are one of the most important parameters in process and power applications. It is therefore very important to be able to predict them and to have experimental data for model validation. The distribution of local heat flux across heat exchanging areas is of special interest due to material strength and durability implications. In the last two decades, a number of research papers can be found where wall heat fluxes are investigated either experimentally (Hayes et al., 2001) or numerically using CFD tools (Vondál and Hájek, 2009). Measurement of local heat loads in industrial conditions is however possible

only using special heat flux probes that cannot provide reliable detailed data covering the whole heat transfer area, but only a limited number of discrete points. Additionally, industrial units typically have only rough estimates of the instantaneous total heat transfer rate, e.g. ± 4 % in (Valero and Cortés, 1996).

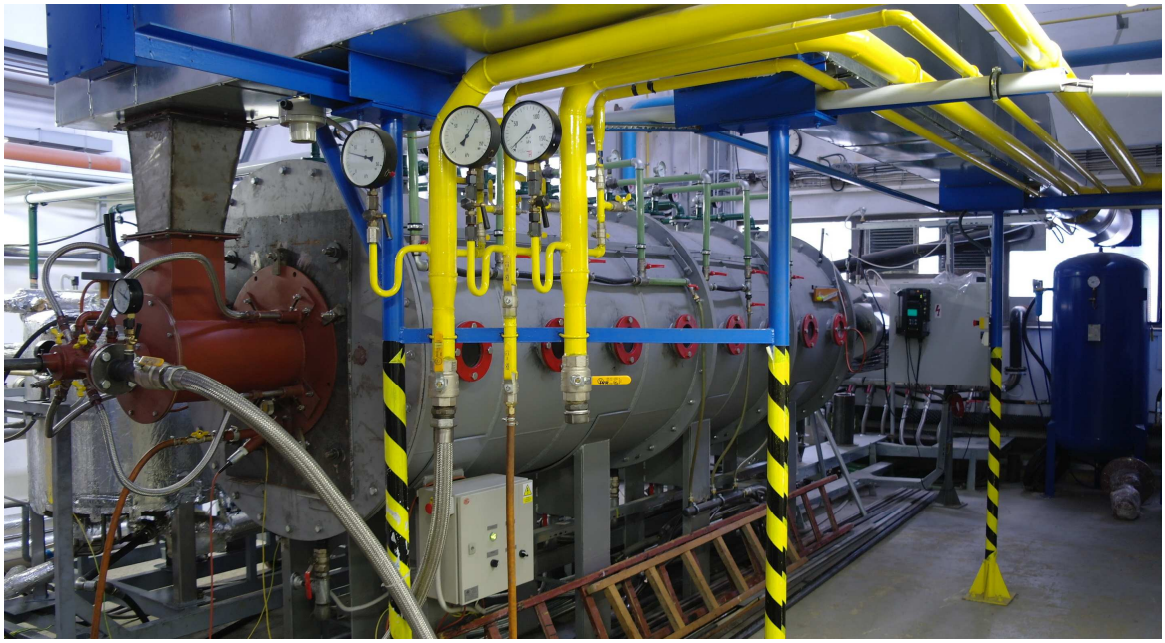

Figure 3-2 Combustion test facility

The measurement of wall heat fluxes was traditionally connected mainly to the identification of fouling and slagging, especially in pulverised-coal boilers. Therefore many of the existing probes are designed to operate in harsh environments. In laboratory experiments the measured heat flux data are naturally more reliable than in industrial combustors. Even though, the accuracy of available measurement methods is on the order of several percent. For instance, for the measurements of thermal irradiation flux ellipsoidal radiometers (accuracy ± 5 %) and water-cooled circular foil heat flux radiometers (accuracy ± 2 %) (Hayes et al., 2001) are often used. The ± 2 % accuracy is about the best one can achieve with heat flux metering probes. However, as reported in (Hayes et al., 2001), differences of values measured by these two methods may reach up to 12 %, thus decreasing the credibility of point heat flux measurements. On the other hand, the measurement of heat transfer rate in a segmental experimental combustion chamber with water cooling is able to provide appreciably more precise values (with average error below 3.2 %) as shown in (Vondál and Hájek, 2009).

The aforementioned segmental experimental chamber was used in this work to obtain wall heat flux measurements (Figure 3-2). This water-cooled horizontal combustion chamber (1 m internal diameter and 4 m length) is located in the Institute of Process and Environmental Engineering of Brno University of Technology. The shell of the chamber is divided into seven sections; each of which has a separate water inlet and outlet and is equipped with a water flow meter and temperature sensors, allowing for accurate local heat transfer rate measurement along the flame. The experimental facility is described in detail in (Kermes et al., 2007) and (Kermes and Bělohradský, 2008).

In order to reduce liquid fuel consumption (due to limited storage capacity), the combustion chamber is usually preheated using natural gas. Thermal duty in the experiments can be set up to 2 MJ. In Figure 3-3 is a simple sketch of the burner and combustion air supply duct. The

stabilization of the experiment is judged according to the stability of local wall heat fluxes in all sections of the furnace, which are monitored continuously. After reaching a steady state, the measurement procedure begins and data are collected for about 30 minutes. The results are post-processed and used as reference when evaluating numerical computations.

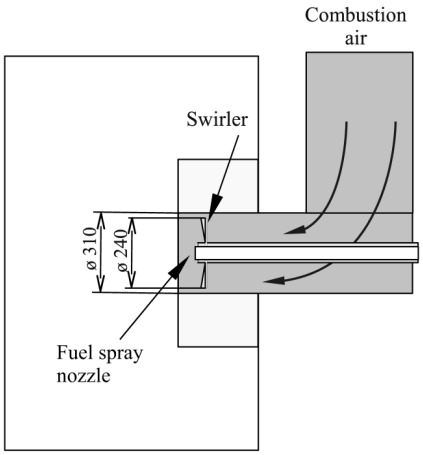

Figure 3-3 Cross-section of the burner

References

Albrecht, H.-E., 2003. Laser Doppler and Phase Doppler Measurement Techniques. Springer.

Avulapati, M.M., Ravikrishna, R.V., 2012. An Experimental Study on Effervescent Atomization of Bio-oil Fuels. Atomization and Sprays 22, 663–685. doi:10.1615/AtomizSpr.2012006482

Babinsky, E., Sojka, P.E., 2002. Modeling drop size distributions. Progress in Energy and Combustion Science 28, 303–329. doi:10.1016/S0360-1285(02)00004-7

Broukal, J., Hájek, J., Jedelský, J., 2010. Effervescent atomization of extra-light fuel-oil: Experiment and statistical evaluation of spray characteristics, in: Proceedings of 23rd European Conference on Liquid Atomization and Spray Systems. Presented at the ILASS-Europe 2010, Brno, Czech Republic, pp. 1–10.

Hayes, R.R., Brewster, S., Webb, B.W., McQuay, M.Q., Huber, A.M., 2001. Crown incident radiant heat flux measurements in an industrial, regenerative, gas-fired, flat-glass furnace. Experimental Thermal and Fluid Science 24, 35–46. doi:10.1016/S0894-1777(00)00055-8

Jedelský, J., Jícha, M., 2012. Spatially and Temporally Resolved Distributions of Liquid in an Effervescent Spray. Atomization and Sprays 22, 603–626. doi:10.1615/AtomizSpr.2012006055

Jedelský, J., Jícha, M., Sláma, J., Otáhal, J., 2009. Development of an Effervescent Atomizer for Industrial Burners. Energy & Fuels 23, 6121–6130. doi: 10.1021/ef900670g

Kermes, V., Bělohradský, P., 2008. Testing of gas and liquid fuel burners for power and process industries. Energy 33, 1551–1561.

Kermes, V., Skryja, P., Stehlík, P., 2007. Up to date experimental facility for testing low-NOx burners. Chemical Engineering Transaction 12, 549–554.

Li, Z., Wu, Y., Cai, C., Zhang, H., Gong, Y., Takeno, K., Hashiguchi, K., Lu, J., 2012. Mixing and atomization characteristics in an internal-mixing twin-fluid atomizer. Fuel 97, 306–314. doi:10.1016/j.fuel.2012.03.006

Liu, M., Duan, Y., Zhang, T., 2010. Evaluation of effervescent atomizer internal design on the spray unsteadiness using a phase/Doppler particle analyzer. Experimental Thermal and Fluid Science 34, 657–665. doi:10.1016/j.expthermflusci.2009.12.007

Panchagnula, M.V., Sojka, P.E., 1999. Spatial droplet velocity and size profiles in effervescent atomizer-produced sprays. Fuel 78, 729–741. doi:10.1016/S0016-2361(98)00192-6

Valero, A., Cortés, C., 1996. Ash fouling in coal-fired utility boilers. Monitoring and optimization of on-load cleaning. Progress in Energy and Combustion Science 22, 189–200. doi:10.1016/0360-1285(96)00004-4

Vondál, J., Hájek, J., 2009. Experimental and numerical analysis of wall heat transfer in non-premixed gas combustor. Chemical Engineering Transactions 18, 587–592.

Wang, X., Wu, X., Liao, G., Wei, Y., Qin, J., 2002. Characterization of a water mist based on digital particle images. Experiments in Fluids 33, 587–593.

4 Numerical Methods

The problem of spray combustion is a highly complex one. Different phenomena (turbulent flow, atomization, evaporation and combustion) interact with each other causing the solution to be very sensitive. The turbulent swirling flow is difficult to model even alone and when chemistry and radiation are added, the resulting problem becomes very complex. In the present, proven approaches that can deal with these complex flows include LES or DNS coupled with advanced chemistry models, e.g. (Sadiki et al., 2006). Those very detailed results come at a price of extremely high computational demands, which are generally unacceptable in industrial applications. That is why even authors of these advanced LES studies are unsure whether the use of LES strategy will in the future prevail over unsteady RANS approach (Sadiki et al., 2006).

More research is therefore needed to find simpler time-effective numerical models from the RANS or unsteady RANS class for the prediction of swirling nonpremixed flames that would yield practically relevant results. The issue of local wall heat flux prediction in swirling combustor has been recently investigated for the case of methane swirling combustion in (Vondál and Hájek, 2009) and it has been shown, that local wall heat flux predictions are very sensitive to the choice of models used to describe the physical and chemical processes occurring in flames. Results in (Vondál and Hájek, 2009) provide guidelines for the selection of several sub-models in computations of swirling nonpremixed gas flames.

The solution in this case is sought using CFD tool Ansys Fluent, which employs the iterative Finite-Volume Method to evaluate the problem equations. The numerical approaches discussed in the following sections will focus on industrial applications. In other words, emphasis will be placed on relatively simple yet sufficiently accurate models which can give reasonable results in a realistic time period. Currently there are very accurate models than employ highly sophisticated methods, but their demands in terms of computational effort and time are far out of reach to be applied to real-life problems.

As mentioned earlier, turbulent spray combustion presents a formidable challenge due to many phenomena involved. Swirling combustion alone (gaseous) still represents an uneasy problem (Vondál and Hájek, 2009; Vondál et al., 2010) and the presence of spray drops further increases the complexity of predicting such flames. Clearly, to minimize the uncertainties and errors that are caused by numerical representation of sprays, appropriate atomization models need to be found and validated.

The following sections discuss numerical approaches adopted in the current work. Additional information about models and approaches are occasionally provided in order to demonstrate the state-of-the-art. Details about the setup procedure for individual models is provided in corresponding sections of chapter 5.

4.1 Governing Equations of the Fluid Flow

Before focusing on more detailed aspects of the two phase flow problems in question, it is helpful to review the governing equations of fluid flow, the so called Navier-Stokes equations. These equations are fundamental to almost any flow problem imaginable and the engineering world relies heavily on them when looking for a solution. A peculiar thing about the Navier-Stokes equations is that we expect them to give us a solution that is unique. However, this has only been proven for two-dimensional flows, not yet for three-dimensional flows. According to the Clay Mathematics Institute this is one of the Millennium Prize Problems.

4.2 Turbulence

As mentioned in paragraph 2.4, turbulence is a very complex phenomenon which causes the flow properties fluctuate. However, when dealing with industrial turbulent flow problems the main interest is usually not in the instantaneous properties, but in the mean values. We can therefore use certain averaging techniques which eliminate the fluctuating components from the governing Navier-Stokes equations, thus getting the so called RANS equations. Nevertheless, this approach introduces new variables called Reynolds stresses which need to be modelled in addition the filtered governing equations.

Turbulence models generally differ in the way they model the Reynolds stresses. A variety of models has been developed ranging from the simplest algebraic models, through one and two equation models to more complex Reynolds stress models. The most common models used in industrial applications are the two equation models, mainly k-ε and k-ω and their variations. A detailed comparison of two equation turbulence models for gas combustion can be found in (Broukal et al., 2012). Over the past few years a great deal of research is being performed around the LES models. These models represent an interesting hybrid combining DNS, where all the fluctuations are resolved, with the RANS models. However promising LES surely is, at the present time it is still not ready to be widely employed in real-life applications.

4.3 Spray Representation

At the present time, two predominant methods for numerical spray representation are used: the Euler–Euler and Euler–Lagrange approach. The first approach is handles both the liquid and gaseous phase as impenetrable continua and tracks their interfaces. Therefore two sets of Navier-Stokes equations (one for each phase) need to be solved along with the coupling interface equations. However, this approach is computationally demanding and so far is used almost exclusively for spray formation investigations without combustion as for example in (Riber et al., 2009; Shinjo and Umemura, 2011). The latter approach is on the other hand less demanding since only the gaseous phase is treated as a continuum while the liquid (or dispersed) phase is handled in a discrete fashion. Only one set of Navier-Stokes equations needs to be solved and the discrete particles (drops) are tracked in a Lagrangian frame of reference using a set of relatively simple ordinary differential equations. The coupling between phases is represented by source terms in the Navier-Stokes equations.

Due to its simplicity the Euler–Lagrange approach allows employment in combustion applications as for example (Yan et al., 2008; Nieckele e al., 2010). However, the simplicity and low computational costs of the Euler–Lagrange approach are compensated by the need to find or develop appropriate sub-models for primary breakup (to determine initial drop parameters like diameter and velocity and their angular variations) and secondary breakup (breakup of drops that occurs further downstream from the nozzle) as well as for all other processes concerning the drops, like momentum, heat and mass transfer in the evaporating spray. Even when taking into account the aforementioned simplification, the problem would still be complex due to the enormous number of particles to track. Another simplification is therefore made which consists in introducing parcels. Parcels are objects that associate particles with similar location, diameter, velocity and other variables of interest. In the tracking algorithm parcels are being tracked instead of individual particles, which greatly reduce the computational time. The concept of parcels also applies to other submodels (secondary breakup, collisions). In the following paragraphs the Euler–Lagrange approach will be discussed in more detail. This approach is adopted in the

numerical analyses performed in this work. A comprehensive overview and review of the spray modelling area can be found in (Jiang et al., 2010).

4.3.1 Particle Tracking

Ansys Fluent predicts the trajectory of a discrete phase particle/parcel (in this case a drop) by integrating the force balance on the particle, which lives in a Lagrangian reference frame. This force balance equates the particle inertia with the forces acting on the particle, and can be written (for the *x* direction in Cartesian coordinates) as

$$\frac{du_p}{dt} = F_D\left(u - u_p\right) + \frac{g_x\left(\rho_l - \rho_g\right)}{\rho_l} \tag{4.1}$$

where g_x is gravity in *x* direction and $F_D(u-u_p)$ is the drag force per unit particle mass.

$$F_D = \frac{18\mu_g C_D \,\mathrm{Re}_{rel}}{24\rho_g D^2}, \tag{4.2}$$

where C_D is the drag coefficient (will be defined in paragraph 5.3.5) and Re_{rel} is the relative Reynolds number defined as

$$\mathrm{Re}_{rel} = \frac{\rho D\left|u_p - u\right|}{\mu_g}. \tag{4.3}$$

In order to take into account the turbulent flow effects on particle motion, the Discrete Random Walk (DRW) can be applied. The DRW model simulates interactions of a particle with a succession of discrete stylized fluid phase turbulent eddies (Gosman and Ioannides, 1983).

4.3.2 Primary Breakup Models

The most crucial step when modelling a spray in the Euler–Lagrangian framework is the primary breakup. The model responsible for this process should ideally provide us with an initial drop size distribution, velocity distribution and mass flow rates, all dependent on spray angle. Available advanced methods that try to approach this idealized model include for example the Maximum Entropy Formalism (MEF) or Discrete Probability Function (DPF) method. These two methods are able to provide us with drop size and velocity distributions (in the case of DPF only with drop size distribution) and can also, to some extent, predict multimodal distributions, as demonstrated for example by Chin et al. (1995). Unfortunately both have also significant drawbacks. MEF requires two representative drop diameters and good predictions are achieved only after adjustments of the model parameters in order to fit experimental data. In the case of DPF, probability density functions of the fluctuating initial conditions are needed. Such fluctuations can be caused by a number of factors, some of which are vibrations of the atomizer, fluctuations in liquid delivery rate, fluctuations in liquid properties (in the case of non-homogenous liquids), fluctuations in exit velocity, etc. However, at the present time we are not able to measure these functions (Babinsky and Sojka, 2002). So far these drawbacks disqualify such methods from being widely used in industrial applications, although they represent a promising research direction.

Since advanced models able to predict the whole range of diameters are not applicable at the moment, simpler primary breakup models are being used. These models usually focus on predictions of a single representative diameter. Papers can be found, e.g. (Qian et al., 2010; Wu et al., 1992), where authors propose empirical correlations between the representative diameter and various physical conditions based on measured data. Such correlations are unfortunately valid

only for a small range of atomizers or even for a small range of operating conditions. In industrial combustion applications, operating conditions are not constant, therefore more flexible models need to be employed. To overcome this obstacle, analytical formulas derived from first principles are needed.

Jet breakup in simple plain orifice atomizers is often modelled by introducing large droplets of the size of the nozzle orifice (Ashgriz, 2011). One of the analytical approaches to describe primary atomization was performed by Senecal et al. (1999). He relates to the pioneering work on jet disintegration by Weber (1931). In his work he investigates liquid sheet atomization and develops the so called LISA (Linearized Instability Sheet Atomization) model. This model predicts the maximum unstable growth rate and wave length, the sheet breakup length and the resulting drop size for pressure-swirl atomizers. The approach of Lund (et al., 1993) is, similarly to the previous case, based on Weber's work (Weber, 1931), but when formulating the model a simpler instability analysis is used to predict a mean drop size of effervescent atomizers. An improvement of Lund's model is proposed by Xiong (et al., 2009), by applying the more rigorous Senecal's instability analysis. As Xiong pointed out, in numerous experimental observations of effervescent atomizers it was concluded that the primary atomization of the liquid undergoes three stages. First, assuming that the two phase flow in the nozzle is annular, an annular sheet forms and breaks up into cylindrical filaments. Second, the filaments break into ligament fragments. Finally, the ligament fragments stabilize to form individual drops. The model assumes that the annular liquid sheet breaks into several cylindrical filaments with almost the same diameter as the thickness of the annular sheet (Figure 4-1). The filaments then break into ligament fragments at the wavelength of the most rapidly growing wave and each fragment only forms one drop. The predicted SMD is later used as the initial diameter of injected drops during the numerical simulation.

The initial particle velocity is yet another unknown, which has to be approximated. One of the possible approximating formulas was derived in Appendix 2 of (Jedelský et al., 2009). However, such formulas only give us a single velocity value and for the sake of precision angular dependency might be necessary.

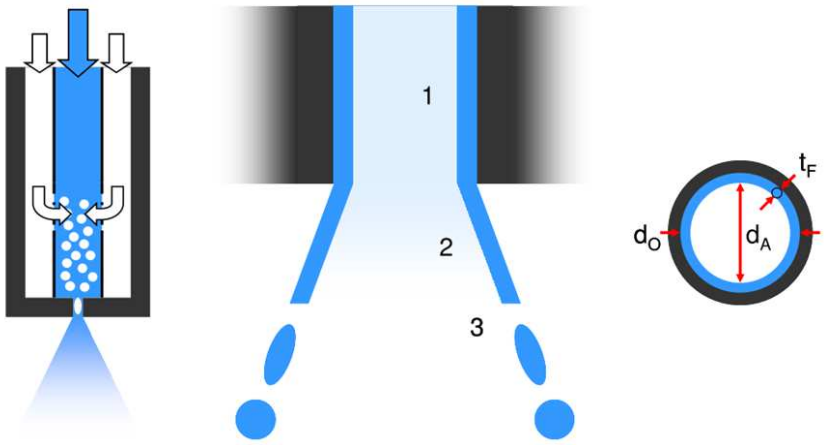

Figure 4-1 Simplified model of effervescent atomization, courtesy of (Schröder et al., 2010)

4.3.3 Secondary Breakup Models

Once the initial drop diameter (or diameter distribution) is obtained, we are interested in how will the drop size change in space and time. When primary breakup model provides a single diameter, the expectation from the secondary breakup model is to create an approximation of the

actual drop size distribution. There are two main branches of secondary breakup models. The first branch is based upon Taylor's analogy between an oscillating and distorting drop and a spring mass system (Taylor, 1963) and it is called Taylor Analogy Breakup (TAB) model, used for example in (Senecal et al., 1999). The second model branch is based on the wave breakup model of Reitz (1987). Here the drop breakup is considered to be induced by the relative velocity between the liquid and gas phase. The relative velocity causes the growth of Kevin-Helmholtz instabilities which are responsible for the final breakup. By using this model it is assumed, that atomization occurs only in the region close to the spray nozzle, since further downstream the relative velocity decreases due to drag and the model no longer predicts any breakup. The model was used for example in (Park et al., 2009) in a study of biodiesel fuel injector.

There are also other approaches to secondary breakup modelling. Xiong (et al., 2009) employs Cascade Analogy Breakup model proposed by Tanner (2004) to simulate an effervescent atomizer. The secondary breakup model based on Fokker – Planck equation proposed Apte (et al., 2003) is adopted by Vuorinen (et al., 2010). These recent models however have yet to be extensively validated and thus have not reached wide acceptance.

4.3.4 Drop Collision Models

There are different models that handle drop collisions. One of the most employed is the algorithm of O'Rourke (1981). Rather than using geometry to see if parcel paths intersect, O'Rourke's method is a stochastic estimate of collisions. Two particles can collide only if they are in the same computational cell. Once it is decided that two parcels of drops collide, the algorithm further determines the type of collision. Only coalescence and bouncing outcomes are considered. The probability of each outcome is calculated from the collisional Weber number We_c and a fit to experimental observations. Here,

$$We_c = \frac{\rho U_{rel}^2 \overline{D}}{\sigma}. \tag{4.4}$$

where U_{rel} is the relative velocity between two drops and $\overline{D}$ is the arithmetic mean diameter of the two drops. The O'Rourke algorithm does not take into account the shattering outcome of the collision, which occurs at high Weber numbers. This drawback does not necessarily need to be significant if the collisions are expected in a region of low Weber number.

New models are being proposed to address the drawbacks of O'Rourke's algorithm. Most recently, Taskiran and Ergeneman (2014) proposed a new collision model taking into account parcel location and velocity data to derive the impact parameter. Their model is therefore no longer mesh dependent but suffers from dependency on parcel number used in the calculations. The authors argue that this drawback could easily be solved in the near future as advances in computer technology will enable us to abandon the parcel approach and track individual droplets.

4.3.5 Drop Drag Models

Accurate determination of drop drag coefficients is crucial for accurate spray modelling and therefore every computational software has a wide array of models to choose from. Ansys Fluent, for example, provides a variety of methods that determine the drop drag coefficient ranging from simple models (Spherical drag law) to dynamic models (Dynamic drag model), where variations in the dropt shape are taken into account. The shape of drops is often assumed to be spherical, but in the case of high Weber numbers, this assumption can distort the final results. The dynamic drag model accounts for the effects of drop distortion, linearly varying the drag between that of a sphere and a value of 1.54 corresponding to a disk. The drag coefficient is given by

$$C_D = C_{D,sph}(1 + 2.632y), \tag{4.5}$$

where $C_{D,sph}$ is the drag coefficient of a sphere and y is the distortion, as determined by the solution of

$$\frac{d^2y}{dt^2} = \frac{C_F \rho_g u^2}{C_b \rho_l r^2} - \frac{C_K y \sigma}{\rho_l r^3} - \frac{C_d \mu_l}{\rho_l r^2}\frac{dy}{dt}. \tag{4.6}$$

where C_F, C_k, C_b, C_d are dimensionless constants (O'Rourke and Amsden, 1987).

4.4 Combustion

The challenge of modelling turbulent reacting flows consists of two interrelated parts, namely the representation of chemical reaction mechanism and its coupling with turbulence. The basic and simple model is Eddy-Dissipation pioneered by Magnussen and Hjertager (1977). This model assumes that combustion is "mixing limited". This means that turbulence slowly mixes fuel and oxidizer into reaction zones where they burn quickly. Due to the Eddy-Dissipation assumption, the model cannot predict intermediate products (e.g. radicals) and can therefore be used only with one-step or two-step global reaction mechanisms. An ignition source is not required, since combustion occurs wherever turbulence is present (Broukal, 2009).

Eddy-Dissipation Concept can be viewed as an extension to the Eddy-Dissipation Model that allows the use of detailed chemical mechanisms and is therefore able to model phenomena such as local extinction and flame lift-off. This advantage comes however with a great computational price.

A compromise between detailed chemistry and computational time may be found in the use of models based on the mixture fraction concept. The power of the mixture fraction modelling approach is that the chemistry description is reduced to two transport equations. Under the assumption of chemical equilibrium, all thermochemical scalars (species fractions, density, and temperature) are uniquely related to the mixture fraction. When taking into account adiabatic systems, the instantaneous values of mass fractions, density and temperature depend only on the instantaneous mixture fraction. The turbulent nonpremixed flame problem is now reduced to tracking the turbulent mixing of the mixture fraction. This tracking can be done from wide variety of levels including DNS, LES and RANS.

4.4.1 Drop Evaporation

As the droplets are heated up by the reaction heat, mass transfer occurs between the discrete Lagrangian entities (fuel droplets) and the continuous gas phase. To take into account such interaction between phases, mass source terms are introduced to the gas phase in appropriate cells, whereas the mass and temperature of droplets are adjusted simultaneously. The evaporative mass fluxes are governed by gradient diffusion, with the flux of droplet vapour into the gas phase related to the difference in vapour concentration at the droplet surface and the bulk gas. No flow inside the droplet is considered and droplet properties such as temperature and density are considered to be uniform over the droplet volume.

References

Apte, S.V., Gorokhovski, M., Moin, P., 2003. LES of atomizing spray with stochastic modeling of secondary breakup. International Journal of Multiphase Flow 29, 1503–1522. doi:10.1016/S0301-9322(03)00111-3

Ashgriz, N., 2011. Handbook of Atomization and Sprays: Theory and Applications. Springer.

Babinsky, E., Sojka, P.E., 2002. Modeling drop size distributions. Progress in Energy and Combustion Science 28, 303–329. doi:10.1016/S0360-1285(02)00004-7

Broukal, J., 2009. Computational modelling of a laboratory burner using FLUENT code. Diploma Thesis, Brno University of Technology.

Broukal, J., Vondál, J., Hájek, J., 2012. Experimental and numerical investigation of wall heat fluxes in a gas fired furnace: Practicable models for swirling non-premixed combustion. Chemical Engineering Transactions 29, 1399–1404. doi:10.3303/CET1229234

Chin, L.P., Switzer, G., Tan Kin, R.S., Jackson, T., Stutrud, J., 1995. BI-Modal Size Distributions Predicted by Maximum Entropy are Compared with Experiments in Sprays. Combustion Science and Technology 109, 35–52. doi:10.1080/00102209508951894

Gosman, A.D., loannides, E., 1983. Aspects of Computer Simulation of Liquid-Fueled Combustors. Journal of Energy 7, 482–490. doi:10.2514/3.62687

Jedelský, J., Jícha, M., Sláma, J., Otáhal, J., 2009. Development of an Effervescent Atomizer for Industrial Burners. Energy & Fuels 23, 6121–6130.doi: 10.1021/ef900670g

Jiang, X., Siamas, G.A., Jagus, K., Karayiannis, T.G., 2010. Physical modelling and advanced simulations of gas-liquid two-phase jet flows in atomization and sprays. Progress in Energy and Combustion Science 36, 131–167. doi:10.1016/j.pecs.2009.09.002

Lund, M.T., Sojka, P.E., Lefebvre, A.H., 1993. Effervescent atomization at low mass flow rates. Part I: The influence of surface tension. Atomization and Sprays 3, 77–89.

Magnussen, B.F., Hjertager, B.H., 1977. On mathematical modeling of turbulent combustion with special emphasis on soot formation and combustion. Symposium (International) on Combustion 16, 719–729. doi:10.1016/S0082-0784(77)80366-4

Nieckele, A.O., Naccache, M.F., Gomes, M.S.P., 2011. Combustion performance of an aluminum melting furnace operating with natural gas and liquid fuel. Applied Thermal Engineering 31, 841–851. doi:10.1016/j.applthermaleng.2010.11.003

O'Rourke, P.J., 1981. Collective Drop Effects on Vaporizing Liquid Sprays (Ph.D. Thesis). Los Alamos National Lab., NM (USA).

O'Rourke, P.J., Amsden, A.A., 1987. The TAB method for numerical calculation of spray droplet breakup. Los Alamos National Lab., NM (USA), USA.

Park, S.H., Kim, H.J., Suh, H.K., Lee, C.S., 2009. Experimental and numerical analysis of spray-atomization characteristics of biodiesel fuel in various fuel and ambient temperatures conditions. International Journal of Heat and Fluid Flow 30, 960–970. doi:10.1016/j.ijheatfluidflow.2009.04.003

Qian, L., Lin, J., Xiong, H., 2010. A Fitting Formula for Predicting Droplet Mean Diameter for Various Liquid in Effervescent Atomization Spray. Journal of Thermal Spray Technology 19, 586–601. doi:10.1007/s11666-009-9457-4

Reitz, R.D., 1987. Mechanisms of Atomization Processes in High-Pressure Vaporizing Sprays. Atomization and Spray Technology 309–337.

Riber, E., Moureau, V., García, M., Poinsot, T., Simonin, O., 2009. Evaluation of numerical strategies for large eddy simulation of particulate two-phase recirculating flows. Journal of Computational Physics 228, 539–564. doi:10.1016/j.jcp.2008.10.001

Sadiki, A., Maltsev, A., Wegner, B., Flemming, F., Kempf, A., Janicka, J., 2006. Unsteady methods (URANS and LES) for simulation of combustion systems. International Journal of Thermal Sciences 45, 760–773. doi:10.1016/j.ijthermalsci.2005.11.001

Senecal, P.K., Schmidt, D.P., Nouar, I., Rutland, C.J., Reitz, R.D., Corradini, M.L., 1999. Modeling high-speed viscous liquid sheet atomization. International Journal of Multiphase Flow 25, 1073–1097. doi:10.1016/S0301-9322(99)00057-9

Shinjo, J., Umemura, A., 2011. Detailed simulation of primary atomization mechanisms in Diesel jet sprays (isolated identification of liquid jet tip effects). Proceedings of the Combustion Institute 33, 2089–2097. doi:10.1016/j.proci.2010.07.006

Tanner, F.X., 2004. Development and validation of a cascade atomization and drop breakup model for high-velocity dense sprays. Atomization and Sprays 14, 211–242.

Taskiran, O.O., Ergeneman, M., 2014. Trajectory based droplet collision model for spray modeling. Fuel 115, 896–900. doi:10.1016/j.fuel.2012.11.053

Taylor, J.I., 1963. The Shape and Acceleration of a Drop in a High Speed Air Stream. Park, S.H., Kim, H.J., Suh, H.K., Lee, C.S., 2009. Experimental and numerical analysis of spray-atomization characteristics of biodiesel fuel in various fuel and ambient temperatures conditions. International Journal of Heat and Fluid Flow 30, 960–970. doi:10.1016/j.ijheatfluidflow.2009.04.003

Technical report, In the Scientific Papers of G. I. Taylor, ed., G. K. Batchelor, University Press, Cambridge.

Vondál, J., Hájek, J., 2009. Experimental and numerical analysis of wall heat transfer in non-premixed gas combustor. Chemical Engineering Transactions 18, 587–592.

Vondál, J., Hájek, J., Kermes, V., 2010. Local wall heat fluxes in swirling non-premixed natural gas flames in large-scale combustor: Data for validation of combustion codes. Chemical Engineering Transactions 21, 1123–1128. doi:10.3303/CET1021188

Vuorinen, V.A., Hillamo, H., Kaario, O., Nuutinen, M., Larmi, M., Fuchs, L., 2010. Effect of Droplet Size and Atomization on Spray Formation: A Priori Study Using Large-Eddy Simulation. Flow Turbulence Combust. doi:10.1007/s10494-010-9266-3

Weber, C., 1931. Disintegration of Liquid Jets. Z. Angew Math. Mech. 11, 136–159.

Wu, P.K., Tseng, L.K., Faeth, G.M., 1992. Primary breakup in gas/liquid mixing layers for turbulent liquids. Atomization and Sprays 2, 295–317.

Xiong, H.-B., Lin, J.-Z., Zhu, Z.-F., 2009. Three-dimensional simulation of effervescent atomization spray. Atomization and Sprays 19, 75–90.

Yan, Y., Zhao, J., Zhang, J., Liu, Y., 2008. Large-eddy simulation of two-phase spray combustion for gas turbine combustors. Applied Thermal Engineering 28, 1365–1374. doi:10.1016/j.applthermaleng.2007.10.008

5 Results

This chapter contains the relevant results in a form of published papers. I chose to order the papers in a chronological fashion since it reflects the way my thoughts and research moved on based on individual results and findings. Since some results have been restated in subsequent publications to lay the groundwork for a new contribution, several articles have been omitted from this chapter. For a full list of the author's articles refer to the Appendix I. The papers collected in this chapter are as follows:

- Broukal, J., Hájek, J., Jedelský, J., 2010. Effervescent atomization of extra-light fuel-oil: Experiment and statistical evaluation of spray characteristics, in: Proceedings of 23rd European Conference on Liquid Atomization and Spray Systems. Presented at the ILASS-Europe 2010, Brno, Czech Republic, pp. 1–10.
- Broukal, J., Hájek, J., 2011. Validation of an effervescent spray model with secondary atomization and its application to modeling of a large-scale furnace. Applied Thermal Engineering 31, 2153–2164. doi:16/j.applthermaleng.2011.04.025
- Broukal, J., Hájek, J., Vondál, J., 2012. Experimental and Numerical Investigation of Wall Heat Fluxes in a Gas Fired Furnace: Practicable Models for Swirling Non-premixed Combustion. Chemical Engineering Transactions 29, 1399–1404. doi:10.3303/CET1229234¨
- Juřena, T., Broukal, J., 2013. Review on validation of CFD models of swirling flows by experimental data, in: Sborník 60. konference chemického a procesního inženýrství, Srní, Czech Republic, pp. 1–8
- Broukal, J., Hájek, J., Sojka, P.E., Juřena, T., 2013. Drop Size Distribution in Effervescent Sprays: An Experimental study Using PDA Technique, in: Proceedings of 6th European Combustion Meeting. Presented at the 6th European Combustion Meeting, Lund, Sweden, pp. 1–6.
- Broukal, J., Hájek, J., 2014. Experimental analysis of spatial evolution of mean droplet diameters in effervescent sprays. Chemical Engineering Transactions, Accepted, awaiting press
- Broukal, J., Hájek, J., Vondál, J., 2014. An experimental study of effervescent sprays: axial evolution of mean drop diameter, 26th European Conference on Liquid Atomization and Spray Systems. To be published

The last section (5.8) contains additional results that have not yet been published. These results are not in a form of a scientific article, since their meaning is to complement the published results and provide additional information to the reader.

5.1 Effervescent Atomization of Extra-light Fuel-oil: Experiment and Statistical Evaluation of Spray Characteristics

Abstract

This paper presents an experimental and statistical analysis of an effervescent atomizer. The spray data were obtained from experimental measurements by means of a Dantec phase/Doppler particle analyser (P/DPA) and analytical and statistical analysis was performed using MATLAB software. The main goal of this work was to analyse the spray characteristics and to find analytical functions that would fit the experimentally obtained drop size distributions. The fitted distributions were then discretized for modelling purposes and the modelled spray was verified against the experimental data. The discrete spray characteristics will be later used for combustion modelling.

5.1.1 Introduction

Liquid sprays can be generated by various atomizers. For combustion purposes, as in this case, effervescent atomizers are gaining on popularity. The effervescent atomizer is a twin-fluid atomizer with internal mixing, which means that besides the liquid there is one more fluid, typically air, that mixes with the liquid before leaving the atomizer body. This type of atomizer was first introduced by Lefebvre and his colleagues in the late 1980s (Lefebvre et al., 1988). Unlike other twin-fluid atomizers, which usually use the air stream to shatter the liquid, the mechanism of drop formation in the case of the effervescent atomizer is rapid air bubble expansion at the atomizer nozzle due to pressure drop. This mechanism makes it possible to use lower injection pressures and larger exit orifice diameters without compromising the drop distribution and has many advantages compared to conventional atomizers (Sovani et al., 2001).

In general, the atomization process is divided into primary and secondary break-up. The primary breakup occurs when the fluid flow exits the orifice and besides being dependent on properties of the fluids involved, it is also strongly dependent on the atomizer type, inner structure and geometry. Secondary atomization is a process during which droplets further break up or collide leading to various outcomes (reflection, coalescence, breakup, etc.). Unlike primary atomization, secondary atomization depends only on properties of the atomized liquid (viscosity, velocity, temperature, surface tension, density, etc.) and the surrounding fluid (typically air).

Recently, several studies appeared, e.g. (Ramamurthi et al., 2009; Jiang et al., 2010; Riber et al., 2009), where the atomization process is modelled directly, meaning that both the internal and external flows are resolved using a single approach, typically the Euler-Euler approach, where the atomized liquid and surrounding air are treated as two continuous impenetrable continua. However, this approach has little applicability in practical applications and although such computational models are emerging, they are not viable in most applications due to extreme computational requirements.

Another approach that is less computationally demanding and therefore acceptable for industrial combustion applications is the Euler-Lagrange approach. In this case the gas phase is modelled as a continuum but the liquid phase is treated as a system of discrete particles (droplets) that are tracked in the gas flow field. It is therefore necessary to use appropriate models for primary and secondary breakup (to determine initial droplet parameters like diameter, velocity and direction) as well as for all other processes concerning the droplets like momentum, heat and mass transfer (evaporation). This is the approach adopted in the present work.

This work concentrates on empirical modelling and numerical representation of the primary break-up process. A strongly simplified approach is to work with only a few representative parameters (e.g. Sauter mean diameter, mass median diameter), but if one wishes to represent the spray more precisely it is necessary to characterize the entire drop size distribution. This method has been developed and studied in numerous papers. Sovani et al. (2001) and Jedelský et al. (2004) suggest that Rosin-Rammler distribution is appropriate for effervescent atomizers. The Rosin-Rammler distribution function reads

$$Q = 1 - e^{-(D/X)^q},$$

where D is the drop diameter and Q represents the mass of drops whose diameter is smaller than D. The parameter X corresponds to the drop diameter for which 63.2 % of the drops' mass is smaller, while the parameter q is a measure of uniformity of the diameters (Rosin and Rammler, 1933).

Moreover, Jedelský et al. also uses log-normal distribution to fit the experimental data. Calay and Holdo (2008) and Cleary et al. (2007) use the two above mentioned distributions to model flashing jets. Ayres et al. (2000) presents a more theoretical approach by predicting joint distribution for both size and velocity of the droplets in sprays using the maximum entropy formalism. A comprehensive list of drop size distributions can be found in (Babinsky and Sojka, 2002).

Modern CFD software codes often allow users to choose from predefined atomizer models and thus avoid laborious manual setting of the spray injection. These models (mostly empirical) use physical atomizer parameters to calculate initial drop sizes, velocities and positions. In the case of Ansys Fluent, a model for the present effervescent atomizer is not available and therefore it is necessary to use a simpler approach (for example cone injection) and to set it up carefully to obtain the spray characteristics as required. Although a great deal of research has been made in CFD modelling of internal combustion engines (Shuai et al., 2009a, 2009b) many papers deal with CFD modelling and numerical studies of non-combustive sprays. Xiong et al. (2009) performed a three-dimensional simulation of an effervescent atomizer. They developed a model for primary and secondary break-up based on the model of Lund et al. (1993). Qian et al. (2009) continued in the footsteps of Xiong et al. and developed a model for effervescent atomizers with an impinging plate. Calay and Holdo (2008) used CFD tools to predict dispersion of flashing jets and a review of physical models and advanced methods used in CFD of sprays can be found in (Jiang et al., 2010).

The scope of this work is to develop a software for analysis of the experimental data and to verify the Fluent‘s ability to represent effervescent sprays. The software will be used firstly to analyse the raw data obtained from measurement and also to find the best possible analytical fit. The fitted data will be discretized and used as input for the CFD software Ansys Fluent, where spray simulations will be performed. Simple models will be preferred in order to focus on the injection models. Finally, the computed data will be compared with the experiment and the results will be discussed.

5.1.2 Measurement and Data Processing

The measured spray of extra-light fuel-oil was generated using the effervescent atomizer and operating conditions described in (Jedelský et al., 2009) as configuration E38. Drop sizes and drop velocities were measured using a Dantec phase/Doppler particle analyser (P/DPA) in 6 radially equidistant sampling points at 150 mm from the atomizer orifice. The angle depicted in

Figure 1 represented the spray half-angle and was estimated as the angle between the axis and the farthermost measurement point. A detailed description of the measurement can be found in (Jedelský et al., 2009).

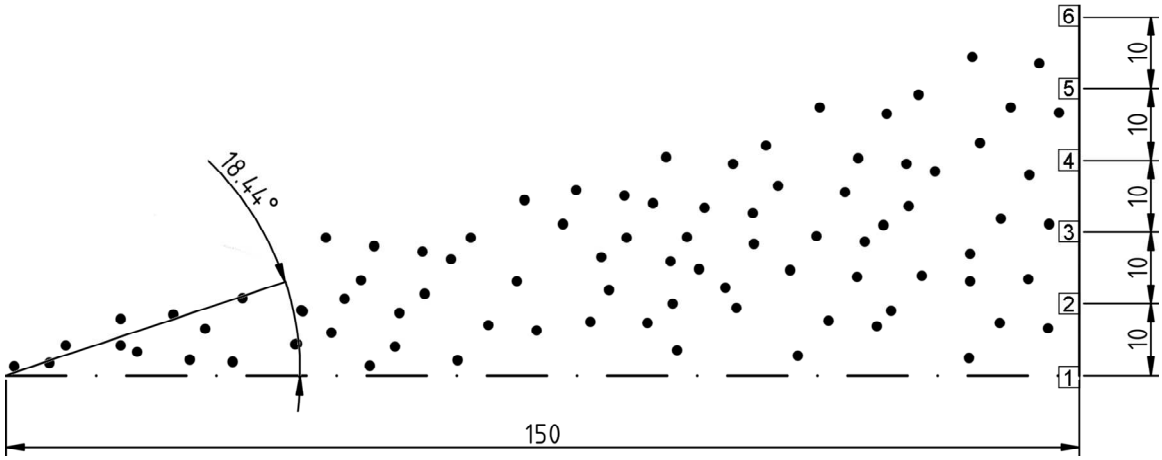

Figure 1. Schematics of the spray measurement

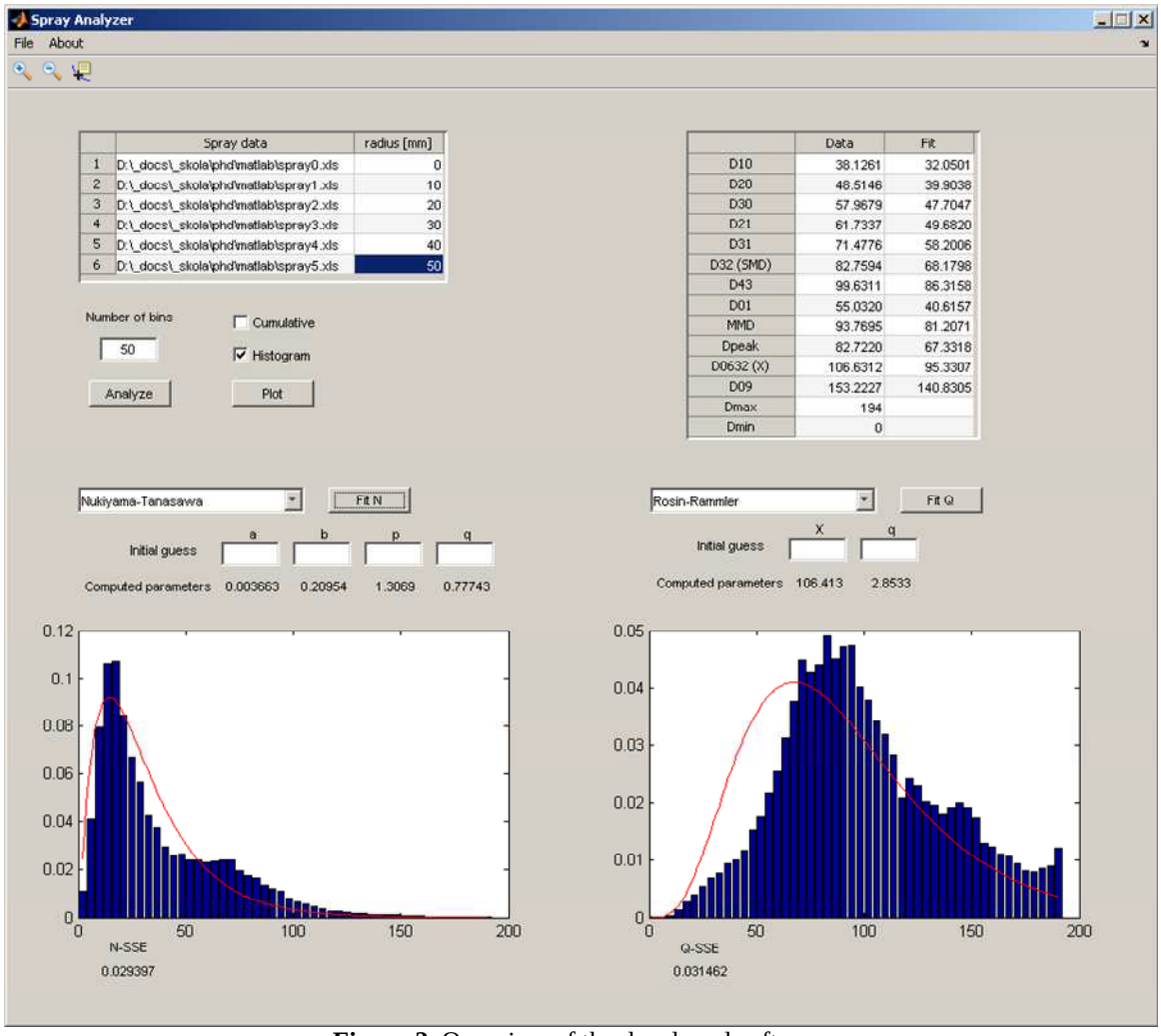

Figure 2. Overview of the developed software

For the purpose of data analysis a software with graphical user interface using MATLAB programming environment (see Figure 2) has been created. The software is able to load experimental data from multiple measuring points as generated by the measuring device and to display frequency and mass histograms together with representative diameters (SMD, MMD, D10, D20, etc.). For simplicity it was assumed that spray properties are piecewise constant in the radial direction, i.e. that a parameter measured in a certain sampling point is the same for the annular area with radiuses $x+d/2$ and $x-d/2$, where r is the radial distance of the sampling point and d is the distance between two adjacent sampling points. The user can then choose from a variety of analytical functions to fit the experimental data. So far the following distributions were implemented: log-normal, root-normal, upper-limit, Rayleigh, Rosin-Rammler, Nukiyama-Tanasawa, Beta and Gamma. To calculate the empirical parameters, the software uses the Nelder-Mead simplex algorithm (Lagarias et al., 1998), in order to accommodate nonlinear regression.

Two cases were studied in this paper. In the first case (A) the spray was considered as a whole and the best Rosin-Rammler fit was found. In the second case (B) the data from the first four sampling points (starting from the centreline) were analysed separately as well as the two remaining sampling points. This separation was performed due to large qualitative differences observed in the three datasets. Best Rosin-Rammler fits have been found for each of these three datasets. Despite of not giving the best approximations the Rosin-Rammler distribution was used in the fitting procedure due to the fact, that Ansys Fluent (used for flow modelling in this work) is equipped with a pre-prepared procedure to discretize this particular distribution function. The best fit in terms of number distribution was the log-normal distribution and in terms of mass weighted distribution the root-normal distribution.

A similar discrepancy, as seen in the work of Babinski and Sojka (2002), has been found between measured and calculated mass flow rates of the atomized liquid. The calculated mass flow rate did not agree with the measured one and therefore needed to be corrected. Such behaviour is probably caused by the low accuracy and error rate of the measurement technique.

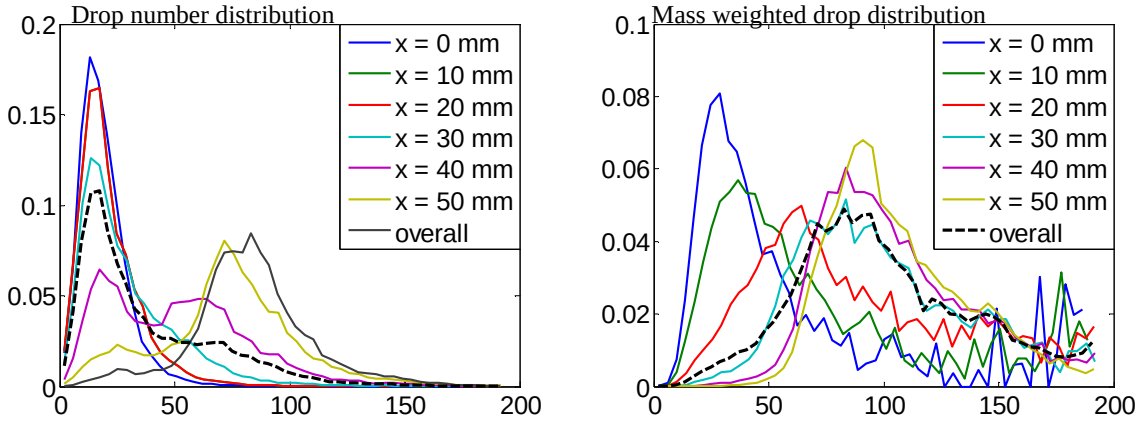

Figure 3. Frequency and mass distributions at different measurement points and average overall distributions, x represents the radial distance of the measurement point

Measurement results

The drop size distributions (notably frequency distributions) in several of the sampling points in the measured spray were bimodal. The distributions obtained from the measurement points close to the atomizer centreline exhibited unimodal behaviour, but bimodality manifested itself as the distance from the centreline increased (see Figure 3). The overall frequency distribution is slightly bimodal (the second peak is around 70 μm).

The mass distributions for respective measurement points on the other hand do not display bimodality, but they generally exhibit discontinuities in the large drop size end of the distribution. These discontinuities might be caused most probably by the measuring technique.

5.1.3 Modelling

The goal of the modelling part of this work was to verify the ability of commercial Ansys Fluent software to re-create a spray according to experimental measurements. This naturally does not mean only the possibility to create suitable boundary conditions, which is a matter of course. The goal was rather to perform a computational virtual experiment repeating the original measurements in which data on the spray were collected. The subjects of evaluation thus include the way how spray boundary conditions are set up, how droplet motion is simulated and how the interaction of the droplets with air deforms the spray on its way from nozzle orifice to the measuring location.

A three-dimensional cylinder-shaped domain was created in Gambit software. The diameter of the domain is 400 mm and it is 2200 mm long. The mesh consists of nearly 80000 hexahedral cells. The domain was filled with air and the spray originated on the centreline 200 mm from air inlet base of the cylinder. The spray was injected from a small circular area of diameter 2.5 mm representing the actual nozzle orifice. In the position of measuring location 150 mm downstream from the injection a series of concentric annular control surfaces has been set up that enabled the virtual measurement. This model served as a test stand for evaluation of the capabilities of the flow solver.

In order to keep the model as simple as possible, gravity was neglected. Turbulence has been accounted for by the $k - \varepsilon$ realizable turbulence model with the default settings (Ansys Fluent, 2009). The spray itself has been modelled as a set of Lagrangian entities using the Discrete Phase Model (DPM). Ansys Fluent offers a variety of atomizer models and injections. Unfortunately none of the implemented atomizer models does correspond to the specific measured effervescent spray; therefore it was chosen to use cone injections instead. In the case A only one injection was created to represent the whole spray, namely a so-called solid cone injection, which means that the spray with a specified half-angle is at the orifice homogeneous with respect to drop size. In case B one solid cone injection and two hollow cone injections were created. The Rosin-Rammler distribution parameters for each injection where found using the previously described MATLAB code. It was also necessary to input the minimal and maximal drop diameter and number of diameters (N) included in the simulations. Each of the drop sizes is in the simulation represented by a specified number of particle streams. Fluent then chooses N diameters equidistantly from between the minimal and maximal diameter and computes for them the Rosin-Rammler probability density using the specified empirical PDF. Then to each stream a different mass flow rate is assigned depending on the computed value of the PDF.

A separate computational analysis was performed to determine the minimal amount of particles that can realistically represent a spray. The criterion used for the evaluation was of the symmetry of temperature distribution in a simple spray combustion problem. The numerical configuration described above is the result of this assessment. The simulations were carried out on the same grid and with the same inlet conditions as in cases A and B. The combustion model was based on a single-step global chemistry with reaction rate controlled by turbulent mixing (so-called eddy dissipation model). Radiative heat transfer has been included using discrete ordinates method to obtain more realistic temperature field. Cases with 500, 2000, 4000, 6000, 8000 and 12000 particles were tested by qualitative comparison of temperature contour plots (see Figure 4).

The smallest number of particles using which the temperature field was still appropriate was found to be 6000.

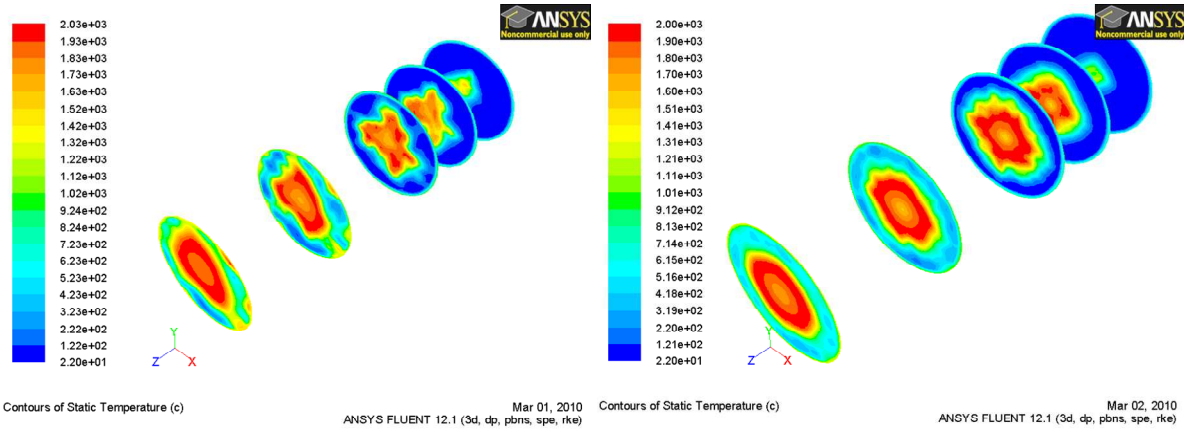

Figure 4. Illustrative demonstration of temperature contour plots. The contours are displayed on cuts perpendicular to the spray axis at 200, 300, 400, 700 and 1100 mm from the spray origin. On the left there are 500 particles while the picture on the right has 6000 particles

The total number of streams both in the case of a single injection (case A) and in the case of three injections (case B) was 200. In the latter case this number has been divided among the injections depending on the area ratios represented by corresponding measurement points. Together with 30 discreet diameters per stream it gives 6000 computational particles.

Another input in the injection definition is the discharge velocity, which was approximated using a formula derived by Jedelský and Sláma in Appendix 2 of (Jedelský et al., 2009). In the case B it was necessary to divide properly the mass flow rates of the three injections. This was done by analysing the partial mass flow rates in respective sampling points and relating them to the total mass flow rate. See Table 1 for injection parameters of the cases A and B.

Although flow in the problem was treated as steady, Ansys Fluent enables to track the particles either as steady (Steady Tracking – StTr) or unsteady (Unsteady Tracking – UnTr). To predict the particle trajectory, one has to integrate the force-balance equation, which can be written (for the *x* direction in Cartesian coordinates) as follows:

$$\frac{du_p}{dt} = F_D\left(u - u_p\right) + \frac{g_x\left(\rho_p - \rho\right)}{\rho_p} + F_x, \tag{1}$$

where u_p is the particle velocity, u the surrounding air flow velocity, F_x and g_x is an additional acceleration in x direction and gravity respectively. $F_D(u - u_p)$ is the drag force per unit particle mass (Ansys Fluent, 2009). The shape of drops is assumed to be spherical and the drag force was calculated using the formula that reads

$$F_D = \frac{18\mu}{\rho_p d^2}\frac{C_D \,\mathrm{Re}}{24}, \tag{2}$$

where d is drop diameter, μ is the molecular viscosity of the fluid (air) and

$$C_D = a_1 + \frac{a_2}{\mathrm{Re}} + \frac{a_3}{\mathrm{Re}^2}. \tag{3}$$

The constants a_1, a_2, a_3 apply to smooth spherical particles over several ranges of Re given by Morsi and Alexander (1972). Ansys Fluent numerically solves the integral by choosing a time step which can be defined using the so called step length factor (SLF). It allows Fluent to compute the time step size in terms of the number of time steps required for a particle to traverse a computational cell (Ansys Fluent, 2009):

$$\Delta t = \frac{\Delta t^*}{SLF}, \tag{4}$$

where Δt^* is the estimated transit time. All units in the previous equations are SI units. In this study two different SLF have been tested: 5 and 15.

In order to take into account the turbulent flow effects on particle motion, the Discrete Random Walk (DRW) model has been applied. The DRW model simulates the interaction of a particle with a succession of discrete stylized fluid phase turbulent eddies.

The discrete phase exchanges only momentum with the continuous phase. Mass and energy exchange (due to evaporation) has been neglected as the analysed cases did not include combustion and the ambient temperature was around 20°C. For such conditions the region of interest is sufficiently small, so that the diameter of drops does not change considerably before reaching the sampling plane. Due to the nature of the studied problem, where we want to model a spray using experimental data at 150 mm from the atomizer orifice, secondary atomization (drop collisions, break-up and coalescence) has not been included.

Sampling in the computational spray was performed by a user-defined function (UDF), which monitored drop parameters at annuluses corresponding to each measuring point 150 mm from the spray origin. After a particle travels further than 250 mm from the spray origin it is deleted in order to decrease computational costs.

Table 1. Injection parameters for cases A and B

	Case A	Case B		
Injection type	Solid cone	Solid cone	Hollow cone	Hollow cone
Half-angle [deg]	18.44	11.31	14.93	18.44
Mass flow [g/s]	21.8	11.3	6	4.5
X[μm]	106.4	103.5	106.7	107.5
q	2.85	2.29	3.56	3.94
measuring points included	1-6	1-4	5	6
# of streams	200	81	53	66
# of diameters (N)	30			
Discharge velocity [m/s]	156.72			
Fuel-oil density [kg/m3]	874			

In the simulation a small air co-flow (1 m/s) was introduced. The co-flow was used in order to improve solution stability. On the opposite side of the domain was used pressure outlet condition. The cylinder's lateral surface was treated as a wall with no slip conditions. This boundary condition deviates from the experiment, but since the volume of interest is relatively small in comparison with the domain dimensions, it should not affect the solution significantly.

Convergence of the simulation was proclaimed upon stabilization of instantaneous flow velocities in various points and total mass of fuel-oil in the computational domain.

5.1.4 Results and Discussion

Discussion of Case A

In this case the whole spray was substituted by a single solid-cone injection. Different cases were studied depending on the tracking scheme and step length factor. The results showed that there is almost no difference between the two values of step length factor (SLF = 5 and SLF = 15) both in the partial and in the overall drop distributions. Such small significance of the SLF is probably induced by the simplicity of the model. In the case of a stronger coupling between the phases (mass and energy exchange, combustion) the significance of SLF would probably increase. Nonetheless future investigation in the area of SLF significance is needed.

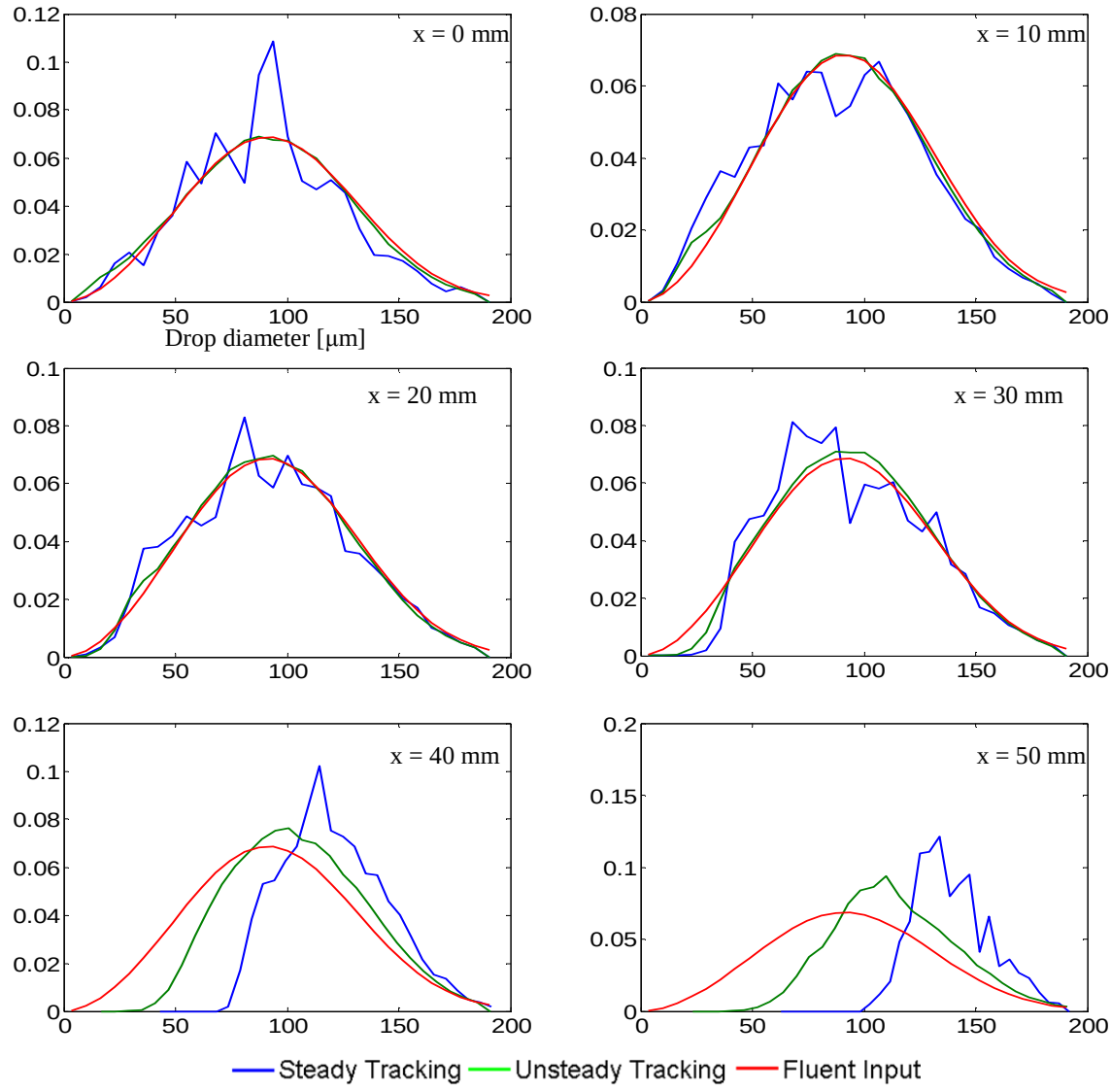

Figure 5. Comparison of steady and unsteady tracking results in case A

On the other hand the tracking scheme has a remarkable effect on the drop distributions. From Figure 5 it is clear that the unsteady tracking scheme gives superior results when compared to steady tracking. Despite the fluctuations of the steady tracking scheme both results are close to the input drop distribution up to the fourth measurement point (at x = 30 mm). In the last two

measurement points the calculated distributions differ from the input distribution; the steady case differs more significantly. This shift is probably caused by the smaller particles being entrained in the spray core. The last two measurement points in Figure 6 show that in the case of unsteady particle tracking, the calculated drop distributions represent surprisingly well the (local) RR fit of actual drop distributions in the respective measurement points. The slight under prediction of smaller diameters in these last two points might be caused by the absence of secondary atomization, which is responsible for the creation of smaller drops in the peripheral regions.

In Figure 6 it can be also clearly seen that closer to the spray core the input distribution is conserved well, however the Rosin-Rammler fits in the individual measurement points (green curves) differ heavily. This is a clear evidence of high complexity of the drop formation process, which cannot be simply replaced by an overall drop distribution when trying to model the spray accurately.

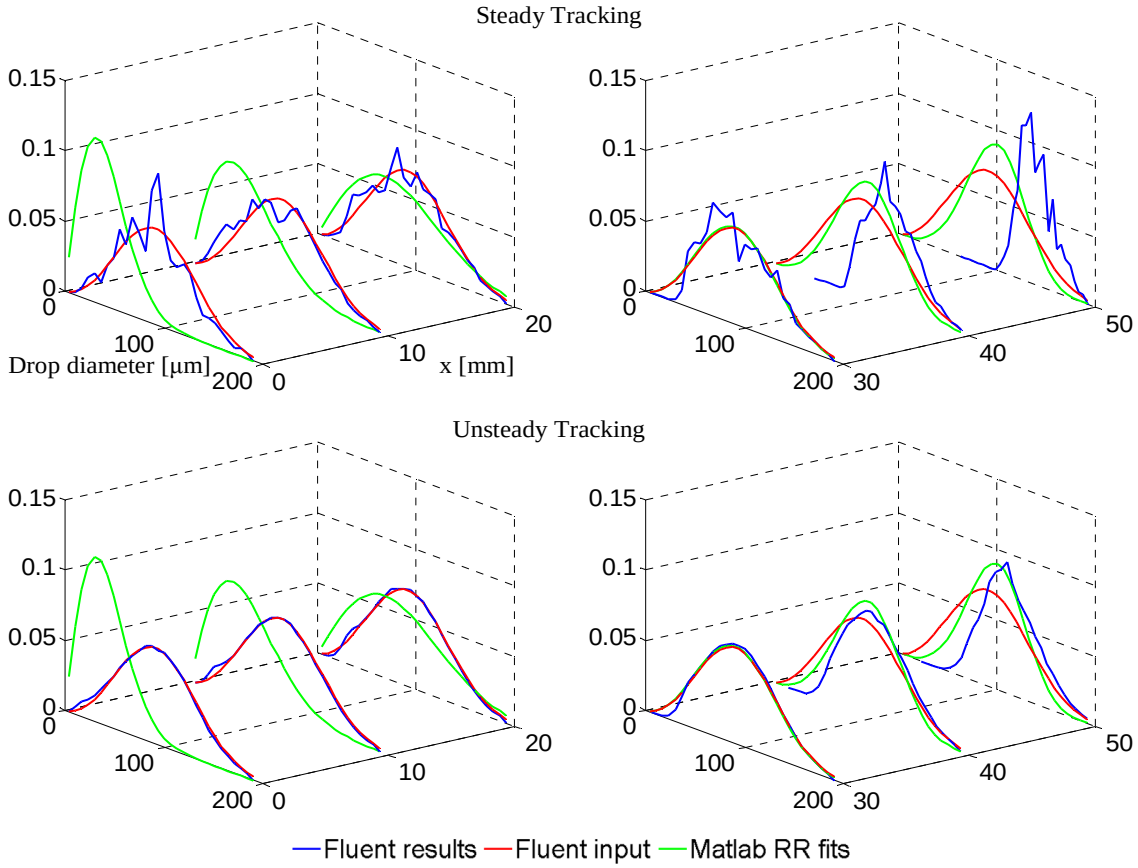

Figure 6. Drop mass PDF for case A, x represents the radial distance of the measurement point

Discussion of Case B

In the second case the whole spray was modelled using one solid cone and two hollow cone injections. The inner solid cone injection averaged the spray cone up to the fourth measuring point (starting from the axis) and each of the two hollow cone injections represented spray sections relative to the last two measurement points. As in the previous case the step length factor did not act as a major deal breaker. Unfortunately the steady tracking results were not examined due to unresolved issues in the user defined function used for numerical spray evaluation. Therefore all results for the case B were produced with the unsteady tracking option. In Figure 7 is evident, that starting from the first measurement point a small peak is building up around the value 70 μm and it reaches its maximum in the fourth measurement point (at x = 30 mm). A possible explanation of this behaviour is a large entrainment of smaller drops at the interface between the inner solid cone

injection and middle hollow cone injection due to the coarse spatial angle discretization. It is also not possible to exclude the possibility that the particle tracking model gives unsatisfactory results when dealing with multiple concentric injections. The peak vanishes almost immediately when moving to the spray outer regions.

An interesting observation can be made when comparing the last two measurement points in case A (Figure 6) and case B (Figure 7). In case A the calculated drop distributions are closer to the Rosin-Rammler fits in the individual measurement points than the calculated drop distributions from case B. This might be again caused by the coarse spatial angle discretization.

Similarly to the previous case A (single cone injection) the calculated distributions in the spray core show good preservation of the input distribution (omitting the measurement point x = 30 mm) while in the last two measurement points a shift is observed. The reason of this shift is identical to the shift discussed in case A. In the measurement points x = 40 mm and x = 50 mm the green curve is missing because in this case it is identical to the red curve.

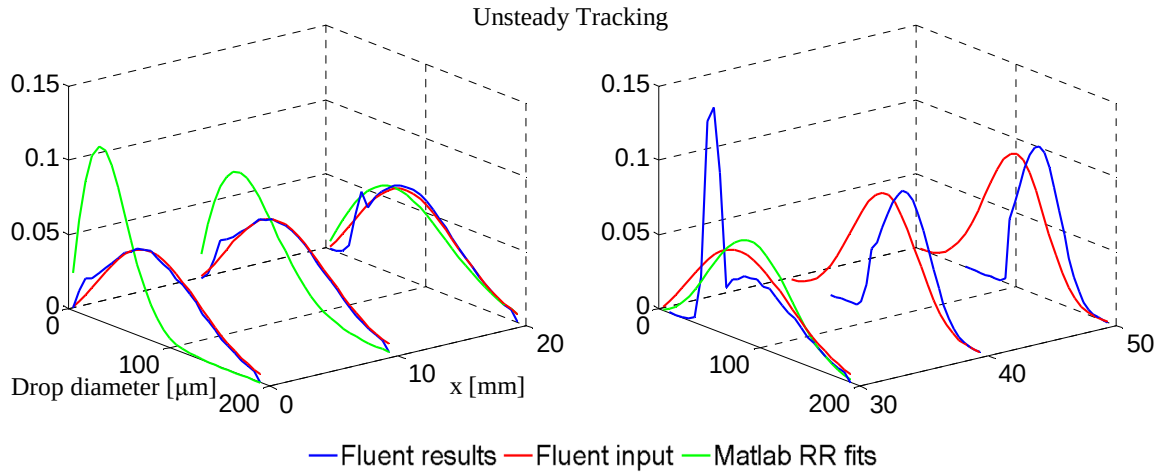

Figure 7. Drop mass PDF for case B, x represents the radial distance of the measurement point

Overall drop distributions of both studied cases can be seen in Figure 8. Concerning the case A, according to Figure 8, it might seem that there is almost no difference between steady and unsteady tracking. However, differences pointed out in previous paragraphs would probably play a much more important role when dealing with more complex flow problems (i.e. spray combustion). A more noticeable difference is found in case B.

In terms of convergence and solution stability the unsteady tracking scheme behaves better than steady tracking scheme in both cases. The obvious drawback of unsteady tracking is higher computational demand, which is in terms of time approximately two to four times higher.

5.1.5 Future Work

The software used for the scope of this work offers only basic fitting procedures at the moment. A bimodal approximation, more accurate than the standard unimodal approximations of the effervescent spray, was investigated as a potential improvement, but has yet to be assessed similarly as the two cases reported in this work. In the future research will be employed also other methods, which do not depend solely on experimental results (Maximum Entropy Formalism (Babinsky and Sojka, 2002), variations of Lund's model (Xiong et al., 2009), etc.).

The developed spray model will be used to model spray combustion of vegetable oils in large scale combustors. The computed results will be verified in terms of wall heat fluxes with experimental results from a large scale experimental facility (Kermes and Bělohradský, 2008).

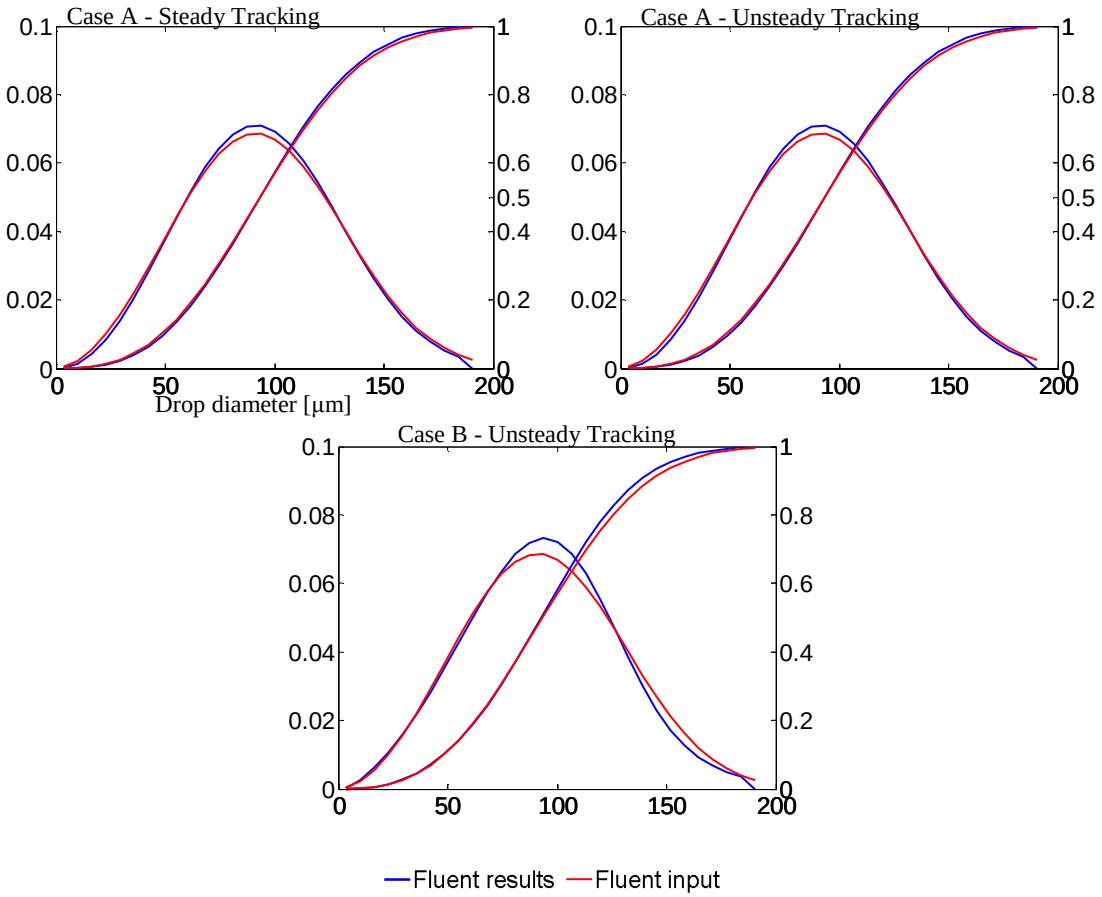

Figure 8. Overall drop mass PDF and distribution functions

5.1.6 Conclusion

Raw data from experimental spray measurement were analysed and fitted using a software tool developed in the MATLAB programming environment. The obtained distribution characteristics were used as input in Ansys Fluent to set up appropriate injections. The spray was properly discretized and represented by a sufficiently large number of computational droplets. The spray simulation was finally validated by comparing the computed data with the experimental data.

It has been shown that Ansys Fluent is able to represent reasonably well sprays in terms of overall drop size distribution. However, in case one is interested in a more detailed spray description then more sophisticated atomizer models or complex injections may be necessary.

Acknowledgement

The authors gratefully acknowledge financial support of the Ministry of Education, Youth and Sports of the Czech Republic within the framework of project No. 2B08048 "Waste as raw material and energy source".

References

Ansys Fluent, 2009. Ansys Fluent 12.1 Documentation.

Ayres, D., Caldas, M., Semiao, V., Carvalho, M. da G., 2000. Prediction of the droplet size and velocity joint distribution for sprays. Fuel 2001, 383–394.

Babinsky, E., Sojka, P.E., 2002. Modeling drop size distributions. Progress in Energy and Combustion Science 28, 303–329. doi:10.1016/S0360-1285(02)00004-7

Calay, R.K., Holdo, A.E., 2008. Modelling the dispersion of flashing jets using CFD. Journal of Hazardous Materials 154, 1198–1209. doi:10.1016/j.jhazmat.2007.11.053

Cleary, V., Bowen, P., Witlox, H., 2007. Flashing liquid jets and two-phase droplet dispersion: I. Experiments for derivation of droplet atomisation correlations. Journal of Hazardous Materials 142, 786–796. doi:10.1016/j.jhazmat.2006.06.125

Jedelský, J., Jícha, M., Sláma, J., 2004. Characteristics And Behaviour Of Multi-Hole Effervescent Atomizers, in: 19th International Conference on Liquid Atomization and Spray Systems - ILASS Europe. Presented at the 19th ILASS Europe, Nottingham, UK, pp. 521–526.

Jedelský, J., Jícha, M., Sláma, J., Otáhal, J., 2009. Development of an Effervescent Atomizer for Industrial Burners. Energy & Fuels 23, 6121–6130. doi: 10.1021/ef900670g

Jiang, X., Siamas, G.A., Jagus, K., Karayiannis, T.G., 2010. Physical modelling and advanced simulations of gas-liquid two-phase jet flows in atomization and sprays. Progress in Energy and Combustion Science 36, 131–167. doi:10.1016/j.pecs.2009.09.002

Kermes, V., Bělohradský, P., 2008. Testing of gas and liquid fuel burners for power and process industries. Energy 33, 1551–1561.

Lagarias, J., Reeds, J., Wright, M., Wright, P., 1998. Convergence Properties of the Nelder--Mead Simplex Method in Low Dimensions. SIAM J. Optim. 9, 112–147. doi:10.1137/S1052623496303470

Lefebvre, A.H., Wang, X.F., Martin, C.A., 1988. Spray Characteristics of Aerated-Liquid Pressure Atomizers. Journal of Propulsion and Power 4, 293–298.

Lund, M.T., Sojka, P.E., Lefebvre, A.H., 1993. Effervescent atomization at low mass flow rates. Part I: The influence of surface tension. Atomization and Sprays 3, 77–89.

Morsi, S.A., Alexander, A.J., 1972. Theoretical Low-Speed Particles Collision with Symmetrical and Cambered Aerofoils. ASME Pap.

Qian, L., Lin, J., Xiong, H., 2009. Simulation of Droplet-gas Flow in the Effervescent Atomization Spray with an Impinging Plate. Chinese Journal of Chemical Engineering 17, 8–19. doi:10.1016/S1004-9541(09)60026-4

Ramamurthi, K., Sarkar, U.K., Raghunandan, B.N., 2009. Performance characteristics of effervescent atomizer in different flow regimes. Atomization and Sprays 19, 41–56.

Riber, E., Moureau, V., García, M., Poinsot, T., Simonin, O., 2009. Evaluation of numerical strategies for large eddy simulation of particulate two-phase recirculating flows. Journal of Computational Physics 228, 539–564. doi:10.1016/j.jcp.2008.10.001

Rosin, P., Rammler, E., 1933. Laws governing the fineness of powdered coal. J. Inst. Fuel 7, 29–36.

Shuai, S., Abani, N., Yoshikawa, T., Reitz, R.D., Park, S.W., 2009a. Evaluation of the effects of injection timing and rate-shape on diesel low temperature combustion using advanced CFD modeling. Fuel 88, 1235–1244. doi:10.1016/j.fuel.2009.01.012

Shuai, S., Abani, N., Yoshikawa, T., Reitz, R.D., Park, S.W., 2009b. Simulating low temperature diesel combustion with improved spray models. International Journal of Thermal Sciences 48, 1786–1799. doi:10.1016/j.ijthermalsci.2009.01.011

Sovani, S.D., Sojka, P.E., Lefebvre, A.H., 2001. Effervescent atomization. Progress in Energy and Combustion Science 27, 483–521. doi:10.1016/S0360-1285(00)00029-0

Xiong, H.-B., Lin, J.-Z., Zhu, Z.-F., 2009. Three-dimensional simulation of effervescent atomization spray. Atomization and Sprays 19, 75–90.

5.2 Validation of an Effervescent Spray Model with Secondary Atomization and its Application to Modeling of a Large-scale Furnace

Abstract

The present work consists of a validation attempt of an effervescent spray model with secondary atomization. The objective is the simulation of a 1 MW industrial-type liquid fuel burner equipped with effervescent spray nozzle. The adopted approach is based on a double experimental validation. Firstly, the evolution of radial drop size distributions of an isothermal spray is investigated. Secondly, the spray model is tested in a swirling combustion simulation by means of measured wall heat flux profile along the flame.

In the first part of the paper, both experiments are described along with the measuring techniques. Drop sizes and velocities measured using a Dantec phase/Doppler particle analyser are analysed in detail for six radial positions. Local heat fluxes are measured by a reliable technique along the furnace walls in a large-scale water-cooled laboratory furnace.

In the second part Euler – Lagrange approach is applied for two-phase flow spray simulations. The adopted spray model is based on the latest industrially relevant (i.e. computationally manageable) primary and secondary breakup sub-models complemented with droplet collision model and a dynamic droplet drag model. Results show discrepancies in the prediction of radial evolution of Sauter mean diameter and exaggerated bimodality in drop size distributions. A partial qualitative agreement is found in radial evolution of drop size distributions. Difficulties in predicting the formation of small drops are highlighted. Comparison of the predicted wall heat fluxes and measured heat loads in swirling flame combustion simulation shows that the absence of the smallest droplets causes a significant elongation of the flame.

Keywords: drop-size distribution, effervescent atomization, modelling, spray combustion

5.2.1 Introduction

Spray combustion is one of the main ways to gain energy in the power and process industries. A great deal of effort is constantly being put into understanding of the fundamental phenomena and processes governing spray formation and swirling combustion. These efforts are motivated by the need to achieve better performance, lower emissions and longer lifetime of furnaces and combustors in various industrial applications.

For combustion purposes, effervescent atomizers are gaining on popularity. They were first introduced by Lefebvre and his colleagues in the late 1980s (Lefebvre et al., 1988). The spray formation process in this type of atomizers does not rely solely on high liquid pressure and aerodynamic forces, instead a small amount of gas (usually air) is introduced in the liquid before it exits the atomizer and a two phase flow is formed (Figure 1). When the mixture exits through the nozzle, pressure suddenly drops, which causes fast expansion of gas bubbles and breakup of the liquid fuel into droplets. This breakup mechanism allows to use lower injection pressures and larger nozzle diameters without compromising the drop-size distribution (Babinsky and Sojka, 2002).

Wall Heat Flux Distribution

When designing a furnace or combustor one of the most important parameters is the distribution of wall heat fluxes, especially on cooled walls (heat exchanging areas). In the last two decades, a number of works can be found where wall heat fluxes are investigated either experimentally, e.g. (Hayes et al., 2001), or numerically using computational fluid dynamics (CFD) tools, e.g. (Vondál and Hájek, 2009a). Measurement of local heat loads in industrial conditions is however possible only using special heat flux probes that cannot provide reliable detailed data covering the whole heat transfer area, but only a limited number of discrete points. Additionally, industrial units typically have only rough estimates of the instantaneous total heat transfer rate, e.g. ± 4 % in (Valero and Cortés, 1996).

The measurement of wall heat fluxes was traditionally connected mainly to the identification of fouling and slagging, especially in pulverised-coal boilers. Therefore many of the existing probes are designed to operate in harsh environments. In laboratory experiments the measured heat flux data are naturally more reliable than in industrial combustors. Even though, the accuracy of available measurement methods is on the order of several percent. E.g. for the measurements of thermal irradiation flux are often used ellipsoidal radiometers (accuracy ± 5 %) and water-cooled circular foil heat flux radiometers (accuracy ± 2 %) (Hayes et al., 2001). The ± 2 % accuracy is about the best one can achieve with heat flux metering probes. However, as reported in (Hayes et al., 2001), differences of values measured by these two methods may reach up to 12 %, thus decreasing the credibility of point heat flux measurements.

On the other hand, the measurement of heat transfer rate in a segmental experimental combustion chamber with water cooling may provide appreciably more precise values, as shown in (Vondál and Hájek, 2009a). This is also the method adopted in the present work.

Swirling Nonpremixed Combustion

The problem complexity is further enhanced when taking into consideration, that the vast majority of power burners use swirl stabilizers, as discussed in (Kermes et al., 2007). The turbulent swirling flow is difficult to model even alone and when chemistry and radiation are added, the resulting problem becomes very complex. In the present, proven approaches that can deal with these complex flows include Large Eddy Simulations (LES) or direct numerical simulations coupled with advanced chemistry models, e.g. (Sadiki at al., 2006). Those very detailed results come at a price of extremely high computational demands, which are generally unacceptable in industrial applications. That is why even authors of these advanced LES studies are unsure whether the use of LES strategy will in the future prevail over unsteady Reynolds-averaged Navier-Stokes (RANS) approach (Jiang et al., 2010).

More research is therefore needed to find simpler time-effective numerical models from the RANS or unsteady RANS class for the prediction of swirling nonpremixed flames that would yield practically relevant results. The issue of local wall heat flux prediction in swirling combustor has been recently investigated for the case of methane swirling combustion in (Vondál and Hájek, 2009a) and it has been shown, that local wall heat flux predictions are very sensitive to the choice of models used to describe the physical and chemical processes occurring in flames. Results in (Vondál and Hájek, 2009a) provide guidelines for the selection of several sub-models in computations of swirling nonpremixed gas flames.

Spray Modelling

The presence of spray droplets in swirling spray combustion further increases complexity of predicting these flames. Clearly, to minimize the uncertainties and errors that are caused by numerical representation of sprays, appropriate spray models need to be found and validated.

At the present time, two predominant methods for numerical spray representation are used: the Euler – Euler and Euler – Lagrange approach (Jiang et al., 2010). The first approach is computationally demanding and so far is used almost exclusively for spray formation investigations without combustion as for example in (Riber et al., 2009; Shinjo and Umemura, 2011). The latter approach is less demanding and allows employment in combustion applications as for example (Yan et al., 2008; Nieckele et al., 2010). The relative simplicity and low computational costs of the Euler – Lagrange approach are compensated by the need to find or develop appropriate sub-models for primary breakup (to determine initial droplet parameters like diameter and velocity and their angular variations) and secondary breakup (breakup of droplets that occurs farther from the nozzle) as well as for all other processes concerning the droplets, like momentum, heat and mass transfer in the evaporating spray.

The most crucial step when modelling a spray in the Euler – Lagrangian framework is the primary breakup. The model responsible for this process should ideally provide us with an initial drop size distribution, velocity distribution and mass flow rates, all dependent on spray angle. Available advanced methods that try to approach this idealized model include for example the Maximum Entropy Formalism (MEF) or Discrete Probability Function (DPF) method. These two methods are able to provide us with drop size and velocity distributions (in the case of DPF only with drop size distribution) and can also, to some extent, predict multimodal distributions, as demonstrated for example in (Chin et al., 1995). Unfortunately both have also significant drawbacks. MEF requires two representative drop diameters and good predictions are achieved only after adjustments of the model parameters in order to fit experimental data. In the case of DPF, probability density functions of the fluctuating initial conditions are needed. Such fluctuations can be caused by a number of factors, some of which are vibrations of the atomizer, fluctuations in liquid delivery rate, fluctuations in liquid properties (in the case of non-homogenous liquids), fluctuations in exit velocity, etc. However, at the present time we are not able to measure these functions (Babinsky and Sojka, 2002). So far these drawbacks disqualify such methods from being widely used in industrial applications, although they represent a promising research direction.

Since advanced models able to predict the whole range of diameters are not applicable at the moment, simpler primary breakup models are being used. These models usually focus on predictions of a single representative diameter. Papers can be found, e.g. (Qian et al., 2010), where authors propose empirical correlations between the representative diameter and various physical conditions based on measured data. Such correlations are unfortunately valid only for a small range of atomizers or even for a small range of operating conditions. In industrial combustion applications, operating conditions are not constant, therefore more flexible models need to be employed. To overcome this obstacle, analytical formulas derived from first principles are needed.

One of the analytical approaches to describe primary atomization was performed by Senecal et al. (1999). He relates to the pioneering work on jet disintegration by Weber (1931). In his work he investigates liquid sheet atomization and develops the so called LISA (Linearized Instability Sheet Atomization) model. Primary atomization of effervescent atomizers has been assessed by Lund et al. (1993). The approach of Lund is, similarly to the previous case, based on Weber's

work (Weber, 1931), but when formulating the model a simpler instability analysis is used. An improvement of Lund's model is proposed by Xiong et al. (2009), by applying the more rigorous Senecal's instability analysis.

Once the initial drop diameter is obtained, we are interested in how will the drop change in space and time. When primary breakup model provides a single diameter, the expectation from the secondary breakup model is to create an approximation of the actual drop size distribution. There are two main branches of secondary breakup models. The first branch is based upon Taylor's analogy between an oscillating and distorting droplet and a spring mass system (Taylor, 1963) and it is called Taylor Analogy Breakup (TAB) model used for example in (Senecal et al., 1999). The second model branch is based on the wave breakup model of Reitz (1987). Here the drop breakup is considered to be induced by the relative velocity between the liquid and gas phase. The relative velocity causes the growth of Kevin-Helmholtz instabilities which are responsible for the final breakup. The model was used for example in (Park et al., 2009).

There are also other approaches to secondary breakup modelling. Xiong (Xiong et al., 2009) employs Cascade Analogy Breakup model proposed by Tanner (2004) to simulate an effervescent atomizer. The secondary breakup model based on Fokker – Planck equation proposed Apte et al. (2003) is adopted by Vuorinen et al. (2010). These recent models however yet have to be extensively validated and thus have not reached wide acceptance.

Spray Model Validations

In the area of combustion, spray models are usually validated based on their ability to predict the Sauter Mean Diameter (SMD). This is a very rough approach as follows from the discussion in the preceding section. Significantly more detailed information would be needed to make really sensible validations. Namely, data about radial (or equivalently depending on spray angle) distribution of droplet size and velocity would be desirable, especially for the case of large nozzles in industrial burners.

Currently, spray model validation studies compare numerical results with experiments usually only in terms of axial SMD evolution. This validation concept is adopted for example in (Qian et al., 2010; Xiong et al., 2009; Apte et al, 2003; Aliseda et al., 2008; Tembely and Lecot, 2010). Apte predicts axial SMD evolution in a diesel engine using a proposed hybrid particle-parcel model coupled with a LES solver, but only a single experimental SMD value is used in the comparison. A model for atomization of viscous and non-Newtonian liquids in an air-blast atomizer is described by Aliseda et al. (2008). The model was validated in terms of axial SMD evolution and good agreement has been achieved in the spray region farther from certain distance downstream from the nozzle. Tembley and Lecot (2010) used MEF to predict drop size distribution in ultrasonic atomizers. He developed a model able to predict initial drop size distribution as well as how does the distribution change along the spray axis. However, this model only predicts the overall drop size distribution of a spray cross-section at a specified axial distance.

Recently, few papers can be found that address the issue of radial drop size distribution and radial SMD evolution. Park et al. (2009) employed the wave breakup model to investigate biodiesel spray in various fuel and ambient conditions in terms of axial and radial SMD evolution. Along with axial SMD evolution, also radial SMD evolution was reported. Unfortunately, only three radial SMD were disclosed. In (Pougatch et al., 2009) a new Euler – Euler spray model is presented and applied to water air-assisted atomization. Radial drop diameter evolution is predicted at various axial positions, but regrettably, no comparison with experimental data has

been made. This illustrates the pressing need for validated spray models that would include sufficient information for an informed choice of models by CFD analysts in the industry.

Although many research papers have been published about atomization and drop breakup, only little attention is given to radial SMD or more detailed spatial drop-size distribution, especially in effervescent atomizers. The present work suggests that the drop diameter evolution in radial direction plays an important role in combustion applications and spray models should be able to predict this feature.

The approach adopted in the present work is the Euler – Lagrange with improved Lund's model (according to Xiong et al. (2009)) applied to account for primary breakup. The secondary breakup is then governed by Reitz's wave model (Reitz, 1987). The motivation of the current study is the prediction of radial drop-size distributions and double experimental validation by isothermal spray measurement and precise local wall heat flux measurement in a large-scale laboratory combustion facility.

5.2.2 Experiments

This work reports data obtained from two different experiments. In the first experiment the effervescent atomizer was analysed in terms of radial drop-size distribution. The purpose of the second experiment was to collect local wall heat flux data in a large-scale combustion chamber (for duties up to 2 MW). Both experimental results are later compared with data obtained from numerical simulations.

Spray Measurement and Data Processing

The measured spray of extra-light fuel-oil was generated using the effervescent atomizer in a vertical position described in (Jedelský et al, 2009) as configuration E38. The atomizer had a single orifice (2.5 mm in diameter) and consisted of a cylindrical body with an inserted aerator tube. The aerator had 80 holes, each 1 mm in diameter, through which the air entered into the liquid. The volume of the mixing chamber inside the aerator tube is given by the length downstream of the last row of air holes (35 mm) and the internal diameter of the aerator tube (14 mm). The oil density, dynamic viscosity and surface tension was 874 kg/m^3, 0.0185 kg/ms and 0.0297 N/m respectively. The atomizing pressure was 0.3 MPa which corresponded to an oil mass flow rate of 21.8 g/s and atomizing air mass flow rate of 2.18 g/s (gas-liquid ratio of 10%). Drop sizes and drop velocities were measured using a Dantec phase/Doppler particle analyser (P/DPA) in 6 radially equidistant sampling points at 150 mm from the atomizer orifice. The drawing in Figure 2 shows the measurement points in a half-angle of the spray (between the axis and the farthermost measurement point). A detailed description of the measurement can be found in (Jedelský et al., 2009). At each of the six measurement points more than 30,000 particles were sampled, leading to a total of approximately 200,000 sampled particles.

For the purpose of data analysis a software with graphical user interface was created using MATLAB programming environment. The software was designed for the processing of experimental data from multiple measuring points as generated by the measuring device. The spray cone was supposed to be symmetrical. The circular cross section of the spray cone at the measurement distance was divided into annular areas corresponding to each measurement point (clearly, for the innermost measurement point the area was circular). The drop-size distribution in each measurement point was assumed to be identical for the whole corresponding area (piecewise constant). From the analysis detailed data were acquired about the total drop-size distribution as well as about the radial evolution of the drop-size distribution as shown in Figure 3.

A similar discrepancy, as seen in the work of Babinski and Sojka (2002), has been found between measured and calculated mass flow rates of the atomized liquid. The calculated mass flow rate was approximately 60% smaller. Such behaviour is probably caused by a non-zero error rate of the measurement technique causing rejection of particles.

The number-based drop-size distributions in several of the sampling points in the measured spray were bimodal. The distributions obtained from the measurement points close to the atomizer centreline exhibited unimodal behaviour, but bimodality manifested itself as the distance from the centreline increased (see Figure 3). The overall number-based drop-size distribution is slightly bimodal.

The volume-based drop-size distributions for respective measurement points on the other hand do not display bimodality, but they generally exhibit discontinuities in the large drop size end of the distribution. These discontinuities might be again caused by the rejection of particles during measurement or by insufficient sampling time. The second option would mean that the number of sampled particles is not high enough to provide statistically meaningful results. Cleary et al. (2007) and Jedelský et al. (2004) both sample 20,000 particles per measuring point while Liu samples 50,000 to 100,000 droplets per measuring point (Liu et al., 2010). A definitive answer to this issue is unfortunately unavailable and a more detailed experimental study would be necessary to provide it.

Large-scale Combustion Facility

Wall heat fluxes in combustion chambers, furnaces and boilers are one of the most important parameters in process and power applications. The distribution of local heat flux across heat exchanging areas is of special interest due to material strength and durability implications. It is therefore very important to have experimental data for validation of computational predictions. In this work local wall heat flux data were obtained from a swirling spray combustion experiment in the test facility located at the Institute of Process and Environmental Engineering of Brno University of Technology (Figure 4).

The combustion experiment has been performed in a water-cooled horizontal combustion chamber (1 m internal diameter and 4 m length). The shell of the chamber is divided into seven sections; each of which has a separate water inlet and outlet and is equipped with a water flow meter and temperature sensors, allowing for accurate local heat transfer rate measurement along the flame as described in (Vondál and Hájek, 2009a). The experimental facility is described in detail in (Kermes et al., 2007; Kermes and Bělohradský, 2008). The fuel was atomized using a single nozzle effervescent atomizer described in the previous section. In Figure 5 is a simple sketch of the burner and combustion air supply duct.

In order to reduce liquid fuel consumption (due to limited storage capacity), the combustion chamber was preheated using natural gas. The liquid fuel and air operating parameters and properties are reported in Table 1. Thermal duty in the experiment was set to 928.7 kW; HHV of the liquid fuel was 42.6 MJ/kg. Stabilization of the experiment was established with respect to local wall heat fluxes in all sections of the furnace, which were monitored continuously. After reaching a steady state, the measurement procedure began and data were collected for about 30 minutes.

5.2.3 Modelling

This section outlines the models applied in the computational part of this work. The objective is to evaluate models that are routinely applied in the industrial practice due to their computational manageability. This implies that trade-offs between accuracy and computational demands were

required in the selection of all sub-models (for turbulence, chemistry, radiation, spray formation and secondary breakup).

The modelling work includes two separate simulations. First is a validation of the primary and secondary atomization model in a setup that mimics conditions during the spray measurements. Numerical drops are sampled in 6 areas corresponding to the experimental measurement points and emphasis is placed on the prediction of drop size distributions in those radial locations and their comparison with experimental results. In the second simulation the same spray model is used to compute the reacting flow in a large-scale oil-fired combustion chamber, focusing on wall heat flux predictions.

The computations were performed in Ansys Fluent code (Ansys Fluent, 2009). To track the liquid particles Discrete Phase model (DPM) has been used, which is based on the Euler – Lagrange approach. The particles were tracked in an unsteady fashion. The particle time step size was set to 0.0001 s and Step Length Factor (SLF) to 15. The SLF controls the accuracy of particle trajectory computation and the chosen value is equal to that recommended in (Broukal et al., 2010).

To predict the particle trajectory, one has to integrate the force-balance equation, which can be written (for the *x* direction in Cartesian coordinates) as follows:

$$\frac{du_p}{dt} = F_D\left(u - u_p\right) + \frac{g_x\left(\rho_l - \rho_g\right)}{\rho_l}, \tag{1}$$

where u_p is the particle velocity, u the surrounding air flow velocity, g_x gravity in x direction, ρ_l and ρ_g are the densities of the liquid and gaseous phase. $F_D(u- u_p)$ is the drag force per unit particle mass.

$$F_D = \frac{18\mu_g C_D \,\mathrm{Re}_{rel}}{24\rho_l d^2}, \tag{2}$$

where d is drop diameter, μ_g is the molecular viscosity of the fluid (air), C_D is the drag coefficient (will be defined in the following sections) and Re_{rel} is the relative Reynolds number defined as

$$\mathrm{Re}_{rel} = \frac{\rho d\left|u_p - u\right|}{\mu_g}. \tag{3}$$

In order to take into account the turbulent flow effects on particle motion, the Discrete Random Walk (DRW) model has been applied. Time scale constant in the DRW model was set to 0.15, which is appropriate for the k-ε turbulence model according to (Ansys Fluent, 2009) and references therein. The DRW model simulates interactions of a particle with a succession of discrete stylized fluid phase turbulent eddies.

Spray Model

Ansys Fluent offers a variety of atomizer models and injections. Unfortunately, it does not offer any atomizer model that corresponds to the atomizer used in the experiments; therefore it was decided to use a so-called solid cone injection instead. The spray is axially symmetrical and therefore, to reduce computational costs, only a 30° cylinder section has been meshed using 15,720 hexahedral cells, with approximately 50, 40 and 8 grid nodes in the axial, radial and tangential directions respectively. The dimensions of the cylindrical computational domain were as follows: 800 mm height and 400 mm diameter. The domain was filled with air and the spray originated on the centreline 200 mm from the air inlet base of the cylinder (see Figure 6). The spray was injected from a small circular area of diameter 2.5 mm representing the actual nozzle

orifice. In the position of measuring location 150 mm downstream from the injection a series of concentric annular control surfaces have been set up that enabled the virtual measurement of droplets. A small air co-flow (0.5 m/s) was introduced to improve solution stability, periodic boundary condition was enforced on the sides of the 30° cylinder section in order to obtain meaningful results for the whole cylinder and finally a pressure outlet condition was used for flow exit. A porous zone was introduced at the end of the domain to prevent possible backflow. The backflow would not have any effect on the spray in the analysed locations due to the large size of the domain, but it is undesirable as it causes problems in simulation convergence. Turbulence was modelled using *k-ε* realizable model (Shih et al., 1995) with the original values of model constants, namely $C_{1\varepsilon}$ and C_2 equal to 1.44 and 1.9 respectively, and turbulent Prandtl numbers σ_k and σ_ε equal to 1 and 1.2 respectively.

The spray measurement was performed in vertical downward configuration and the influence of gravity on drop velocity in the sampling location was therefore negligible.

Primary Breakup

As pointed out in (Xiong et al., 2009), in numerous experimental observations of effervescent atomizers it was concluded, that the primary atomization of the liquid undergoes three stages. First, assuming that the two phase flow in the nozzle is annular, an annular sheet forms and breaks up into cylindrical filaments. Second, the filaments break into ligament fragments. Finally, the ligament fragments stabilize to form individual droplets. In this work, a one-dimensional breakup model based on Lund (Lund et al., 1993) and further developed in (Xiong et al., 2009) is used to predict the spray SMD after primary breakup. The model assumes that the annular liquid sheet breaks into several cylindrical filaments with almost the same diameter as the thickness of the annular sheet. The filaments then break into ligament fragments at the wavelength of the most rapidly growing wave and each fragment only forms one drop.

Regrettably, the model does not give any information about the initial droplet velocity nor about the spray angle. These parameters therefore need to be estimated alternatively. The initial particle velocity was approximated as 154 m/s using the formula

$$w_2 = \sqrt{2xp_1v_{g1}\frac{K}{K-1}\left[1-\left(\frac{p_2}{p_1}\right)^{\frac{K-1}{K}}\right]+2(1-x)v_l(p_1-p_2)+w_1^2} \qquad (4)$$

derived by Jedelský and Sláma in Appendix 2 of (Jedelský et al., 2009), where w_2 is the discharge velocity, w_1 is the velocity of the two-phase mixture in the mixing chamber, p_2 is the pressure at the discharge orifice, p_1 is the pressure inside the mixing chamber, v_l is the specific volume of the liquid phase, v_{g1} is the specific volume of the gas phase inside the mixing chamber, x is the gas-liquid ratio and K is the isentropic exponent of the two-phase mixture. The spray angle 18.44° was determined from the experimental measurement (Figure 2). Lund's model is entirely based on first principles and its variations are often adopted due to its simplicity and satisfactory predictions ((Xiong et al., 2009; Schröder et al., 2010). The predicted SMD is later used as the initial diameter of injected droplets during the numerical simulation.

Secondary Breakup

Secondary breakup was taken into account by including the wave model by Reitz (1987). This model was developed for high-Weber-number flows and considers the breakup to be induced by the relative velocity between the gas and liquid phases. The model assumes that the time of breakup and the resulting droplet size are related to the fastest-growing Kelvin-Helmholtz instability. The wavelength and growth rate of this instability are used to predict details of the

newly-formed droplets. This model is also often used in the area of internal combustion engines (Fu-shui et al., 2008). The wave model requires two parameters. The first parameter (C_1) affects the radius of the child droplets and has been set to 0.61 based on the work of Reitz (1987). The breakup time scale is governed by the second parameter (C_2), which can range from 1 to 60 depending on the spray characteristics. The parameter C_2 is a measure of how quickly the parent droplet will lose mass. A larger value means that it takes longer for a droplet to lose a given amount of mass. In their work Liu et al. (1993) recommended 1.73 as a default value. In this work, together with the default value, two other values are tested, namely $C_2 = 2.5$ and $C_2 = 10$.

By using this model it is assumed, that atomization occurs only in the region close to the spray nozzle, since farther downstream the relative velocity decreases due to aerodynamic drag and the model no longer predicts any breakup. In reality, secondary breakup occurs even further downstream from the nozzle. However, for the current case a reasonable assumption is made that the highest rate of drop breakup is concentrated in the region close to the spray nozzle and therefore breakup in low-velocity regions is neglected.

Droplet Collision

The algorithm of O'Rourke (1981) was used to determine the outcome of drop collisions. Rather than calculating exact trajectories to see if parcel paths intersect, O'Rourke's method is a stochastic estimate of collisions. Two particles can collide only if they are in the same computational cell. Once it is decided that two parcels of droplets collide, the algorithm further determines the type of collision. Only coalescence and bouncing outcomes are considered. The probability of each outcome is calculated from the collisional Weber number (We_c) and a fit to experimental observations. Here,

$$We_c = \frac{\rho U_{rel}^2 D}{\sigma}, \tag{5}$$

where U_{rel} is the relative velocity between two droplets, D is the arithmetic mean diameter of the two drops, ρ is the liquid density and σ the surface tension.

The O'Rourke algorithm does not take into account the shattering outcome of the collision, which occurs at high Weber numbers. This drawback does not necessarily need to be significant, as the Weber number is expected to decrease rapidly (Qian et al., 2010). However, this can cause absence of small droplets in the region close to the spray nozzle.

Droplet Drag Model

Accurate determination of droplet drag coefficients is crucial for accurate spray modelling. Ansys Fluent provides a method that determines the droplet drag coefficient dynamically, accounting for variations in the droplet shape. The shape of drops is often assumed to be spherical, but in the case of high Weber numbers, this assumption can distort the final results. The dynamic drag model accounts for the effects of droplet distortion, linearly varying the drag between that of a sphere and a value of 1.54 corresponding to a disk. The drag coefficient is given by

$$C_D = C_{D,sph}\left(1 + 2.632y\right), \tag{6}$$

where $C_{D,sph}$ is the drag coefficient of a sphere and y is the distortion, as determined by the solution of

$$\frac{d^2 y}{dt^2} = \frac{C_F \rho_g u^2}{C_b \rho_l r^2} - \frac{C_k \sigma}{\rho_l r^3} y - \frac{C_d \mu_l}{\rho_l r^2} \frac{dy}{dt}, \tag{7}$$

where t is time, r the undisturbed drop radius, μ_l the drop viscosity and C_F, C_k, C_b, C_d are dimensionless constants equal to 1/3, 8, 0.5 and 5, respectively, as determined by O'Rourke and Amsden (1987).

Combustion Model

The swirling combustion simulation was performed using commercial CFD code Ansys Fluent as well. The main goal of these simulations was to predict heat fluxes absorbed by the cylindrical water-cooled combustion chamber walls. For the purposes of numerical analysis a mesh was constructed in the software Gambit (Figure 7). The total number of computational cells (97 % of which are hexahedral) was nearly 1,200,000, with approximately 200, 65 and 135 grid nodes in the axial, radial and tangential directions respectively. Four boundary conditions were applied – mass flow inlet (for combustion air, see Table 1), pressure outlet, prescribed temperature on the water-cooled walls (80°C (Vondál and Hájek, 2009b)) and adiabatic condition for the remaining walls.

The flow field was obtained by solving the unsteady Reynolds-averaged Navier-Stokes equations together with turbulent mixing controlled eddy breakup model (Magnussen and Hjertager, 1977) to account for turbulence chemistry interactions. Turbulence was modelled using the k-ε realizable model used for the isothermal spray simulation. In combustion chambers, the main mechanism of heat transfer is radiation. As shown by Baek et al. (2002), the discrete ordinates model offers good results and reasonable computational demand. The absorption coefficients were obtained using the domain-based approach of the weighted sum of grey gases model, which reportedly gives good prediction for heat transfer according to (Ströhle, 2004). The fuel droplets were modelled as discrete Lagrangian entities – particles. The atomized fuel was modelled using the models specified in section 5.2.3. The operating conditions were identical to the combustion experiment (Table 1) and gravity was taken into account, since the combustion chamber is in horizontal position.

Evaporation

As the droplets are heated up by the reaction heat, mass transfer occurs between the discrete Lagrangian entities (fuel droplets) and the continuous gas phase. To take into account such interaction between phases, mass source terms are introduced to the gas phase in appropriate cells, whereas the mass and temperature of droplets are adjusted simultaneously. The evaporative mass fluxes are governed by gradient diffusion, with the flux of droplet vapour into the gas phase related to the difference in vapour concentration at the droplet surface and the bulk gas. No flow inside the droplet is considered and droplet properties such as temperature and density are considered to be uniform over the droplet volume.

5.2.4 Results and Discussion

In the following subsections results will be presented and compared with experimental data. Shortcomings will be mentioned and their sources will be discussed. First, the results of the isothermal effervescent spray simulation will be presented and discussed, followed by the combustion simulation of large-scale combustor.

Spray Simulations

The initialization, motion and breakup of droplets and their interaction with the gaseous phase were governed by sub-models presented in section 5.2.3. For this isothermal non-reactive simulation the sub-model for droplet evaporation was disabled. The initial droplet diameter predicted by the primary atomization model was 225.2 μm.

Data on the resulting numerical spray were collected in a similar manner as in the experiment. The only difference was that data were collected from concentric annular areas and not points as in the physical experiment. The raw data were imported into Matlab environment and further analysed and visualized in the same way as the experimental data. The objective was to investigate predictive capabilities of the selected spray model in terms of radial and overall drop size distributions.

Form Figure 8 it is apparent that the model in all three cases (as defined in section 5.2.3) fails to predict drop diameters smaller than approximately 31 μm and on the other hand the maximal predicted diameter is greater (245 μm) than the maximal experimentally measured diameter (194 μm). This may be caused by the wave model, which does not predict any breakup at low Weber numbers. Additionally, drop coalescence is not diminished in these conditions, thus increasing the drop diameter in spray regions with low Weber number. Also, for all the three cases the maximal diameter decreases while moving radially to the spray peripheral region, which is contradictory to the experimental results.

The overall SMD obtained from simulations (67.6 μm) under predicts the experimental value (83.2 μm). This mismatch is opposite than the one reported in (Schröder et al., 2010), where the simulated SMD over predicted experimental SMD.

The radial evolution of predicted and measured SMD is shown in Figure 9. The experimental measurement shows that SMD is smallest at the spray core and then increases when moving radially to the edge of the spray. The predicted SMD evolution is however different. At the spray core the biggest SMD value is predicted and SMD further decreases. After the third measurement point it remains almost constant. This discrepancy clearly shows the poor prediction of radial spray drop-size distribution regardless of the C_2 parameter value.

The comparison of radial evolution of the number-based drop-size distributions at the sampling locations 150 mm downstream from the atomizer (same as in the experiment) are shown in Figure 10. In the first three measuring points a shift towards the right hand side of the predicted distribution is observed for all three C_2 parameters. In addition, bimodal behaviour is predicted in all measurement points for the case C_2 = 1.73 and in the last two measurement points for the case C_2 = 10. The predicted drop sizes in the peripheral regions are also smaller than the experimentally measured values.

In Figure 11 are presented volume-based drop-size distributions corresponding to appropriate measuring points at the same locations as in the previous paragraph. Except for the measurement point on the spray axis (r=0mm), all three cases give very similar results and are relatively closer to the experimentally measured distribution than in the case of number-based distributions. In all measurement points the case C_2 = 10 has the “heaviest” tail, meaning it predicts the largest droplets. This is expected, since as mentioned in section 5.2.3 the higher the value of C_2, the slower the atomization process is.

Figure 12 reports the comparison of overall drop-size distributions based on number and volume. Similarly as in Figure 10, bimodality is predicted in the case C_2 = 1.73 and also the “heavy” tail in the case C_2 = 10 is again apparent. The deficiency of numerical results is marked by the absence of small numerical drops.

The phenomenon of bimodality manifested itself in both experimental as well as in the simulated drop size distributions (mainly in the case C2 = 1.73). Such behaviour is not uncommon in spray applications and it would be a significant aid to be able to predict it. Bimodality, in some cases even multimodality, also raises the question about legitimacy of using a single representative diameters (e.g. SMD) to represent the drop size distributions.

For a really detailed analysis of the quality of the secondary breakup model, more experimental data at different axial locations would be desirable, but are unfortunately not available.

Combustion Simulation

This section presents a comparison between experimentally obtained local heat transfer rates and numerical prediction. Although none of the three cases discussed in the previous sections can be claimed to be superior, in the combustion simulation the case C_2 = 1.73 has been used. The reason is that it captured the bimodality phenomena better with respect to the other cases. The numerical results are also compared with the results of authors' previously proposed model (Broukal and Hájek, 2010), where no breakup was taken into account and the particle diameters were initialized with a Rosin-Rammler drop size distribution, which was based on experimental results. The previous spray model was therefore based a priory on experimental data, which is not the case in this study. Despite the older results do not present a better alternative, they have been compared with the current simulation in order to point out some interesting consequences.

Numerous experimental measurements have been performed in the last few years for the case of natural gas combustion in the same testing facility (Vondál and Hájek, 2009a; Vondál et al., 2010). Repeatability of the applied heat flux measurements and accuracy of the method that measures heat extracted in individual sections of the furnace has been addressed in (Vondál et al., 2010). Overall, the method provides highly reliable and accurate data, unlike point measurements using heat flux probes as discussed in the Introduction.

In Figure 13 it can be seen that the wall heat fluxes obtained from simulations do not agree well with the experimental measurements. The simulation peak occurs between the 5th and 6th section while the experiment suggests the peak is around the 4th section. The simulation also under predicts the maximal wall heat flux. One of the reasons of these discrepancies is clearly the representation of the effervescent spray, whose drawbacks were discussed in the previous section. The figure suggests that the smallest drops might be missing and therefore it takes longer for the spray to evaporate and subsequently to burn, thus moving the flame farther downstream.

It is interesting that the predicted wall heat fluxes are quite close to the results obtained using author’s previous model (Broukal et al., 2010) despite significant differences in the spray representation. This may be caused by the fact that both spray representations suffer from significant deficiencies. At this point it is difficult to tell the reason of this occurrence, since also other phenomena involved in the simulation (turbulence, radiation, chemistry) present a great deal of uncertainty. Further examination is needed in order to determine the nature of this behaviour. Related work focusing on the case of natural gas combustion as documented e.g.in (Vondál and Hájek, 2009a) shows these effects of other modelling options. Swirling combustion applications clearly present a very complex task for numerical modelling.

Another possible cause could be the simplification of the effervescent atomizer model. The simulations did not take into account the atomizing air exiting the atomizer nozzle together with the liquid drops. Although the flow rate of the atomizing air is very small compared to the combustion air (0.5 %), it might have important effects on the mixing process of the evaporated fuel with air. This issue is closely related to turbulence modelling, which has major effects on the predicted wall heat fluxes as observed in the investigations concerning natural gas combustion (Vondál and Hájek, 2009a; Vondál and Hájek, 2009b).

5.2.5 Conclusions

The present work provides a detailed analysis and an unsuccessful validation attempt of a modern industrially relevant (i.e. computationally manageable) effervescent spray modelling approach. The investigated application is a 1 MW swirling flame of light fuel oil in a large-scale water-cooled laboratory furnace. Data for validation include spray characteristics in six locations along the spray radius at 150 mm axial distance from the nozzle and distribution of local heat flux along furnace walls. The following conclusions were drawn:

- The measured number-based drop size distribution of effervescent spray is unimodal around the axis and bimodal in the external part of the spray. Volume-based distributions are much less smooth and rather than bimodality they display irregularities among the larger drops. The volume-based distributions are clearly much more sensitive to the number of measured drops.
- The measurements prove that in effervescent sprays it is insufficient to measure a single total drop size distribution for a given axial position, as the distributions change very significantly in the radial direction. Single SMD value that is often provided in the literature is even less representative.
- Comparisons between predicted and experimentally measured radial drop size distributions show that the spray model implemented in this work based on Lund's primary breakup model (Lund et al., 1993) and secondary breakup model by Reitz (1987) is insufficient to describe the formation of effervescent spray.
- The computational model does not predict the formation of small drops below 30 μm, which is in contrast with drops down to 3 μm observed in the measurements.
- Comparison of the predicted and measured heat loads on furnace walls shows that the real flame is significantly shorter. As predictions for natural gas combustion in the same furnace with a similar gas burner do not display this discrepancy (Vondál and Hájek, 2009a), it may be attributed to the deficiencies of the spray model, mainly to the missing small drops below 30 μm.
- Drop dynamics at the atomizer exit seems to be an important factor that should be reflected by the primary breakup model. Drop size, velocity, and mass flow rate should be functions of the spray angle.
- The C_2 parameter value in the secondary breakup sub-model (Reitz, 1987) is shown to have only little effect on the drop size distributions studied in this case.
- The proposed method of spray model validation by analysing radial (i.e. depending on spray angle) drop size distributions provides valuable insights and indeed seems to be necessary for effervescent sprays.

Acknowledgement

The authors gratefully acknowledge financial support of the Ministry of Education, Youth and Sports of the Czech Republic within the framework of project No. 2B08048 "Waste as raw material and energy source" and within the framework of Operational Programme "Research and Development for Innovations" – "NETME Centre – New Technologies for Mechanical Engineering".

References

Aliseda, A., Hopfinger, E.J., Lasheras, J.C., Kremer, D.M., Berchielli, A., Connolly, E.K., 2008. Atomization of viscous and non-newtonian liquids by a coaxial, high-speed gas jet. Experiments and droplet size modeling. International Journal of Multiphase Flow 34, 161–175. doi:10.1016/j.ijmultiphaseflow.2007.09.003

Ansys Fluent, 2009. Ansys Fluent 12.1 Documentation.

Apte, S.V., Gorokhovski, M., Moin, P., 2003. LES of atomizing spray with stochastic modeling of secondary breakup. International Journal of Multiphase Flow 29, 1503–1522. doi:10.1016/S0301-9322(03)00111-3

Babinsky, E., Sojka, P.E., 2002. Modeling drop size distributions. Progress in Energy and Combustion Science 28, 303–329. doi:10.1016/S0360-1285(02)00004-7

Baek, S.W., Kim, H.S., Yu, M.J., Kang, S.J., Kim, M.Y., 2002. Application of the extended weighted sum of gray gases model to light fuel oil spray combustion. Combustion Science and Technology 174, 37–70.

Broukal, J., Hájek, J., 2010. Wall heat fluxes in swirling combustion of extra-light fuel-oil in large-scale test combustor: experiment and modeling using eddy dissipation model. CET 21, 1111–1116. doi:10.3303/CET1021186

Broukal, J., Hájek, J., Jedelský, J., 2010. Effervescent atomization of extra-light fuel-oil: Experiment and statistical evaluation of spray characteristics. Presented at the ILASS-Europe 2010, Brno, Czech Republic, pp. 1–10.

Chin, L.P., Switzer, G., Tan Kin, R.S., Jackson, T., Stutrud, J., 1995. BI-Modal Size Distributions Predicted by Maximum Entropy are Compared with Experiments in Sprays. Combustion Science and Technology 109, 35–52. doi:10.1080/00102209508951894

Cleary, V., Bowen, P., Witlox, H., 2007. Flashing liquid jets and two-phase droplet dispersion: I. Experiments for derivation of droplet atomisation correlations. Journal of Hazardous Materials 142, 786–796. doi:10.1016/j.jhazmat.2006.06.125

Fu-shui, L., Lei, Z., Bai-gang Sun, Zhi-jie, L., Schock, H.J., 2008. Validation and modification of WAVE spray model for diesel combustion simulation. Fuel 87, 3420–3427. doi:10.1016/j.fuel.2008.05.001

Hayes, R.R., Brewster, S., Webb, B.W., McQuay, M.Q., Huber, A.M., 2001. Crown incident radiant heat flux measurements in an industrial, regenerative, gas-fired, flat-glass furnace. Experimental Thermal and Fluid Science 24, 35–46. doi:10.1016/S0894-1777(00)00055-8

Jedelský, J., Jícha, M., Otáhal, J., Katolický, J., Landsmann, M., 2007. Velocity field in spray of twin-fluid atomizers. Presented at the 21st Sympozium on Anemometry, Prague, Czech Republic, pp. 67–74.

Jedelský, J., Jícha, M., Sláma, J., 2004. Characteristics And Behaviour Of Multi-Hole Effervescent Atomizers. Presented at the 19th ILASS Europe, Nottingham, UK, pp. 521–526.

Jedelský, J., Jícha, M., Sláma, J., Otáhal, J., 2009. Development of an Effervescent Atomizer for Industrial Burners. Energy & Fuels 23, 6121–6130. doi: 10.1021/ef900670g

Jiang, X., Siamas, G.A., Jagus, K., Karayiannis, T.G., 2010. Physical modelling and advanced simulations of gas-liquid two-phase jet flows in atomization and sprays. Progress in Energy and Combustion Science 36, 131–167. doi:10.1016/j.pecs.2009.09.002

Kermes, V., Bělohradský, P., 2008. Testing of gas and liquid fuel burners for power and process industries. Energy 33, 1551–1561.

Kermes, V., Skryja, P., Stehlík, P., 2007. Up to date experimental facility for testing low-NOx burners. Chemical Engineering Transaction 12, 549–554.

Lefebvre, A.H., Wang, X.F., Martin, C.A., 1988. Spray Characteristics of Aerated-Liquid Pressure Atomizers. Journal of Propulsion and Power 4, 293–298.

Liu, A.B., Mather, D., Reitz, R.D., 1993. Modeling the Effects of Drop Drag and Breakup on Fuel Sprays (Technical paper No. A056362). University of Wisconsin-Madison, Engine Research Center.

Liu, M., Duan, Y., Zhang, T., 2010. Evaluation of effervescent atomizer internal design on the spray unsteadiness using a phase/Doppler particle analyzer. Experimental Thermal and Fluid Science 34, 657–665. doi:10.1016/j.expthermflusci.2009.12.007

Lund, M.T., Sojka, P.E., Lefebvre, A.H., 1993. Effervescent atomization at low mass flow rates. Part I: The influence of surface tension. Atomization and Sprays 3, 77–89.

Magnussen, B.F., Hjertager, B.H., 1977. On mathematical modeling of turbulent combustion with special emphasis on soot formation and combustion. Symposium (International) on Combustion 16, 719–729. doi:10.1016/S0082-0784(77)80366-4

Nieckele, A.O., Naccache, M.F., Gomes, M.S.P., 2011. Combustion performance of an aluminum melting furnace operating with natural gas and liquid fuel. Applied Thermal Engineering 31, 841–851. doi:10.1016/j.applthermaleng.2010.11.003

O'Rourke, P.J., 1981. Collective Drop Effects on Vaporizing Liquid Sprays (Ph.D. Thesis). Los Alamos National Lab., NM (USA).

O'Rourke, P.J., Amsden, A.A., 1987. The TAB method for numerical calculation of spray droplet breakup. Los Alamos National Lab., NM (USA), USA.

Park, S.H., Kim, H.J., Suh, H.K., Lee, C.S., 2009. Experimental and numerical analysis of spray-atomization characteristics of biodiesel fuel in various fuel and ambient temperatures conditions. International Journal of Heat and Fluid Flow 30, 960–970. doi:10.1016/j.ijheatfluidflow.2009.04.003

Pougatch, K., Salcudean, M., Chan, E., Knapper, B., 2009. A two-fluid model of gas-assisted atomization including flow through the nozzle, phase inversion, and spray dispersion. International Journal of Multiphase Flow 35, 661–675. doi:10.1016/j.ijmultiphaseflow.2009.03.001

Qian, L., Lin, J., Xiong, H., 2010. A Fitting Formula for Predicting Droplet Mean Diameter for Various Liquid in Effervescent Atomization Spray. Journal of Thermal Spray Technology 19, 586–601. doi:10.1007/s11666-009-9457-4

Reitz, R.D., 1987. Mechanisms of Atomization Processes in High-Pressure Vaporizing Sprays. Atomization and Spray Technology 309–337.

Riber, E., Moureau, V., García, M., Poinsot, T., Simonin, O., 2009. Evaluation of numerical strategies for large eddy simulation of particulate two-phase recirculating flows. Journal of Computational Physics 228, 539–564. doi:10.1016/j.jcp.2008.10.001

Sadiki, A., Maltsev, A., Wegner, B., Flemming, F., Kempf, A., Janicka, J., 2006. Unsteady methods (URANS and LES) for simulation of combustion systems. International Journal of Thermal Sciences 45, 760–773. doi:10.1016/j.ijthermalsci.2005.11.001

Schröder, J., Schlender, M., Sojka, P.E., Gaukel, V., Schuchmann, H.P., 2010. Modeling of drop sizes from effervescent atomization of gelatinized starch suspensions. Presented at the ILASS-Europe 2010, Brno, Czech Republic.

Senecal, P.K., Schmidt, D.P., Nouar, I., Rutland, C.J., Reitz, R.D., Corradini, M.L., 1999. Modeling high-speed viscous liquid sheet atomization. International Journal of Multiphase Flow 25, 1073–1097. doi:10.1016/S0301-9322(99)00057-9

Shih, T.-H., Liou, W.W., Shabbir, A., Yang, Z., Zhu, J., 1995. A new k-ε eddy viscosity model for high reynolds number turbulent flows. Computers & Fluids 24, 227–238. doi:10.1016/0045-7930(94)00032-T

Shinjo, J., Umemura, A., 2011. Detailed simulation of primary atomization mechanisms in Diesel jet sprays (isolated identification of liquid jet tip effects). Proceedings of the Combustion Institute 33, 2089–2097. doi:10.1016/j.proci.2010.07.006

Ströhle, J., 2004. Spectral Modelling of Radiative Heat Transfer in Industrial Furnaces. Shaker Verlag GmbH, Germany, Aachen, Germany.

Tanner, F.X., 2004. Development and validation of a cascade atomization and drop breakup model for high-velocity dense sprays. Atomization and Sprays 14, 211–242.

Taylor, J.I., 1963. The Shape and Acceleration of a Drop in a High Speed Air Stream. Technical report, In the Scientific Papers of G. I. Taylor, ed., G. K. Batchelor, University Press, Cambridge.

Tembely, M., Lecot, C., Soucemarianadin, A., 2011. Prediction and evolution of drop-size distribution for a new ultrasonic atomizer. Applied Thermal Engineering 31, 656–667. doi:10.1016/j.applthermaleng.2010.09.027

Valero, A., Cortés, C., 1996. Ash fouling in coal-fired utility boilers. Monitoring and optimization of on-load cleaning. Progress in Energy and Combustion Science 22, 189–200. doi:10.1016/0360-1285(96)00004-4

Vondál, J., Hájek, J., 2009a. Experimental and numerical analysis of wall heat transfer in non-premixed gas combustor. Chemical Engineering Transactions 18, 587–592.

Vondál, J., Hájek, J., 2009b. Boundary condition evaluation and stability issues in swirling flame gas combustion. Presented at the 1st International Conference on Computational Methods for Thermal Problems, Napoli, Italy, pp. 314–317.

Vondál, J., Hájek, J., Kermes, V., 2010. Local wall heat fluxes in swirling non-premixed natural gas flames in large-scale combustor: Data for validation of combustion codes. Chemical Engineering Transactions 21, 1123–1128. doi:10.3303/CET1021188

Vuorinen, V.A., Hillamo, H., Kaario, O., Nuutinen, M., Larmi, M., Fuchs, L., 2010. Effect of Droplet Size and Atomization on Spray Formation: A Priori Study Using Large-Eddy Simulation. Flow Turbulence Combust. doi:10.1007/s10494-010-9266-3

Weber, C., 1931. Disintegration of Liquid Jets. Z. Angew Math. Mech. 11, 136–159.

Xiong, H.-B., Lin, J.-Z., Zhu, Z.-F., 2009. Three-dimensional simulation of effervescent atomization spray. Atomization and Sprays 19, 75–90.

Yan, Y., Zhao, J., Zhang, J., Liu, Y., 2008. Large-eddy simulation of two-phase spray combustion for gas turbine combustors. Applied Thermal Engineering 28, 1365–1374. doi:10.1016/j.applthermaleng.2007.10.008

Figures

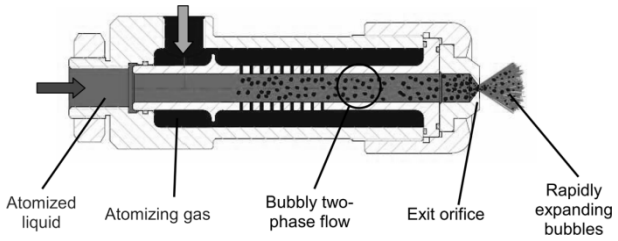

Figure 1. Schematics of the effervescent atomization process, courtesy of (Jedelský et al, 2007)

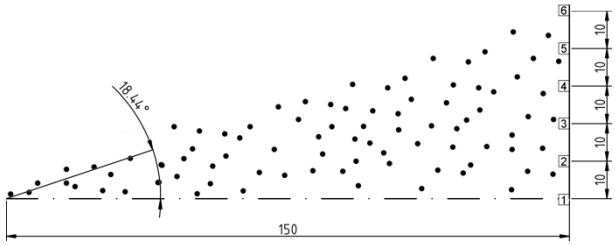

Figure 2. Schematics of the spray measurement (dimensions are expressed in mm)

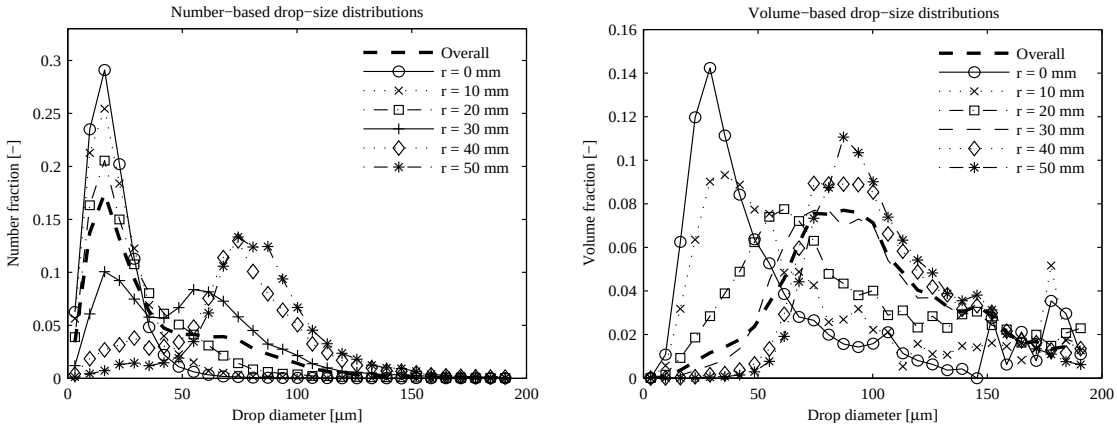

Figure 3. Drop-size distributions based on number and volume at various measurement points and overall distributions; *r* represents the radial distance of the measurement point form the spray centreline at 150 mm downstream from the spray nozzle.

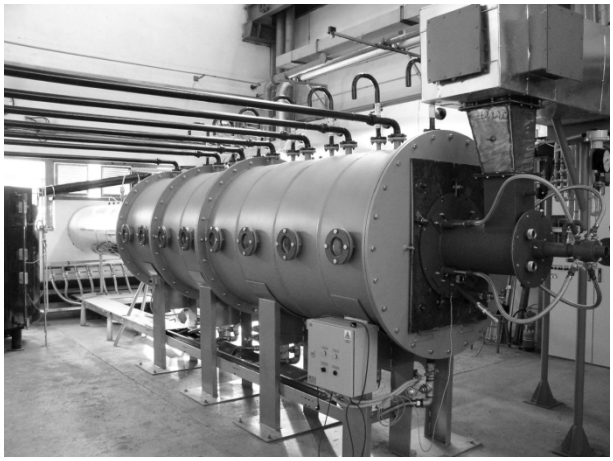

Figure 4. Combustion test facility

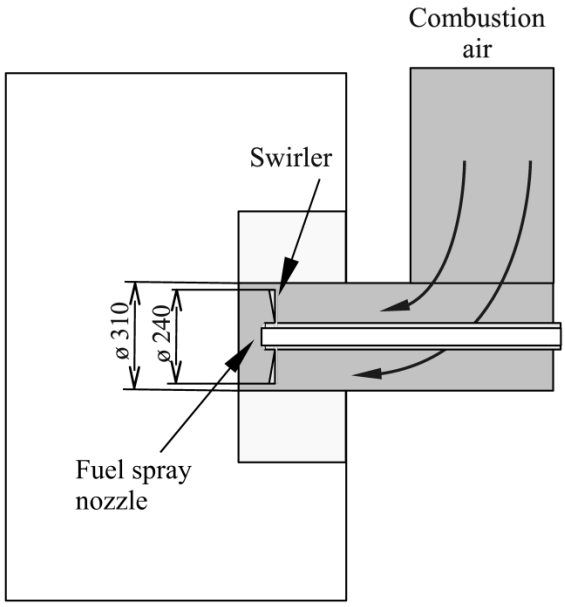

Figure 5. Cross-section of the burner (dimensions are expressed in mm)

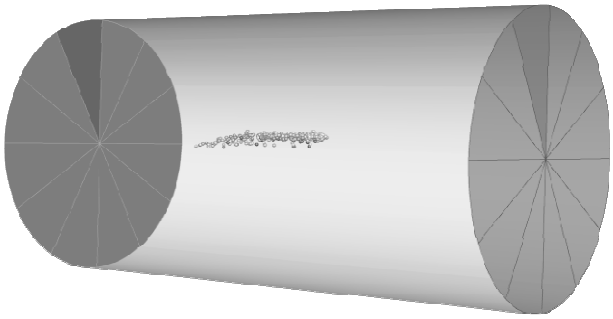

Figure 6. Geometry of the cylindrical computational domain

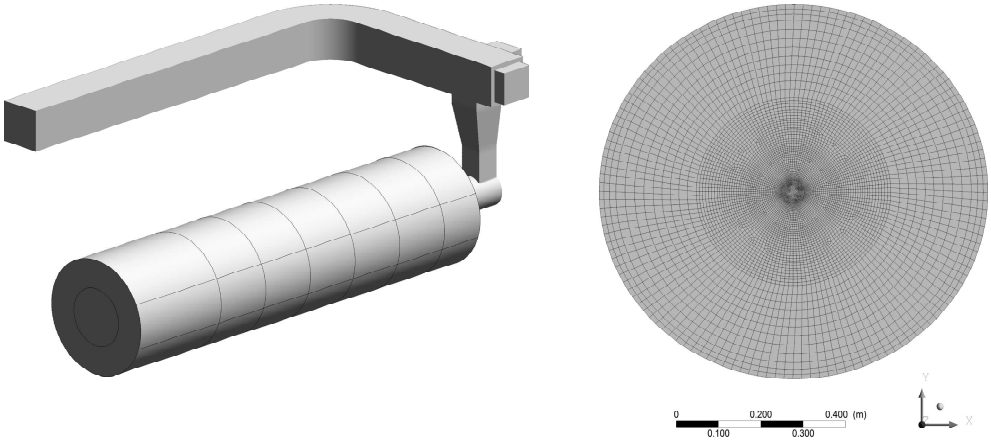

Figure 7. Geometry of the combustion chamber with air duct and a detail of the mesh in axial cut

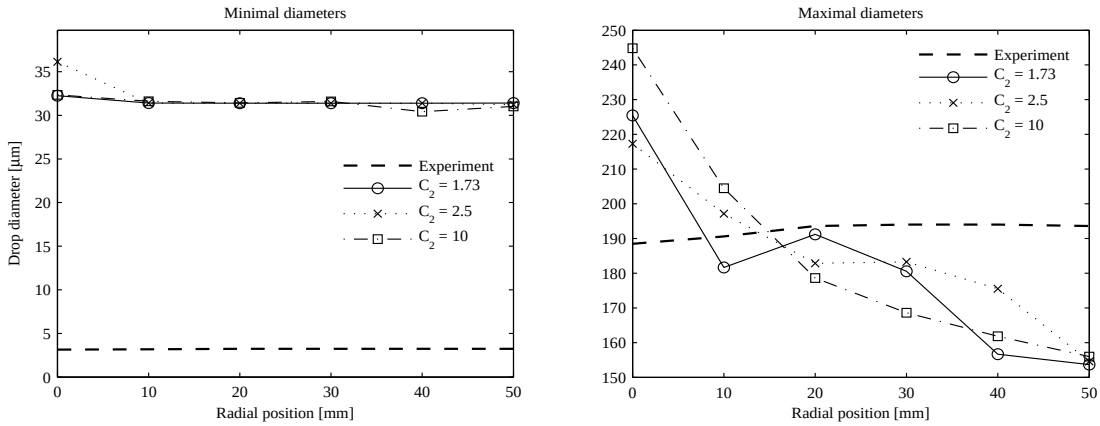

Figure 8. Minimal and maximal drop diameters (at axial distance 150 mm)

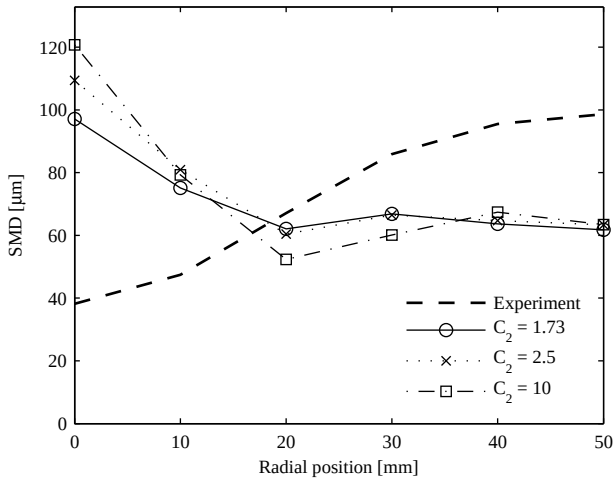

Figure 9. Comparison of measured and computed radial SMD evolution (at axial distance 150 mm)

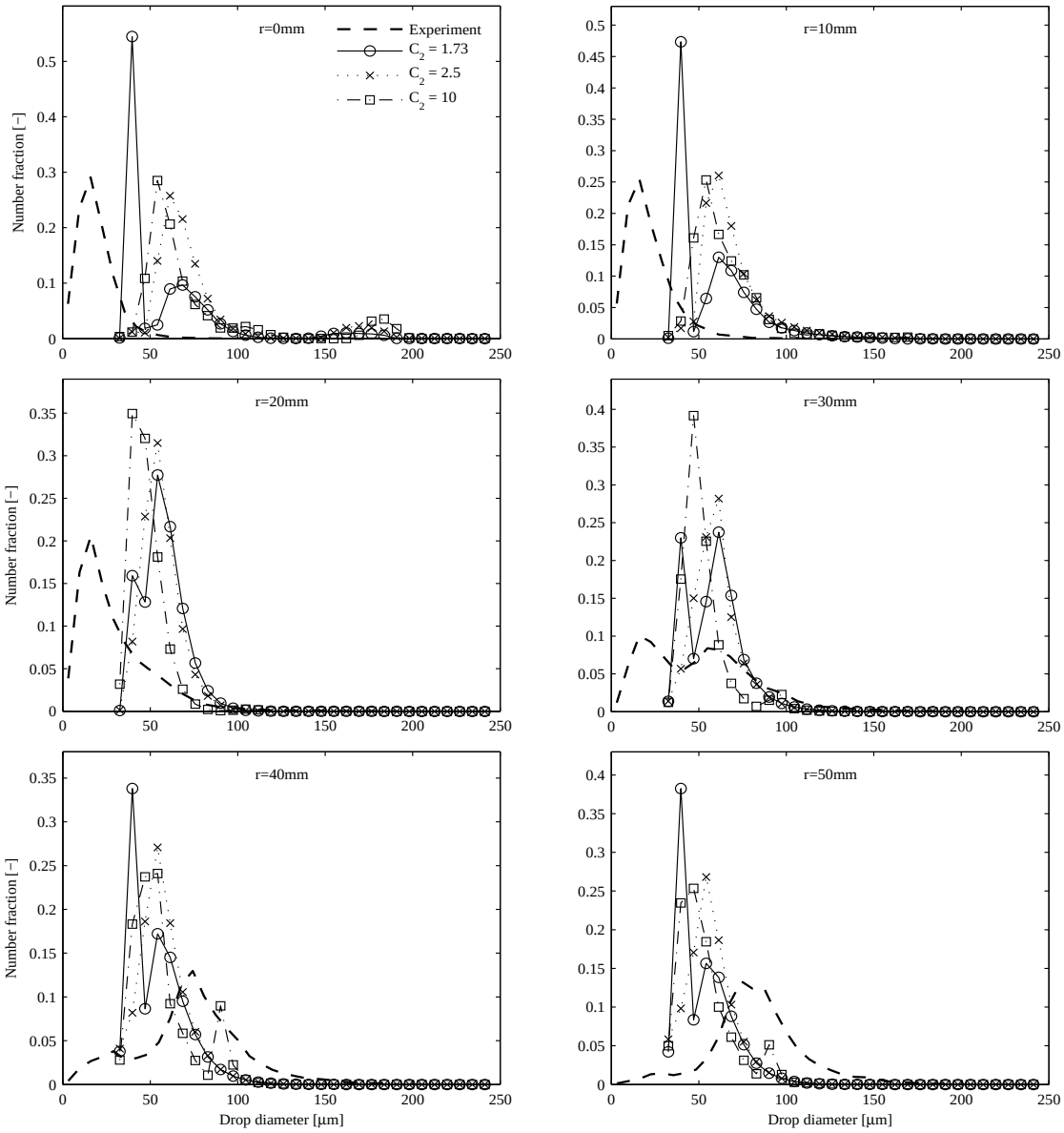

Figure 10. Plots of number-based drop-size distributions at various radial locations *r* (at axial distance 150 mm)

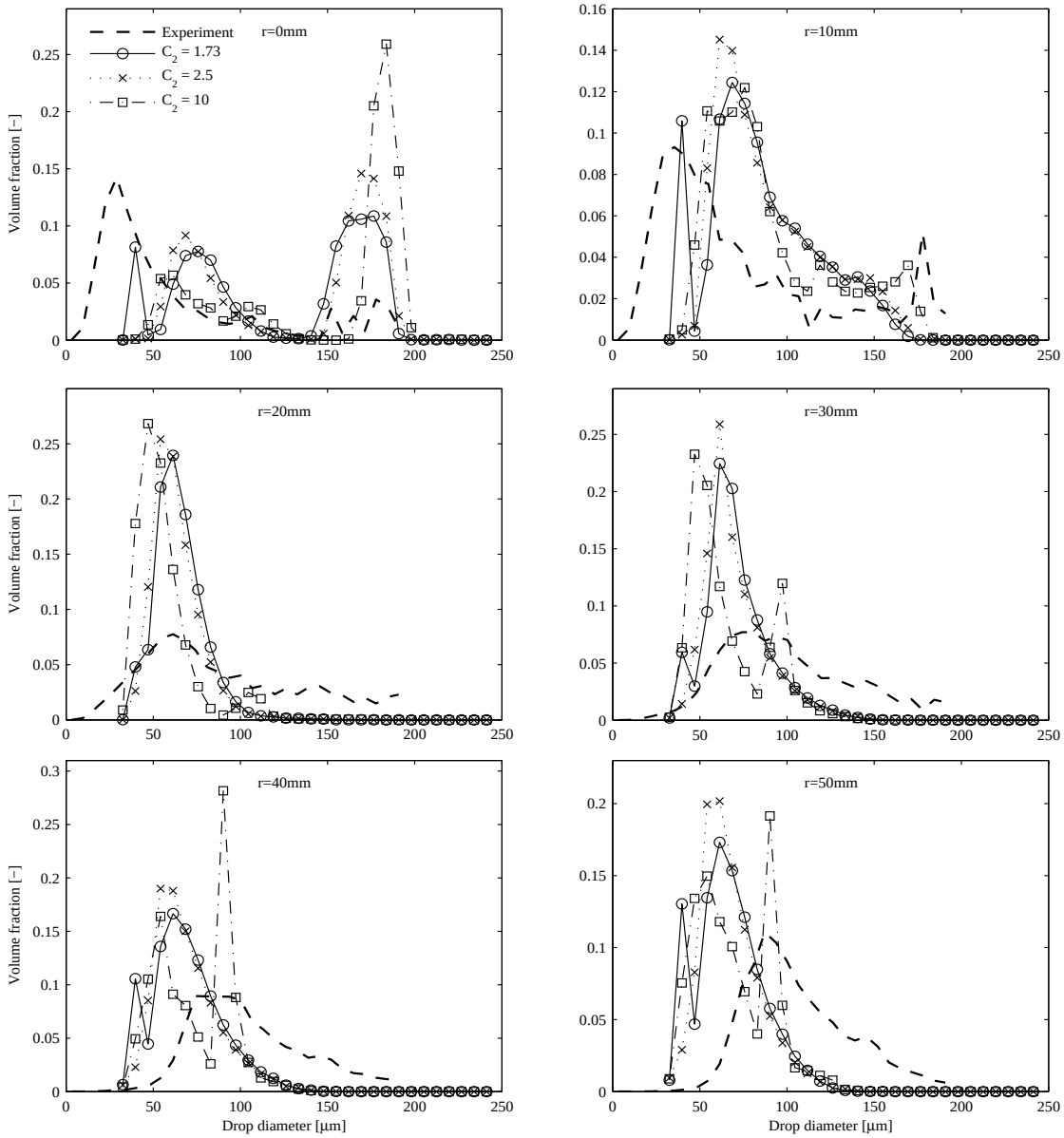

Figure 11. Plots of volume-based drop-size distributions at various radial locations *r* (at axial distance 150 mm)

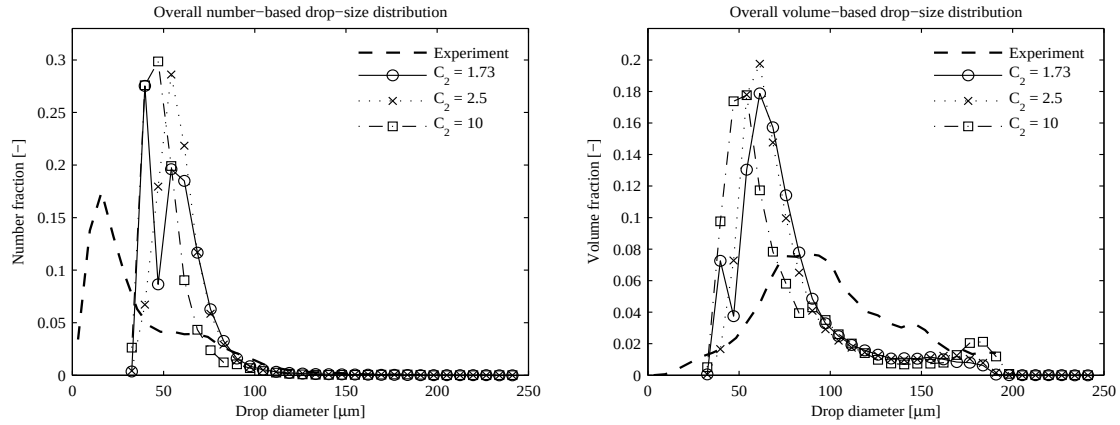

Figure 12. Overall drop-size distributions (at axial distance 150 mm)

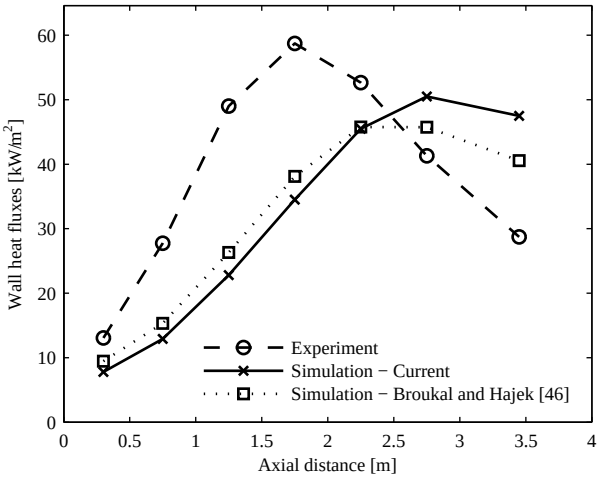

Figure 13. Comparison of measured and computed wall heat fluxes

Tables

Table 1. Experiment parameters

Fuel mass flow	78.48 [kg/h]
Atomizing air mass flow	7.85 [kg/h]
Gas-Liquid ratio (GLR)	10% [–]
Combustion air mass flow	1280 [m3/h]
Global air equivalence ratio	1.46 [–]
Fuel density	820.7 [kg/m3]
Combustion air temperature	4 [°C]
Fuel temperature	32 [°C]
Atomizing air temperature	20 [°C]

5.3 Experimental and Numerical Investigation of Wall Heat Fluxes in a Gas Fired Furnace: Practicable Models for Swirling Non-premixed Combustion

Abstract

Natural gas combustion and combustion of other light hydrocarbon gases is still one of the primary means of gaining heat. This applies especially for process and energy industries, where gas combustion is used as heat source for various processes. It is therefore of crucial importance, that the combustion chamber is designed properly in order to optimize the heat transfer process. Recently, CFD (Computational Fluid Dynamics) tools have proved themselves as a great potential aid for designers and engineers. These tools allow predicting of various phenomena of practical interest.

The main focus of this study is to validate a numerical model for swirling combustion in terms of wall heat fluxes using reliable measured data. The first part of this study deals with the experimental measurement of wall heat fluxes. Two burner duties are taken into account: 745 kW and 1120 kW. The second part consists in a numerical analysis of the problem. The simulations are performed using unsteady RANS with four different turbulence models coupled with chemistry and radiation models. Boundary conditions are set identically to the experiment.

Two simulations are performed (one for each burner duty) and fine-tuned. The measured and simulated wall heat flux profiles are finally compared and shortcomings if the numerical model are reported and discussed.

5.3.1 Introduction

The study of flame structure is the subject of long-lasting interest within the combustion modelling community. Detailed in-flame measurements of temperature, velocity and species concentrations have served as validation of many of the existing combustion models. Unlike the in-flame properties, wall heat fluxes have been used for model validation only rarely. Heat flux measurements reported in the literature are either spot measurements or global heat transfer rates. Spot measurements however mostly provide just the thermal irradiation flux, not the actual radiative or total heat transfer rate as demonstrated in some studies of industrial furnaces and boilers (Hayes et al., 2001; Ströhle, 2004). Likewise, global heat transfer rates calculated from the total hot water (steam) production are insufficient for the validation of detailed predictions.

In contrast to that, the interest of engineering community focuses primarily on local heat fluxes and pollutant emissions. Emissions are studied namely to ensure compliance with legislative regulations, while heat fluxes are required to check proper furnace design and to ensure safe operation and durability. It is thus apparent that the correct prediction of local heat fluxes on heat transfer surfaces is one of the most important aspects of practical combustion simulations that should receive adequate attention.

Swirl-stabilised non-premixed flames are frequently used in industrial burners, but at the same time they present a huge challenge, since numerical prediction of swirling flows is very difficult. Only with the advances in large eddy simulations (LES), successful predictions of in-flame properties were reported (Fureby et al., 2007; James et al., 2007; Sadiki et al., 2006). However, the LES approach is still too computationally expensive for the simulation of large-scale fired heaters due to their huge dimensions (in the order of 10 m) and the need to resolve fine features like gas nozzles with diameters on the order of 1 mm. The only viable alternative for

practical predictions in the present as well as for a number of years to come thus consists of models based on first or second-order turbulence closures.

5.3.2 Experimental Measurement

Experimental Facility

The wall heat fluxes measurements were performed in the experimental facility located at Brno University of Technology. The chamber has a form of a water-cooled horizontal combustion chamber with 1 m internal diameter and 4 m length (see Figure 1). The shell of the chamber is divided into seven sections; each of which has a separate water inlet and outlet and is equipped with a water flow meter and temperature sensors, allowing for accurate heat transfer rate measurement. The experimental facility is described in (Kermes and Bělohradský, 2008; Kermes et al., 2007) and details about the measurement precision can be found in (Vondál et al., 2010). A low-NOx staged-gas burner with axial swirl generator was employed and fired by natural gas. Flame ignition and stabilization is performed by a small (25 kW) premixed natural-draft pilot burner. Its thermal duty was included in the total thermal duty.

This facility has been used for several measurements. Although with different scope (Bělohradský et al., 2008; Kermes and Bělohradský, 2008; Kermes et al., 2008).

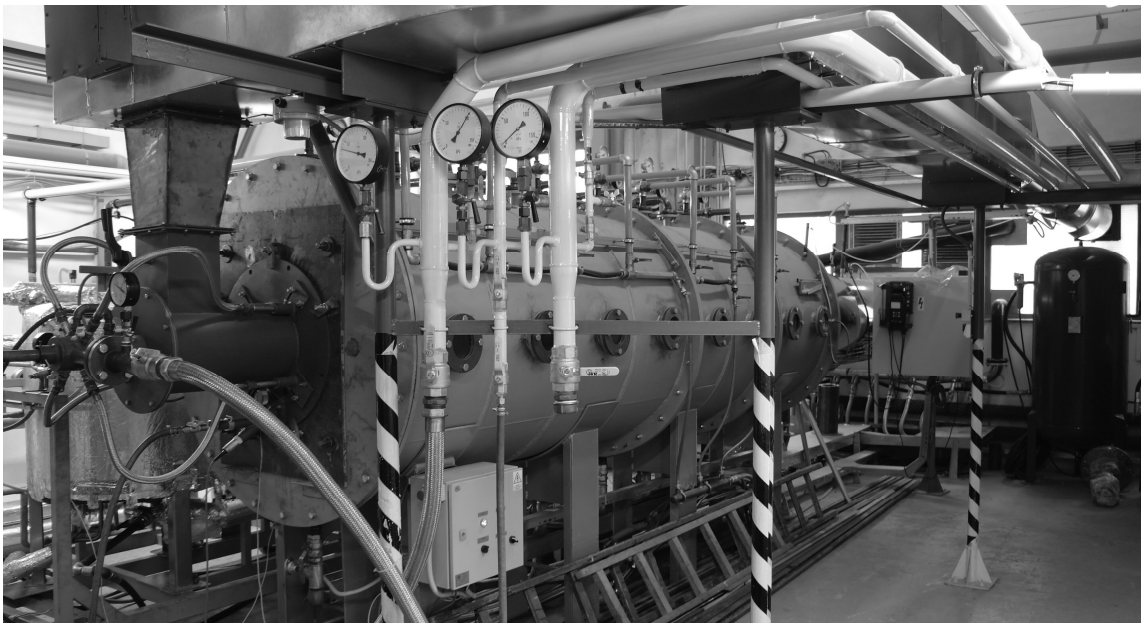

Figure 1. Testing facility

Table 1. Operating conditions

		Case 1	Case 2
Thermal duty	[kW]	746.9	1119.6
Natural gas flow rate	[kg/s]	0.0152	0.02278
Air flow rate	[kg/s]	0.29	0.436
Natural gas temperature	[°C]	16.31	16.83
Air temperature	[°C]	11.75	14.54

Wall Heat Fluxes Measurements

Two different burner duties were tested: 745 kW (case 1) and 1120 kW (case 2). The local wall heat fluxes were measured based on the heat absorbed by the cooling water. Stabilization of the experiment was established with respect to local wall heat fluxes in all sections of the furnace, which were monitored continuously. After reaching a steady state, the measurement procedure began and data were collected for about 30 minutes. The operating conditions for both cases are presented in Table 1.

5.3.3 Modelling

For each of the two cases a combustion simulation was performed using commercial CFD package Ansys Fluent. The problem was carefully set up taking into account recent results of a related investigation (Vondál and Hájek, 2011). The main goal of these simulations was to predict heat fluxes absorbed by the cylindrical water-cooled combustion chamber walls for two different burner duties, namely 745 kW and 1120 kW.

Computational Grid and Setup

For the purposes of numerical analysis a mesh was constructed in the software Gambit. The total number of computational cells (97% of which are hexahedral) was nearly 1,200,000, with approximately 200, 65 and 135 grid nodes in the axial, radial and tangential directions respectively. During the computations the mesh was adapted according to temperature and vorticity gradients, leading to a total of approximately 1,500,000 computational cells.

Four boundary conditions types were applied – mass flow inlets (for combustion air and methane), pressure outlet, prescribed temperature on the water-cooled walls of 80°C (Vondál and Hájek, 2009) and adiabatic condition for the remaining walls. Boundary and operating conditions were set identical to the experiment.

Turbulence and Chemistry

The flow field was obtained by solving the unsteady Reynolds-averaged Navier-Stokes equations. Four different turbulence models were tested: k-ε realizable, k-ε RNG (based on renormalization group theory), k-ω SST (Shear-Stress Transport) and RSM (Reynolds Stress Model).

To account for turbulence chemistry interactions and combustion the Eddy-Dissipation model (Magnussen and Hjertager, 1977) has been employed. This model falls into the family of eddy breakup models and therefore combustion occurs as soon as fuel and oxidants are mixed. Due to the simplifying assumptions only a single-step reaction mechanism has been used.

Radiation

In combustion chambers, the main mechanism of heat transfer is radiation. However, by this time no generally accepted model has been developed. For this study the discrete ordinates model has been used due to its reasonable computational demand. A recent model for the absorption coefficients has been implemented (Yin et al., 2010), which is based on approach of the weighted sum of grey gases model.

5.3.4 Results and Discussion

This section provides a summary of computed results and comparison of the various turbulence models employed. Both comparisons of the predicted local wall heat fluxes with experimental measurement can be seen in Figure 2 and Figure 3. The error bars in the figures represent the standard deviation.

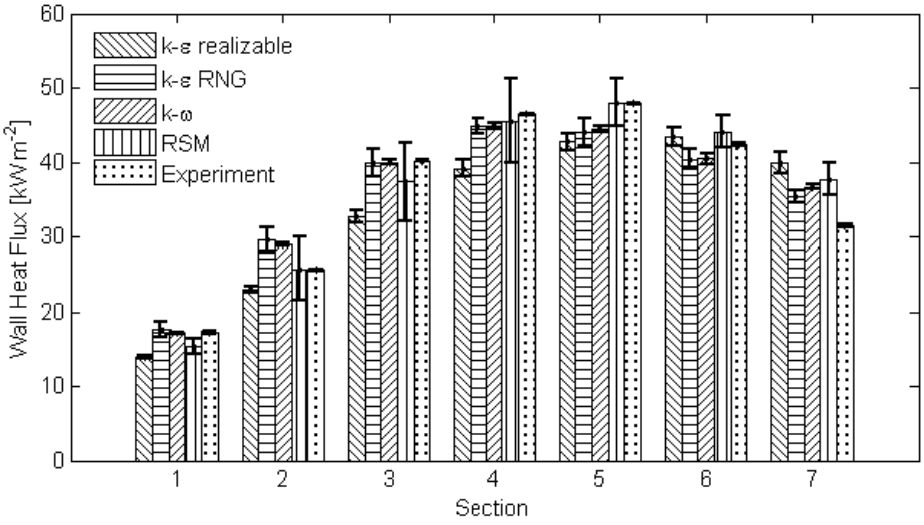

Figure 2. Comparison of predicted local wall heat fluxes between simulation and experiment – 745 kW

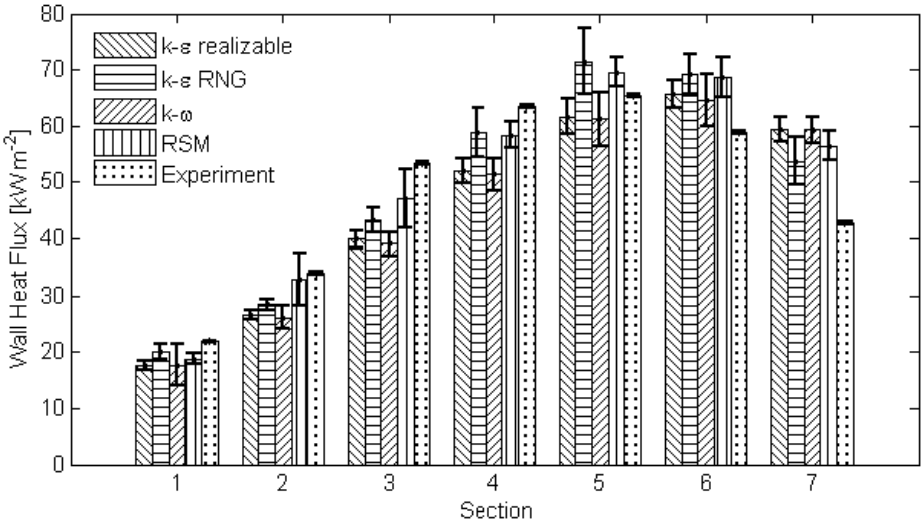

Figure 3. Comparison of predicted local wall heat fluxes between simulation and experiment – 1120 kW

Table 2. Total Wall Heat Fluxes

	Case 1 [kW]	Deviation [%]	Case 2 [kW]	Deviation [%]
k-ε realizable	426.8	2.59	595.3	0.19
k-ε RNG	445.3	1.63	619.9	4.33
k-ω SST	448.6	2.37	589.3	0.82
RSM	452.9	3.35	635.7	7
Experiment	438.2		594.1	

In case 1 it can be said that good agreement is achieved with all turbulence models (see Figure 2). After a closer look the RSM model provides the best agreement (only in the last section it is surpassed by the other models). However, it is important not to forget, that the RSM model is by far the most computationally expensive among the other models. The k-ε RNG and k-ω SST

models give very similar results, while the k-ε realizable model, compared to the others, gives the poorest predictions. Overall, the section where the least agreement is achieved is the 7th section.

The comparison of case 2 is reported in Figure 3. When compared to the previous case, the prediction is not as successful. Again, all models have only small deviations. In the first four sections all models underpredict the wall heat fluxes, while in the last two sections they are overpredicted. Similar trends can be also found in the previous case, but they are not as distinct as in this case. It is also interesting to note, that most models predict an increase of wall heat flux between section 5 and 6, while the experimental data have the opposite trend. No model can be clearly said to give best agreement. The k-ε realizable and k-ω SST models give very similar results similarly and a similar resemblance can be found among the k-ε RNG and RSM models. The 7th section is, as in the previous case, where all models struggle to give acceptable predictions.

Although the only difference between the two simulated cases was the burner duty, in the case 1 good agreement was achieved unlike in case 2. Even with the up-to-date radiation approach (Yin et al., 2010) the simulation results in case 2 cannot be considered good. From Figure 3 it can be seen that the predicted flame is longer, which means that the mixing of fuel and oxidizer is occurs at a smaller rate then in reality. This clearly shows the difficulty of modeling swirling flows. As the burner duty is increased, the gas velocities increase as well accentuating the role of swirling in the mixing process. The swirling phenomenon has not yet been fully understood and current turbulence models are not able to capture its complex flow structure properly (Mitrofanova, 2003).

In general it cannot be said the RSM model is superior compared to the two-equation models. Although it gives slightly better predictions of local heat fluxes the growth of computational effort is significant and is likely to disqualify this model when it comes to industrial applications.

An overview of total heat fluxes in the combustion chamber is reported in Table 2. In case 1 all models give reasonable agreement with only small differences among them. In case 2 k-ε realizable and k-ω SST give very accurate prediction of the total wall heat flux while k-ε RNG and RSM gives much worse predictions. It is worth noting that the RSM model gives in both cases the least accurate predictions.

5.3.5 Conclusion and Future work

This study addresses the issue of turbulent swirling gas combustion. Two cases with different burner duties (745 kW and 1120 kW) were addressed both experimentally and numerically. Four commonly used turbulence models were compared in terms of local wall heat fluxes predictions and confronted with experimental measurements. The results indicate that in the case of higher duties (case 2) the used models struggle to capture the swirling effect, which results in slower mixing of fuel and oxidizer leading to longer flames and mismatch between predicted and measured wall heat fluxes. It can be argued, that there are turbulence models able to overcome these shortcomings, but unfortunately they are still too computationally expensive to be employed across the board. Furthermore it is shown that the advanced RSM model has difficulties predicting total wall heat fluxes as accurately as simpler two-equation models. More research is therefore needed to better understand the swirling process and to find efficient ways to improve current models or to develop new ones.

Acknowledgement

Ministry of Education, Youth and Sports of the Czech Republic within the framework of research plan No. MSM 0021630502 “Waste and Biomass Utilization focused on Environment Protection and Energy Generation” and within the framework of Operational Programme “Research and Development for Innovations” – “NETME Centre – New Technologies for Mechanical Engineering”.

References

Bělohradský, P., Kermes, V., Stehlík, P., 2008. Design and analysis of experiment for low-NOx burners design for process industries. Presented at the 8th European Conference on Industrial Furnaces and Boilers, Vilamouria, Portugal.

Fureby, C., Grinstein, F.F., Li, G., Gutmark, E.J., 2007. An experimental and computational study of a multi-swirl gas turbine combustor. Proc. Combust. Inst. 31, 3107–3114. doi:10.1016/j.proci.2006.07.127

Hayes, R.R., Brewster, S., Webb, B.W., McQuay, M.Q., Huber, A.M., 2001. Crown incident radiant heat flux measurements in an industrial, regenerative, gas-fired, flat-glass furnace. Experimental Thermal and Fluid Science 24, 35–46. doi:10.1016/S0894-1777(00)00055-8

James, S., Zhu, J., Anand, M.S., 2007. Large eddy simulations of turbulent flames using the filtered density function model. Proc. Combust. Inst. 31, 1737–1745. doi:10.1016/j.proci.2006.07.160

Kermes, V., Bělohradský, P., 2008. Testing of gas and liquid fuel burners for power and process industries. Energy 33, 1551–1561.

Kermes, V., Bělohradský, P., Stehlík, P., 2008. Influence of burner geometry with staged gas supply on the formation of nitrogen oxides. Presented at the 8th European Conference on Industrial Furnaces and Boilers, Vilamouria, Portugal.

Kermes, V., Skryja, P., Stehlík, P., 2007. Up to date experimental facility for testing low-NOx burners. Chemical Engineering Transaction 12, 549–554.

Magnussen, B.F., Hjertager, B.H., 1977. On mathematical modeling of turbulent combustion with special emphasis on soot formation and combustion. Symposium (International) on Combustion 16, 719–729. doi:10.1016/S0082-0784(77)80366-4

Mitrofanova, O.V., 2003. Hydrodynamics and Heat Transfer in Swirling Flows in Channels with Swirlers (Analytical Review). High Temperature 41, 518–559. doi:10.1023/A:1025172018351

Sadiki, A., Maltsev, A., Wegner, B., Flemming, F., Kempf, A., Janicka, J., 2006. Unsteady methods (URANS and LES) for simulation of combustion systems. International Journal of Thermal Sciences 45, 760–773. doi:10.1016/j.ijthermalsci.2005.11.001

Ströhle, J., 2004. Spectral Modelling of Radiative Heat Transfer in Industrial Furnaces. Shaker Verlag GmbH, Germany, Aachen, Germany.

Vondál, J., Hájek, J., 2009. Boundary condition evaluation and stability issues in swirling flame gas combustion, in: 1st International Conference on Computational Methods for Thermal Problems. Presented at the 1st International Conference on Computational Methods for Thermal Problems, Napoli, Italy, pp. 314–317.

Vondál, J., Hájek, J., 2011. Experimental and numerical investigation of swirling non-premixed gas flames in industrial-scale furnace, in: Proceedings of 9th European Conference on Industrial Furnaces and Boilers. Presented at the INFUB-9, Estoril, Portugal, pp. 1–9.

Vondál, J., Hájek, J., Kermes, V., 2010. Local wall heat fluxes in swirling non-premixed natural gas flames in large-scale combustor: Data for validation of combustion codes. Chemical Engineering Transactions 21, 1123–1128. doi:10.3303/CET1021188

Yin, C., Johansen, L.C.R., Rosendahl, L.A., Kær, S.K., 2010. New Weighted Sum of Gray Gases Model Applicable to Computational Fluid Dynamics (CFD) Modeling of Oxy−Fuel Combustion: Derivation, Validation, and Implementation. Energy Fuels 24, 6275–6282. doi:10.1021/ef101211p

5.4 Review on Validation of CFD Models of Swirling Flows by Experimental Data

Abstract

Efficient research and development of combustion applications is not possible without an experimental facility. Recently, development has also been supported by Computational Fluid Dynamics (CFD). CFD models, however, have to be validated against experimental data to become reliable tools for predictions. This article reviews available experimental data that are necessary for validation of CFD models of swirling turbulent reacting or nonreacting flows. The review is primarily concerned with measurements and CFD model validations of swirling turbulent combustion. However, swirling turbulent isothermal flows are included as well for sake of completeness. Experiments under well-defined conditions are stressed. These experiments are identified as popular with CFD modelers as they provide for complete experimental data, that are appropriate for validation.

5.4.1 Introduction

One of the most important components in industrial combustion applications is a burner. Since different applications may require more or less specific designs of burners, numerous special types of burners are developed and found in practice (Baukal, 2003). Beside experimental methods, Computational Fluid Dynamics has also proved to be helpful in development and optimization of burners. However, CFD simulation of turbulent combustion is complex as it includes modeling of turbulent reactive flow with radiative heat transfer. There is no general method or procedure that could be applied to modeling of any kind of burner or combustion system to correctly describe all features of the simulated flow. For instance, Franzelli et al. (2012) showed effects of perfect premixing assumption on results of Large Eddy Simulation (LES) of combustion instabilities in swirl burners. Even in case of swirling turbulent flow without presence of chemical reactions or additional radiation models, care must be taken when choosing an appropriate turbulence model for the description of main flow properties as demonstrated e.g. in (Benim et al., 2007). From this point of view, modeling of swirling flows is still challenging task and further development and validation of computational methods are needed.

There is a lot of published literature with measurements of turbulent flows under various conditions. The range of investigated phenomena is wide and covers, for example, studies on recirculation and flow field regimes, thermo-acoustic instabilities, vortex breakdown, the effect of pressure on flow field, fuel-air premixing and flame shapes. A comprehensive review in the area of development of low-emission lean-premixed gas turbine combustion systems with respect to combustion instabilities can be found in (Huang and Yang, 2009). Since not all experimental studies are suitable for validation of CFD models, e.g. due to incomplete description of the geometry or ill-defined boundary conditions, much effort has been made to establish solid databases of measurements, that can be accessed online and provide for all data necessary for proper definition and evaluation of the CFD model, thus serving CFD analysts for the model validation. Masri (2011) discusses six key issues for design of experiments that provide not only a better understanding of studied physics, but also a quality base for validation of calculations.

Many studies have been done on validation of CFD models of turbulent flows (both reactive and non-reactive) using the experimental data archives available either directly from TNF Workshop web site (“International Workshop on Measurement and Computation of Turbulent

Nonpremixed Flames," 2013), or web sites of laboratories, that have been involved in TNF Workshop. During the last ten years, a number of LES of turbulent flows has notably increased. Gicquel et al. (2012) review advances in LES of flames in gas turbine combustion chambers. More general review on LES validation from experiments is provided in (Kempf, 2008) and ideas and notes on experiments for LES validation of combustion models are presented in (Böhm et al., 2008). In addition, correct representation of inlet boundary conditions has also been widely discussed topic as it plays very important role in LES to produce accurate results (Malalasekera et al., 2007). Various methods to introduce turbulent boundary conditions at the inlet are reviewed e.g. in (Tabor and Baba-Ahmadi, 2010). Finally, some research groups have validated their models against data sets that are not included in the TNF experimental data archives, but still available elsewhere in published literature. It is found, that some experimental setups are more popular with modellers for validation. Therefore some kinds of burners are studied more frequently than others. Both experimental and theoretical (i.e. validation) works are subject of the present contribution and are discussed in the following sections.

This article follows the work of Vondál (Vondál and Hájek, 2011a). Their selection of the most important experiments on confined swirling flows is extended. It is not intended to provide a comprehensive review. The aim is to explore the extent to which published experimental data are used to validate CFD models.

5.4.2 Structure and Classification

As it has already been mentioned, there are numerous types of burners, only a few of which have been studied both experimentally and theoretically. For the purpose of the article, the paper is structured according to the type of flow - reacting/non-reacting (isothermal) - and various studies are classified according to a principle of swirl generation. Although the review is primarily concerned with measurements and CFD model validation of swirling turbulent combustion, swirling turbulent isothermal flows are included for sake of completeness.

Several methods to generate swirling flows are reported in literature. These can be divided into three groups (Vondál and Hájek, 2011a). This classification is also adopted in the present work.

Guide vanes (possibly adjustable) are typically used e.g. in industrial burners for process engineering applications mainly due to operational reliability and simple design. The number and design of vanes (i.e. shape, dimensions and angle with respect to the flow direction) are important parameters influencing flow characteristics downstream of the vanes. A study on the effect of these parameters on the flow characteristics is presented in (Raj and Ganesan, 2008).

Tangential inlet is probably the most often used method to introduce turbulent component to the flow. For example, Coghe et al. (2004) use an experimental configuration which is similar to diffusive atmospheric pressure burners.

Direct rotation caused by, for instance, rotating tubes is not used in combustion applications. It is found mostly in water systems. This kind of swirl generator is applied e.g. in the work of Liang (Liang and Maxworthy, 2005).

5.4.3 Isothermal Flows

There is a substantial amount of literature published on measurements and validation of swirling turbulent isothermal flows. One of the most popular measurements of such flows in terms of the number of various validations was carried out and published by Dellenback et al. (1988), who used a swirl generator with tangential inlets. The published experimental data

including both axial and tangential velocities are well-documented for flows with Reynolds numbers ranging from 30000 to 100000 and swirl numbers from zero to 1.2. These data have been used for validation by many research groups. Congedo et al. (2012) tested Raynolds-Averaged Navier-Stokes (RANS) and LES models finding LES to outperform RANS model, Sentyabov et al. (2011) compared RANS and Detached Eddy Simulation (DES) models and found DES to predict tangential velocity component more accurately than RANS. Chen (Chen and Chang, 1995) modified the standard *k*-ε turbulence model so that the hybrid one performed better than the original one. The problem of generating the inlet boundary conditions for LES was examined by Ahmadi (Baba-Ahmadi and Tabor, 2008), who developed a procedure for estimation of the inlet profiles by applying a body force. There are many other works referring to Dellenback et al. (1988), most of which compare performance and accuracy of various turbulence models, e.g. (Kumar and Ghoniem, 2012; Nilsson, 2012).

Some examples of other validations of isothermal flows against experimental data are listed in the Table 1. Turbulence models used in the listed studies (DNS – Direct Numerical Simulation, URANS – Unsteady RANS) were examined with respect to accuracy of predictions of vortex breakdown (VB), recirculation zones (RZ) and coherent structures (CS). To the best author‘s knowledge, no validation with experimental setup identical to that of Escudier (Escudier and Keller, 1985) has been carried out. Only qualitative comparison of numerical results with the experimental ones is presented in (Jochmann et al., 2006). Although the list of works is not complete, it can be concluded, that experimental configurations with tangential inlets dominate over others in validations of isothermal turbulent flows.

Table 1. Selection of Validations of Isothermal Flows

Type of Swirl Generator	Ref.to Experiment	Ref.to Validation	Turbulence models	Subject of Study
Tangential inlet	(Al-Abdeli and Masri, 2003)	(Malalasekera et al., 2007)	LES	VB, RZ
	(Al-Abdeli and Masri, 2003)	(Ranga Dinesh and Kirkpatrick, 2009)	LES	VB, RZ
Rotating tube (cylinder, honeycomb, etc.)	(Billant et al., 1998)	(Gui et al., 2010)	DNS	VB, CS
Guide vanes	(Escudier and Keller, 1985)	-	-	VB
	(Benim et al., 2010)	(Benim et al., 2010)	LES, URANS	
	(Lilley David G., 1985)	(Lilley David G., 1985)	*k*-ε	

Finally, it is worth to note that certain studies have also been extended for reacting flows using the same geometry allowing for comparison of both cases of flows. This is an important issue, because it is argued in one of the earlier works by Escudier (Escudier and Keller, 1985), that isothermal flows might not be representative of reacting flows through the same

experimental setup. Therefore care must be taken when transferring results from one experiment to another.

5.4.4 Reacting Flows

As it is noted in (Vondál and Hájek, 2011b), much of the research work in the area of turbulent reacting flows has recently concentrated mainly on the flame itself. Flames have been investigated mostly under well-defined conditions using laboratory-scale burners. Detailed experimental data sets have been obtained for flames of several specific types of burners, two of which have become target of a vast number of CFD validations, namely Sydney burner (see, for instance, experimental studies of Al-Abdeli (Al-Abdeli et al., 2006) and Kalt (Kalt et al., 2002)) and TECFLAM burner (see e.g. Schmittel et al. (Schmittel et al., 2000), Landenfeld et al. (Landenfeld et al., 1998), Meier. (Meier et al., 2000)). While turbulent velocity components are introduced by tangential inlets in Sydney burner, TECFLAM burner has a movable block.

Several LES validations by data from Sydney burner flames experiments can be found in literature. Three Sydney burner flames, namely swirl methane flame SM1 and swirl methane-hydrogen flames SMH1 and SMH2, were simulated by Kempf (Kempf et al., 2008) using different numerical techniques implemented in their codes PUFFIN and FLOWSI. SMH flames were found to be the most difficult to predict. Stein (Stein and Kempf, 2007) also reported problematic capture of vortex breakdown in SMH1 flame. SM1 flame was examined by other research groups as well, e.g. by Hu (Hu et al., 2008), who tested different Smagorinsky subgrid-scale (SGS) stress models in combination with two different combustion models (second-order moment - SOM - and probability density function - PDF). Olbricht (Olbricht et al., 2010) investigated a set of seven swirled/non-swirled and reacting/non-reacting Sydney flames including SM1. In addition, instabilities of SM1 and SM2 flames were explored by Dinesh (Dinesh et al., 2010). LES seems to be employed almost exclusively in validations of Sydney burners. However, other turbulence models have also been tested. In order to study turbulence-chemistry interactions, De Meester (De Meester et al., 2012) used k-ε RANS turbulence model with transported scalar PDF approach in simulations of SM1 flame. A good agreement of results with experimental measurements was reported and comparable to those obtained by LES in earlier works.

The effect of turbulence-chemistry interactions on predictions of flow was also investigated for the TECFLAM burner, however using Monte Carlo-PDF method and presumed-PDF model (Repp et al., 2002). A presumed PDF model for temperature fluctuation was proposed and applied to simulation of TECFLAM flame by Yang (Yang and Zhang, 2009). One of the first CFD simulation of TECFLAM burner flame was attempted by Meier (Meier et al., 2000) using FLUENT 5 code. Since general behavior of the flow was not predicted correctly, the results were considered unsatisfactory. Better results were reported five years later in (Frassoldati et al., 2005) (using FLUENT 6), which was attributed mainly to appropriate inlet velocity profiles as boundary conditions and specific convergence strategy. Finally, very recent investigation of TECFLAM burner using LES is presented in (Ayache and Mastorakos, 2013). All mentioned simulation studies of TECFLAM referred to the S09C flame case.

Beside these well-known flames, there are also other well-documented experiments for validation of CFD turbulent combustion models. Meier (Meier et al., 2007) and Lartigue (Lartigue et al., 2004) carried out experiments on a gas turbine combustor, which is based on Turbomeca design. Swirling flow is generated by guide vanes. For this configuration, Franzelli (Franzelli et al., 2012) studied combustion instabilities using LES, while Moureau (Moureau et al., 2011) applied a methodology of successive LES with increasing resolution up to DNS.

Experimental data for piloted Delft III natural gas burner is available online at TNF Workshop web site ("International Workshop on Measurement and Computation of Turbulent Nonpremixed Flames," 2013). Data were applied to validation of LES coupled with Conditional Moment Closure, see (Ayache and Mastorakos, 2012). Mass fractions of major species were captured reasonably well, however concentration of NO was overpredicted. Some examples of other validations of reacting swirling flows against experimental data are listed in the Table 2.

Table 2. Selection of Validations of Reacting Flows

Type of Swirl Generator	Ref.to Experiment	Ref.to Validation	Turbulence models	Subject of Study
Guide vanes	(Petersson et al., 2007)	(Karl-Johan et al., 2008)	LES	Flame
	(Mak and Balabani, 2007)	(Vondál and Hájek, 2011b)	RNG k-ε, SST k-ω, RSM	Grid sensitivity, RZ
	(Khezzar, 1998)	-	-	Velocity
	(Grinstein et al., 2002)	(Grinstein et al., 2002)	LES	Inlet conditions
	(Wu, H.L., n.d.)	(Fudihara et al., 2007)	RNG k-ε	Axial velocity, RZ
	(Ballester et al., 1997)	-	-	NOx emissions

Recently, a number of studies on coal combustion burners have increased dealing mostly with pollutant emission levels, see e.g. (Chen et al., 2011) and (Hu et al., 2013). Although CFD results of such studies are compared to experimental data, the experimental configuration and data are not well-documented (or well-defined) to serve for general validation of CFD models.

5.4.5 Conclusion

The review has revealed, that quality experimental data for validation of numerical models of swirling turbulent reactive flows are available mainly for gas swirl burner with tangential inlet swirl generators such as Sydney burner. This is supported by a large number of validation reports, in which LES and DES are the most often used methods for predictions. However, other turbulence models are also tested as they still dominate in practical industrial applications due to lower computational requirements. Other types of configuration (e.g. burners with guide vanes swirl generators) seem to be less frequently studied, which is given probably by the fact that the experimental database is not so extensive with respect to the number of different case studies. Available documentation of such experimental setups for tests under well-defined conditions includes description of TECFLAM burners (with movable blocks) and several gas combustion turbine configurations (e.g. based on Turbomeca design). A set of measurements on burners with axial guide vanes is very limited. To the best author's knowledge, no experimental measurement for validation of CFD turbulent combustion models is available for natural-draft burners, which are typical in process engineering applications.

Acknowledgement

The authors gratefully acknowledge financial support within the framework of Operational Programme “Investment in education development” CZ.1.07/2.3.00/20.0020 and within the framework of Operational Programme “Research and Development for Innovations” – “NETME Centre – New Technologies for Mechanical Engineering”.

References

Al-Abdeli, Y.M., Masri, A.R., 2003. Recirculation and flowfield regimes of unconfined non-reacting swirling flows. Exp. Therm. Fluid Sci. 27, 655–665. doi:10.1016/S0894-1777(02)00280-7

Al-Abdeli, Y.M., Masri, A.R., Marquez, G.R., Starner, S.H., 2006. Time-varying behaviour of turbulent swirling nonpremixed flames. Combust. Flame 146, 200–214. doi:16/j.combustflame.2006.03.009

Ayache, S., Mastorakos, E., 2012. Conditional Moment Closure/Large Eddy Simulation of the Delft-III Natural Gas Non-premixed Jet Flame. Flow Turbul. Combust. 88, 207–231. doi:10.1007/s10494-011-9368-6

Ayache, S., Mastorakos, E., 2013. Investigation of the “TECFLAM” Non-premixed Flame Using Large Eddy Simulation and Proper Orthogonal Decomposition. Flow Turbul. Combust. 90, 219–241. doi:10.1007/s10494-012-9428-6

Baba-Ahmadi, A.H., Tabor, G.R., 2008. Inlet conditions for large eddy simulation of gas-turbine swirl injectors. Aiaa J. 46, 1782–1790. doi:10.2514/1.35259

Ballester, J.M., Dopazo, C., Fueyo, N., Hernández, M., Vidal, P.J., 1997. Investigation of low-NOx strategies for natural gas combustion. Fuel 76, 435–446. doi:10.1016/S0016-2361(97)85521-4

Baukal, C.E., 2003. Industrial Burners Handbook, 1st ed. CRC Press.

Benim, A.C., Escudier, M.P., Nahavandi, A., Nickson, A.K., Syed, K.J., Joos, F., 2010. Experimental and numerical investigation of isothermal flow in an idealized swirl combustor. Int. J. Numer. Methods Heat Fluid Flow 20, 348–370. doi:10.1108/09615531011024084

Benim, A.C., Escudier, M.P., Nahavandi, A., Nickson, K., Syed, K.J., 2007. Computational analysis of isothermal flow in a test swirl combustor. World Scientific and Engineering Acad and Soc, Athens.

Billant, P., Chomaz, J.-M., Huerre, P., 1998. Experimental study of vortex breakdown in swirling jets. J. Fluid Mech. 376, 183–219. doi:10.1017/S0022112098002870

Böhm, B., Brübach, J., Ertem, C., Dreizler, A., 2008. Experiments for Combustion-LES Validation. Flow Turbul. Combust. 80, 507–529. doi:10.1007/s10494-008-9144-4

CHEN, C.-S., CHANG, K.-C., 1995. MODIFICATION OF THE κ-ε TURBULENCE MODEL FOR SWIRLING RECIRCULATING FLOW IN A PIPE EXPANSION. Int. J. Comput. Fluid Dyn. 5, 263–279. doi:10.1080/10618569508940746

Chen, Z., Li, Z., Zhu, Q., Jing, J., 2011. Gas/particle flow and combustion characteristics and NOx emissions of a new swirl coal burner. Energy 36, 709–723. doi:10.1016/j.energy.2010.12.037

Coghe, A., Solero, G., Scribano, G., 2004. Recirculation phenomena in a natural gas swirl combustor. Exp. Therm. Fluid Sci. 28, 709–714. doi:10.1016/j.expthermflusci.2003.12.007

Congedo, P.M., Duprat, C., Balarac, G., Corre, C., 2012. Numerical prediction of turbulent flows using Reynolds-averaged Navier–Stokes and large-eddy simulation with uncertain inflow conditions. Int. J. Numer. Methods Fluids n/a–n/a. doi:10.1002/fld.3743

De Meester, R., Naud, B., Maas, U., Merci, B., 2012. Transported scalar PDF calculations of a swirling bluff body flame ("SM1") with a reaction diffusion manifold. Combust. Flame 159, 2415–2429. doi:10.1016/j.combustflame.2012.01.026

Dellenback, P.A., Metzger, D.E., Neitzel, G.P., 1988. Measurements in turbulent swirling flow through an abrupt axisymmetric expansion. AIAA J. 26, 669–681. doi:10.2514/3.9952

Dinesh, K.K.J.R., Jenkins, K.W., Kirkpatrick, M.P., Malalasekera, W., 2010. Modelling of instabilities in turbulent swirling flames. Fuel 89, 10–18. doi:10.1016/j.fuel.2009.06.024

Escudier, M.P., Keller, J.J., 1985. Recirculation in swirling flow: a manifestation of vortex breakdown. AIAA J. 23, 111–116.

Franzelli, B., Riber, E., Gicquel, L.Y.M., Poinsot, T., 2012. Large Eddy Simulation of combustion instabilities in a lean partially premixed swirled flame. Combust. Flame 159, 621–637. doi:10.1016/j.combustflame.2011.08.004

Frassoldati, A., Frigerio, S., Colombo, E., Inzoli, F., Faravelli, T., 2005. Determination of NOx emissions from strong swirling confined flames with an integrated CFD-based procedure. Chem. Eng. Sci. 60, 2851–2869. doi:10.1016/j.ces.2004.12.038

Fudihara, T.J., Goldstein Jr., L., Mori, M., 2007. A numerical investigation of the aerodynamics of a furnace with a movable block burner. Braz. J. Chem. Eng. 24, 233–248.

Gicquel, L.Y.M., Staffelbach, G., Poinsot, T., 2012. Large Eddy Simulations of gaseous flames in gas turbine combustion chambers. Prog. Energy Combust. Sci. 38, 782–817. doi:10.1016/j.pecs.2012.04.004

Grinstein, F., Young, T., Gutmark, E., Li, G., Hsiao, G., Mongia, H., 2002. Flow dynamics in a swirl combustor. J. Turbul. 3, 1–19. doi:10.1088/1468-5248/3/1/030

Gui, N., Fan, J., Cen, K., Chen, S., 2010. A direct numerical simulation study of coherent oscillation effects of swirling flows. Fuel 89, 3926–3933. doi:10.1016/j.fuel.2010.06.037

Hu, L., ZHOU, L., Luo, Y., Xu, C., 2013. Measurement and simulation of swirling coal combustion. Particuology 11, 189–197. doi:10.1016/j.partic.2012.05.009

Hu, L.Y., Zhou, L.X., Luo, Y.H., 2008. Large-Eddy Simulation of the Sydney Swirling NonPremixed Flame and Validation of Several Subgrid-Scale Models. Numer. Heat Transf. Part B Fundam. 53, 39–58. doi:10.1080/10407790701632477

Huang, Y., Yang, V., 2009. Dynamics and stability of lean-premixed swirl-stabilized combustion. Prog. Energy Combust. Sci. 35, 293–364. doi:10.1016/j.pecs.2009.01.002

International Workshop on Measurement and Computation of Turbulent Nonpremixed Flames [WWW Document], 2013. URL http://www.sandia.gov/TNF/abstract.html

Jochmann, P., Sinigersky, A., Hehle, M., Schäfer, O., Koch, R., Bauer, H.-J., 2006. Numerical simulation of a precessing vortex breakdown. Int. J. Heat Fluid Flow 27, 192–203. doi:10.1016/j.ijheatfluidflow.2005.08.003

Kalt, P.A.M., Al-Abdell, Y.M., Masri, A.R., Barlow, R.S., 2002. Swirling turbulent non-premixed flames of methane: Flow field and compositional structure. Proc. Combust. Inst. 29, 1913–1919. doi:16/S1540-7489(02)80232-2

Karl-Johan, N., Xue-Song, B., C., F., P., P., 2008. A Comparative Study of LES Turbulent Combustion Models Applied to a Low Swirl Lean Premixed Burner.

Kempf, A., Malalasekera, W., Ranga-Dinesh, K.K.J., Stein, O., 2008. Large eddy simulations of swirling non-premixed flames with flamelet models: A comparison of numerical methods. Flow Turbul. Combust. 81, 523–561. doi:10.1007/s10494-008-9147-1

Kempf, A.M., 2008. LES Validation from Experiments. Flow Turbul. Combust. 80, 351–373. doi:10.1007/s10494-007-9128-9

Khezzar, L., 1998. Velocity measurements in the near field of a radial swirler. Exp. Therm. Fluid Sci. 16, 230–236. doi:10.1016/S0894-1777(97)10027-9

Kumar, M., Ghoniem, A.F., 2012. Multiphysics Simulations of Entrained Flow Gasification. Part I: Validating the Nonreacting Flow Solver and the Particle Turbulent Dispersion Model. Energy Fuels 26, 451–463. doi:10.1021/ef200884j

Landenfeld, T., Kremer, A., Hassel, E.P., Janicka, J., Schäfer, T., Kazenwadel, J., Schulz, C., Wolfrum, J., 1998. Laser-diagnostic and numerical study of strongly swirling natural gas flames. Symp. Int. Combust. 27, 1023–1029. doi:10.1016/S0082-0784(98)80502-X

Lartigue, G., Meier, U., Bérat, C., 2004. Experimental and numerical investigation of self-excited combustion oscillations in a scaled gas turbine combustor. Appl. Therm. Eng. 24, 1583–1592. doi:10.1016/j.applthermaleng.2003.10.026

Liang, H., Maxworthy, T., 2005. An experimental investigation of swirling jets. J. Fluid Mech. 525, 115–159. doi:10.1017/S0022112004002629

Lilley David G., 1985. NASA-Investigation of Flowfields Found in Typical Combustor Geometries (No. NASA CR 3869).

Mak, H., Balabani, S., 2007. Near field characteristics of swirling flow past a sudden expansion. Chem. Eng. Sci. 62, 6726–6746. doi:10.1016/j.ces.2007.07.009

Malalasekera, W., Ranga Dinesh, K.K.J., Ibrahim, S.S., Kirkpatrick, M.P., 2007. Large Eddy Simulation of Isothermal Turbulent Swirling Jets. Combust. Sci. Technol. 179, 1481–1525. doi:10.1080/00102200701196472

Masri, A.R., 2011. Design of experiments for gaining insights and validating modeling of turbulent combustion, in: Turbulent Combustion Modeling - Fluid Mechanics and Its Applications. Springer Netherlands, pp. 355–380.

Meier, W., Keck, O., Noll, B., Kunz, O., Stricker, W., 2000. Investigations in the TECFLAM swirling diffusion flame: Laser Raman measurements and CFD calculations. Appl. Phys. B Lasers Opt. 71, 725–731. doi:10.1007/s003400000436

Meier, W., Weigand, P., Duan, X.R., Giezendanner-Thoben, R., 2007. Detailed characterization of the dynamics of thermoacoustic pulsations in a lean premixed swirl flame. Combust. Flame 150, 2–26. doi:10.1016/j.combustflame.2007.04.002

Moureau, V., Domingo, P., Vervisch, L., 2011. From Large-Eddy Simulation to Direct Numerical Simulation of a lean premixed swirl flame: Filtered laminar flame-PDF modeling. Combust. Flame 158, 1340–1357. doi:10.1016/j.combustflame.2010.12.004

Nilsson, H., 2012. Simulations of the vortex in the Dellenback abrupt expansion, resembling a hydro turbine draft tube operating at part-load. IOP Conf. Ser. Earth Environ. Sci. 15, 022016. doi:10.1088/1755-1315/15/2/022016

Olbricht, C., Ketelheun, A., Hahn, F., Janicka, J., 2010. Assessing the Predictive Capabilities of Combustion LES as Applied to the Sydney Flame Series. Flow Turbul. Combust. 85, 513–547. doi:10.1007/s10494-010-9300-5

Petersson, P., Olofsson, J., Brackman, C., Seyfried, H., Zetterberg, J., Richter, M., Aldén, M., Linne, M.A., Cheng, R.K., Nauert, A., Geyer, D., Dreizler, A., 2007. Simultaneous PIV/OH-PLIF, Rayleigh thermometry/OH-PLIF and stereo PIV measurements in a low-swirl flame. Appl. Opt. 46, 3928–3936. doi:10.1364/AO.46.003928

Raj, R.T.K., Ganesan, V., 2008. Study on the effect of various parameters on flow development behind vane swirlers. Int. J. Therm. Sci. 47, 1204–1225. doi:16/j.ijthermalsci.2007.10.019

Ranga Dinesh, K.K.J., Kirkpatrick, M.P., 2009. Study of jet precession, recirculation and vortex breakdown in turbulent swirling jets using LES. Comput. Fluids 38, 1232–1242. doi:10.1016/j.compfluid.2008.11.015

Repp, S., Sadiki, A., Schneider, C., Hinz, A., Landenfeld, T., Janicka, J., 2002. Prediction of swirling confined diffusion flame with a Monte Carlo and a presumed-PDF-model. Int. J. Heat Mass Transf. 45, 1271–1285. doi:10.1016/S0017-9310(01)00243-5

Schmittel, P., Günther, B., Lenze, B., Leuckel, W., Bockhorn, H., 2000. Turbulent swirling flames: Experimental investigation of the flow field and formation of nitrogen oxide. Symp. Int. Combust. 28, 303–309. doi:10.1016/S0082-0784(00)80224-6

Sentyabov, A.V., Gavrilov, A.A., Dekterev, A.A., 2011. Investigation of turbulence models for computation of swirling flows. Thermophys. Aeromechanics 18, 73–85. doi:10.1134/S0869864311010094

Stein, O., Kempf, A., 2007. LES of the Sydney swirl flame series: A study of vortex breakdown in isothermal and reacting flows. Proc. Combust. Inst. 31, 1755–1763. doi:10.1016/j.proci.2006.07.255

Tabor, G.R., Baba-Ahmadi, M.H., 2010. Inlet conditions for large eddy simulation: A review. Comput. Fluids 39, 553–567. doi:10.1016/j.compfluid.2009.10.007

Vondál, J., Hájek, J., 2011a. Experimental and numerical investigation of swirling non-premixed gas flames in industrial-scale furnace. Presented at the 9th European Conference on Industrial Furnaces and Boilers, Estoril, Portugal.

Vondál, J., Hájek, J., 2011b. Prediction of flow through swirl generator and validation by measured data. J. Phys. Conf. Ser. 318, 022026. doi:10.1088/1742-6596/318/2/022026

Wu, H.L., F., N., n.d. An Investigation of the Behavior of Swirling Jet Flames in a Narrow Cylindrical Furnace, in: IFRF Technical Paper.

Yang, W., Zhang, J., 2009. Simulation of methane turbulent swirling flame in the TECFLAM combustor. Appl. Math. Model. 33, 2818–2830. doi:10.1016/j.apm.2008.08.014

5.5 Drop Size Distributions in Effervescent Sprays: An Experimental Study Using PDA Technique

Abstract

Although effervescent atomizers (twin fluid atomizers with internal mixing) represent one of the most recent atomization techniques, they have already shown great usability especially in combustion applications. Due to their different drop formation mechanism they are able to produce smaller droplets than many other conventional atomizers at similar operating conditions, thus making the combustion process more efficient. However, one of the shortcomings of effervescent atomization is the complexity of the atomization mechanism, which involves a two-phase flow. This complexity presents a challenging obstacle when trying to devise computational models describing effervescent sprays. In the past few years many various models have been proposed, but their verification and validation often relies only on very limited data, such as only few representative diameters or global drop size distribution. The purpose of this paper is to review the previous experimental studies on effervescent atomization in order to identify areas that need to be more deeply investigated. The parameters that need more detailed analysis include especially radially (or angularly) and axially dependent representative drop diameters or drop distributions and mass fluxes. It is shown that previous measurements did not collect sufficient amount of data across the whole spectrum of drop sizes and thus parts of the previously measured spectra might be unreliable. A methodology for effervescent spray measurement for verification and validation of numerical models for combustion applications is suggested. Preliminary results are shown indicating the importance of appropriate mask choice.

5.5.1 Introduction

Spray combustion is one of the main ways to gain energy in the power and process industries. A great deal of effort is therefore constantly being put into understanding of the fundamental phenomena and processes governing spray formation. These efforts are motivated by the need to achieve better performance, lower emissions and longer lifetime of furnaces and combustors in various industrial applications.

For combustion purposes, effervescent atomizers are gaining on popularity. They were first introduced by Lefebvre and his colleagues in the late 1980s (Lefebvre et al., 1988). The spray formation process in this type of atomizers does not rely solely on high liquid pressure and aerodynamic forces. Instead, a small amount of gas (typically air) is introduced in the liquid before it exits the atomizer and a two phase flow is formed (Figure 1). When the mixture exits through the nozzle, pressure suddenly drops, which causes fast expansion of gas bubbles and breakup of the liquid fuel into ligaments and subsequently droplets. As noted in (Babinsky and Sojka, 2002), this breakup mechanism allows to use lower injection pressures and larger nozzle diameters without compromising the drop-size distribution.

Recently a great effort has been put into finding reliable numerical models that would describe effervescent spray formation. Many models for various applications have been proposed, however, before they can be successfully applied to industrial applications proper verification and validation needs to be done.

In the area of combustion, spray models are usually validated based on their ability to predict the Sauter Mean Diameter (SMD). The Sauter Mean Diameter is defined as a diameter of a representative droplet having the same volume/surface area ratio as the whole spray. As pointed

out in (Broukal and Hájek, 2011a) and (Broukal and Hájek, 2011b), this can be a very rough approach, since even if the global SMD of the spray in question is in good agreement with measurements, local SMD values might be different and thus cause faulty numerical predictions. Moreover, as shown in (Broukal and Hájek, 2011a; Juslin et al., 1995), effervescent sprays often exhibit multimodal behaviour in drop size distributions, which further raises the question about legitimacy of using a single representative diameter (see Figure 2). To remedy this, more detailed information would be needed to make really sensible validations. Namely, data about radial (or equivalently depending on spray angle) distribution of droplet size and velocity would be desirable, especially for the case of large nozzles in industrial burners.

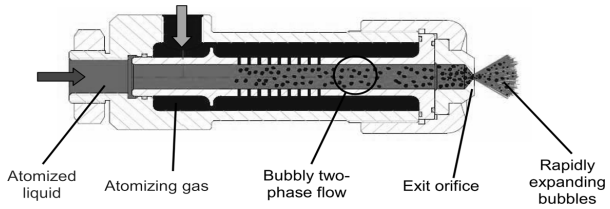

Figure 1. Schematics of the effervescent atomization process, reprinted from (Jedelský et al., 2007)

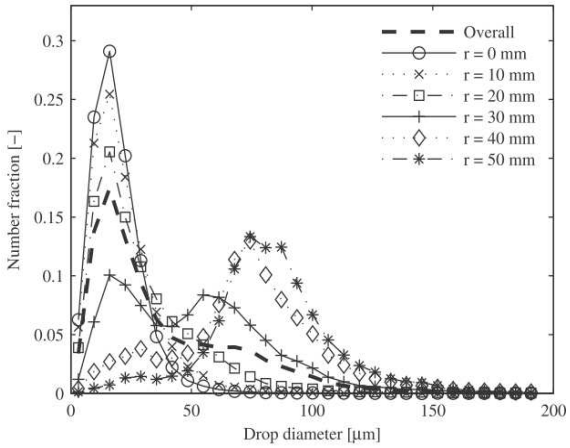

Figure 2. Example of bimodality, reprinted from (Broukal and Hájek, 2011)

5.5.2 Current Measurement Approaches

Currently, spray model validation studies compare numerical results with experiments usually only in terms of global SMD or its axial evolution. Apte et al. (2003) predict axial SMD evolution in a diesel engine using a proposed hybrid particle-parcel model coupled with a LES solver, but only a single experimental SMD value is used in the comparison. A model for atomization of viscous and non-Newtonian liquids in an air-blast atomizer is described by Aliseda et al. (2008) and validated in terms of axial SMD evolution. Tembley et al. (2011) predicted drop size distribution in ultrasonic atomizers. His group developed a model able to predict initial drop size distribution as well as how does the distribution change along the spray axis. However, this model only predicts the overall drop size distribution of a spray cross-section at a specified axial distance. In (Mandato et al., 2012) both single and two-fluid atomizers are examined. A model for spray formation based on dimensional analysis is developed, which is validated using a single point measurement

In the last decade few papers can be found that address the issue of radial drop size distribution and radial SMD evolution. Park et al. (2009) employed the wave breakup model to

investigate biodiesel spray in various fuel and ambient conditions in terms of axial and radial SMD evolution. Along with axial SMD evolution, also radial SMD evolution was reported. Unfortunately, only three radial SMD were disclosed. In (Pougatch et al., 2009) a spray model is presented and applied to water air-assisted atomization. Radial drop diameter evolution is predicted at various axial positions, but no comparison with experimental data has been made. Recently the situation has improved as more researchers focus in more detail on a complex spray measurement (Li et al., 2012). Lian-sheng et al. (2012) performs a detailed experimental measurement of effervescent spray combustion. The work reports various radial SMD and axial drop size distributions. Also, a swirl effervescent atomizer is employed and the influence of swirl on spray angle is demonstrated. However, the liquid mass flow rates are still in a lab-scale region with a maximum of only 10 kg/h.

These examples illustrate the pressing need for validated spray models that would include sufficient information for an informed choice of models by Computational Fluid Dynamics (CFD) analysts in the industry. Although many research papers have been published about atomization and drop breakup, so far only little attention is given to radial SMD or more detailed spatial drop-size distribution, especially in large-scale effervescent atomizers.

5.5.3 Measurement Techniques

In this section the main idea is to provide the reader with an overview of the most used measurement techniques used in the area of spray measurements, especially droplet size measurements, with emphasis on the Phase/Doppler Particle Analyser (P/DPA) or sometimes also called Phase Doppler Anemometry (PDA).

Phase Doppler Anemometry

The Phase Doppler Anemometry is an extension of the Laser Doppler Anemometry used mainly to study local velocities (up to 3 components) in fluid flows. The extension lies in the ability to measure diameters of particles present in the fluid flow (bubbles in liquid, droplets in gas …). The PDA is a non-intrusive optical technique, on-line and in-situ. Due to the nature of the technique, optical access to the measurement area is needed, which can be sometimes limiting for on-site industrial measurements. Since the method requires particles to be spherical (or only slightly deformed), measurements must be taken at a sufficient distance from the discharge orifice. Also, the method is not suitable for very dense spray regions. The measurement device consists of a laser based optical transmitter, an optical receiver, a signal processor and a software for data analysis. The laser beams emitted by the transmitter intersect creating a small sample volume. When a droplet passes through this laser intersection the scattered light forms a fringe pattern. As the drop moves, the scattered interference pattern is registered by the receiver at the Doppler difference frequency, which is proportional to the drop velocity. The droplet diameter is then inversely proportional to the spatial frequency of the fringe pattern. Due to the purely optical nature of the measurement process, no calibration is required and since the sampling volume is usually very small (1 mm^3) high spatial resolution can easily be achieved.

This technique is ideal for high precision measurements of liquid sprays and its results can be used to perform detailed validation of numerical models. Although it gives excellent qualitative representation of the spray (local drop size and velocity distributions), quantitative results, such as mass concentration, can be misleading as reported by (Babinsky and Sojka, 2002; Broukal et al., 2010). This is most probably the result of the trade-off for high spatial resolution and possibly also due to rejection of non-spherical droplets.

Other Techniques

An alternative to PDA is provided by the so called whole-flow-field techniques, like Particle/Droplet Imaging Analysis (PDIA) or Particle Image Velocimetry (PIV). These non-intrusive techniques were originally devised to measure velocity fields of seeded flows. The basic principle of these methods is to take two consecutive images of an illuminated cross-section of the flow and by comparing the displacement of the particles compute the velocity vector field. However, information about drop diameters can be gathered as well by employing advanced image processing algorithms (Avulapati and Ravikrishna, 2012; Wang et al., 2002).

To remedy the potential inaccuracy of mass concentration measurements in the PDA measurements, Planar Laser-Induced Fluorescence (PLIF) can be employed (Jedelsky and Jicha, 2012). During the measurement, a spray cross-section is shortly illuminated by a laser sheet and after some time (in the order of nano- or microseconds) the droplets de-excite and emit a portion of the light which is captured by a camera. The emitted light intensity is proportional to the liquid concentration.

5.5.4 Methodology of Spray Characterization

This section will aim at providing guidelines for gathering ideal experimental data of effervescent sprays to be used for validation of numerical spray models. From the previous section it is evident, that in order to get high resolution drop size and velocity measurement together with accurate mass concentration information, two measurement techniques need to be employed. However, in this part emphasis will be put on the PDA measurement technique.

For the purpose of model development and validation, the primary breakup region of the spray is the most important. Unfortunately, due to the limitations of the PDA technique we cannot measure the spray at its origin, since the droplets are far from being spherical and also the liquid density might be too high. The goal then is to get as close to the spray nozzle as possible. In (Li et al., 2012) it is demonstrated that PDA measurements can be taken at distance from the spray origin $x^* = x/d_0 = 3.3$ (where x is axial distance and d_0 is the discharge orifice diameter), which can still be regarded as area dominated by primary atomization. Data collected here can be a good starting point for the model validation and can even be used as boundary conditions for CFD simulation if needed. After the closest possible location to the spray nozzle has been identified, the set of measurement points should be then expanded in the radial direction to the spray edge using at least two new locations. If the drop size distributions or SMD measurements vary substantially between these points, additional measurement locations should be introduced. To understand the axial evolution of the spray, this process should be repeated at least once more further downstream. The number of radial measurement points should be increased since the spray cone naturally widens. The radial measurements can be taken in multiple directions to check the symmetric behaviour of the spray.

When performing a PDA measurement the user has to choose a receiver mask based on the expected range of drop diameters. If the range of generated droplets does not fall in the range specified by the mask, a part of the drop size distribution will be trimmed. It is therefore advisable to perform measurements with multiple masks and eventually merge resulting distributions. In such case the distributions must be weighted properly prior to merging and also, attention must be paid to whether the mask ranges overlap.

One of the parameters influencing the quality of measured data is the number of sampled droplets. It is reasonable to expect, that the actual drop size distributions are smooth, including the peripheries or so called tails, where the droplet fraction is small. To obtain such distribution it is

important to sample a sufficient number of droplets. Various sampling numbers are adopted, form 2,000 (Li et al., 2012), 10,000 (Panchagnula and Sojka, 1999), 20,000 (Jedelský et al., 2004) up to 50,000 and 100,000 (Liu et al., 2010). There is no universal rule to determine this number, but it can be derived during the measurement itself by judging on the convergence of the drop size distribution. In some cases the smoothness of the drop size distribution might be also compromised by a wrong choice of mask, or by high noise. The latter case can be remedied by shielding the measurement area from any other light sources and/or by increasing the PDA lasers power.

As mentioned above, accurate measurement of liquid mass concentration and mass flux are a vital part for successful numerical validation, especially in the area of spray combustion. The PDA technique is known to have issues when measuring mass concentration. However, in (Dullenkopf et al., 1998) it is shown, that the Dual PDA technique (an extension of PDA combining conventional PDA and planar PDA) gives much better results. Dullenkopf compares flux measurements of PDA, Dual PDA and patternator, showing a noticeable improvement for Dual PDA over the conventional PDA (see Figure 3). He takes into account a pressure swirl and airblast atomizer and there is no reason not to assume a similar improvement would be observed in the case of effervescent atomizers. Naturally, this needs to be confirmed by dedicated experimental measurement.

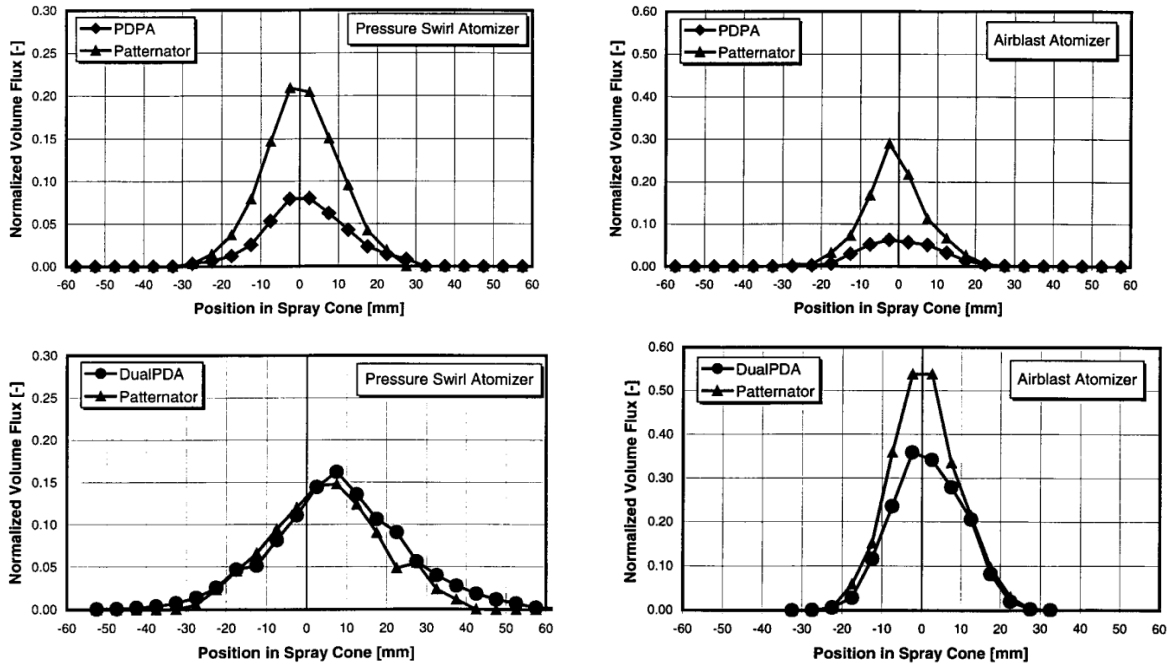

Figure 3. Comparison of volume flux measurements for two types of atomizer using different measurement techniques, reprinted from (Dullenkopf et al., 1998)

Table 1. Experiment details

Liquid	Water
Gas	Air
Liquid mass flow rate	31.2 kg/h
GLR	11%
Discharge orifice diameter	2.5 mm

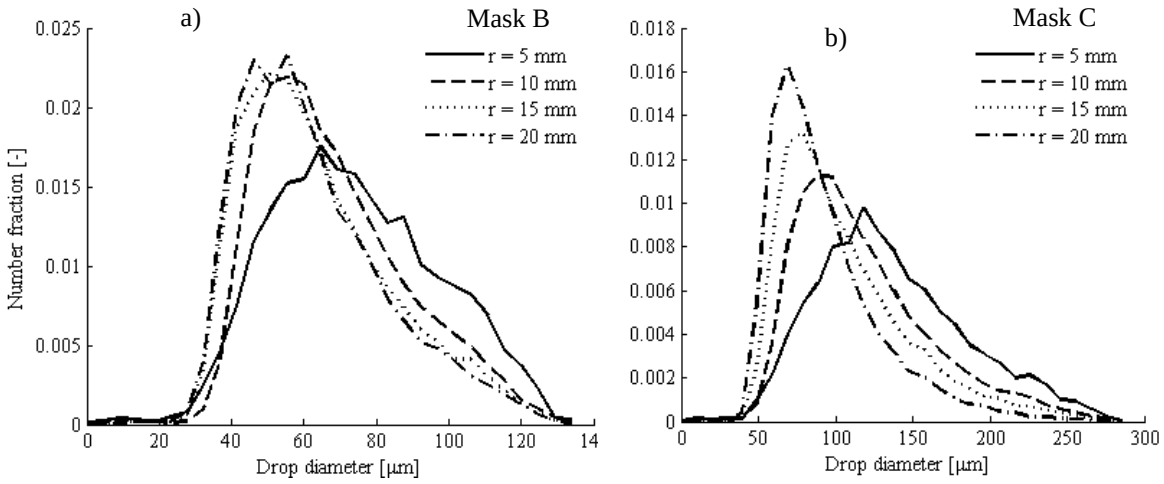

Figure 4. Drop size distribution functions 50 mm downstream from nozzle, r is radial distance from spray centreline

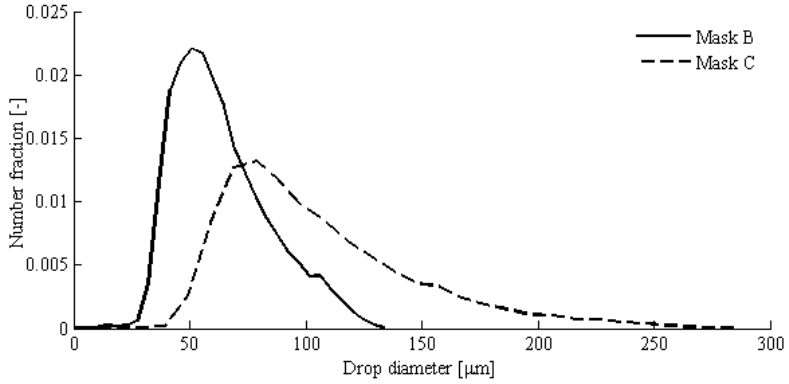

Figure 5. Comparison of drop size distributions for different mask choices at r = 15 mm

5.5.5 Results and Discussion

In this section preliminary results will be shown with focus on mask choice and its implications. The experimental measurements are being conducted at Maurice J. Zucrow Laboratories at Purdue University, USA using a Dual PDA apparatus. The spray was generated using the effervescent atomizer in vertical position described in (Jedelský et al., 2009) as E38. Operating conditions and details of the measurements are noted in Table 1. As mentioned in the previous sections, a wrong mask choice can cause trimming of the resulting drop size distributions and therefore loss of important data. Moreover, it is often not obvious or easy to notice that a wrong mask is being used.

Two sets of measurement of drop size distributions have been performed (see Figure 4). Data were taken 50 mm downstream from the discharge orifice at 4 equidistant radial positions. Two different masks were employed. Mask B allows detection of droplets up to 130 μm and mask C up to 270 μm. At each measurement location, the same amount of droplets has been recorder for each of the two masks.

From Figure 4a) alone it is hard to determine if any trimming is occurring. The most suspicious measurement point is at r = 5 mm, but it is still impossible to even approximately determine the amount of trimmed droplets. Only when comparing with Figure 4b) the amount of trimming can be fully seen. A detailed comparison showing the substantial amount of trimmed

droplets in the case of mask B can be seen in Figure 5. Evidently it can be very misleading to judge the mask choice based only on the distribution tails. Even if these tails are very small, it does not necessarily mean there is no trimming. As shown in Figure 4 and Figure 5 even a rapidly decreasing drop size distributions are not proof of right mask choice. It is a question to what extent the trimmed data can be used. Even if the mass flow rates were known, which as mentioned before is a challenge on its own, it is unclear whether the merged distribution would be closer to reality. Also, even with the seemingly convergent distribution in the case of mask C, it is still impossible to rule out further trimming, since as in the case with mask B, the distribution curve goes all the way to the maximal diameter the mask is able to detect.

5.5.6 Conclusions

The present work provides an overview of spray measurements with emphasis on effervescent spray formation and stresses the need of experimental data for verification and validation of numerical spray models for combustion purposes. It is shown that a great deal of available experimental results are insufficient for validation of numerical models, since only a coarse and global representation of the spray is given. Furthermore it is highlighted, that higher spatial resolution of measurements is needed, although recently detailed studies started to appear (Li et al., 2012; Lian-sheng et al., 2012).

Furthermore, a methodology for effervescent spray measurement using PDA technique is suggested that produces experimental results suitable for numerical model validations. Ideally, at least two sets of radial measurements points at various axial locations should be performed focusing on drop size and velocity distributions and also on mass flux distribution. Attention must be paid to the mask choice in order to prevent trimming of the drop distributions. The issue of unreliable mass flux measurements using PDA is addressed, but it is shown, that the Dual PDA extension of the original technique is able to at least partially overcome this problem. However, a similar study to that of (Dullenkopf et al., 1998) needs to be performed for the case of effervescent atomization.

In the last section experimental data are shown that demonstrate how a wrong mask choice can greatly skew obtained drop size distributions. Moreover, such mistake might be hard to notice, therefore a great caution should be addressed to this issue.

Acknowledgement

The present work has been supported by European Regional Development Fund in the framework of the research project NETME Centre under the Operational Programme Research and Development for Innovation, reg. number CZ. 1.05/2.1.00/01.0002 and by the Fulbright Scholarship Grant

References

Aliseda, A., Hopfinger, E.J., Lasheras, J.C., Kremer, D.M., Berchielli, A., Connolly, E.K., 2008. Atomization of viscous and non-newtonian liquids by a coaxial, high-speed gas jet. Experiments and droplet size modeling. International Journal of Multiphase Flow 34, 161–175. doi:10.1016/j.ijmultiphaseflow.2007.09.003

Apte, S.V., Gorokhovski, M., Moin, P., 2003. LES of atomizing spray with stochastic modeling of secondary breakup. International Journal of Multiphase Flow 29, 1503–1522. doi:10.1016/S0301-9322(03)00111-3

Avulapati, M.M., Ravikrishna, R.V., 2012. An Experimental Study on Effervescent Atomization of Bio-oil Fuels. Atomization and Sprays 22, 663–685. doi:10.1615/AtomizSpr.2012006482

Babinsky, E., Sojka, P.E., 2002. Modeling drop size distributions. Progress in Energy and Combustion Science 28, 303–329. doi:10.1016/S0360-1285(02)00004-7

Broukal, J., Hájek, J., 2011a. Validation of an effervescent spray model with secondary atomization and its application to modeling of a large-scale furnace. Applied Thermal Engineering 31, 2153–2164. doi:16/j.applthermaleng.2011.04.025

Broukal, J., Hájek, J., 2011b. Effervescent Spray Modelling: Investigation of Drop Momentum Models and Validation by Measured Data. Chemical Engineering Transactions 25, 797–802. doi:10.3303/CET1021186

Broukal, J., Hájek, J., Jedelský, J., 2010. Effervescent atomization of extra-light fuel-oil: Experiment and statistical evaluation of spray characteristics, in: Proceedings of 23rd European Conference on Liquid Atomization and Spray Systems. Presented at the ILASS-Europe 2010, Brno, Czech Republic, pp. 1–10.

Dullenkopf, K., Willmann, M., Wittig, S., Schöne, F., Stieglmeier, M., Tropea, C., Mundo, C., 1998. Comparative Mass Flux Measurements in Sprays using a Patternator and the Phase-Doppler Technique. Particle & Particle Systems Characterization 15, 81–89. doi:10.1002/(SICI)1521-4117(199804)15:2<81::AID-PPSC81>3.0.CO;2-A

Jedelsky, J., Jicha, M., 2012. Spatially and Temporally Resolved Distributions of Liquid in an Effervescent Spray. Atomization and Sprays 22, 603–626. doi:10.1615/AtomizSpr.2012006055

Jedelský, J., Jícha, M., Otáhal, J., Katolický, J., Landsmann, M., 2007. Velocity field in spray of twin-fluid atomizers, in: 21st Sympozium on Anemometry, Proceedings. Presented at the 21st Sympozium on Anemometry, Prague, Czech Republic, pp. 67–74.

Jedelský, J., Jícha, M., Sláma, J., 2004. Characteristics And Behaviour Of Multi-Hole Effervescent Atomizers, in: 19th International Conference on Liquid Atomization and Spray Systems - ILASS Europe. Presented at the 19th ILASS Europe, Nottingham, UK, pp. 521–526.

Jedelský, J., Jícha, M., Sláma, J., Otáhal, J., 2009. Development of an Effervescent Atomizer for Industrial Burners. Energy & Fuels 23, 6121–6130. doi: 10.1021/ef900670g

Juslin, L., Antikainen, O., Merkku, P., Yliruusi, J., 1995. Droplet size measurement: I. Effect of three independent variables on droplet size distribution and spray angle from a pneumatic nozzle. International Journal of Pharmaceutics 123, 247–256. doi:10.1016/0378-5173(95)00081-S

Lefebvre, A.H., Wang, X.F., Martin, C.A., 1988. Spray Characteristics of Aerated-Liquid Pressure Atomizers. Journal of Propulsion and Power 4, 293–298.

Li, Z., Wu, Y., Cai, C., Zhang, H., Gong, Y., Takeno, K., Hashiguchi, K., Lu, J., 2012. Mixing and atomization characteristics in an internal-mixing twin-fluid atomizer. Fuel 97, 306–314. doi:10.1016/j.fuel.2012.03.006

Lian-sheng, L., Hua, Y., Xiang, G., Runze, D., Yan, Y., 2012. Experimental Investigations on the Spray Combustion Produced by Effervescent Atomizers, in: 2012 International Conference on Computer Distributed Control and Intelligent Environmental Monitoring (CDCIEM). Presented at the 2012 International Conference on Computer Distributed Control and Intelligent Environmental Monitoring (CDCIEM), pp. 305 –311. doi:10.1109/CDCIEM.2012.79

Liu, M., Duan, Y., Zhang, T., 2010. Evaluation of effervescent atomizer internal design on the spray unsteadiness using a phase/Doppler particle analyzer. Experimental Thermal and Fluid Science 34, 657–665. doi:10.1016/j.expthermflusci.2009.12.007

Mandato, S., Rondet, E., Delaplace, G., Barkouti, A., Galet, L., Accart, P., Ruiz, T., Cuq, B., 2012. Liquids' atomization with two different nozzles: Modeling of the effects of some processing and formulation conditions by dimensional analysis. Powder Technology 224, 323–330. doi:10.1016/j.powtec.2012.03.014

Panchagnula, M.V., Sojka, P.E., 1999. Spatial droplet velocity and size profiles in effervescent atomizer-produced sprays. Fuel 78, 729–741. doi:10.1016/S0016-2361(98)00192-6

Park, S.H., Kim, H.J., Suh, H.K., Lee, C.S., 2009. Experimental and numerical analysis of spray-atomization characteristics of biodiesel fuel in various fuel and ambient temperatures conditions. International Journal of Heat and Fluid Flow 30, 960–970. doi:10.1016/j.ijheatfluidflow.2009.04.003

Pougatch, K., Salcudean, M., Chan, E., Knapper, B., 2009. A two-fluid model of gas-assisted atomization including flow through the nozzle, phase inversion, and spray dispersion. International Journal of Multiphase Flow 35, 661–675. doi:10.1016/j.ijmultiphaseflow.2009.03.001

Tembely, M., Lecot, C., Soucemarianadin, A., 2011. Prediction and evolution of drop-size distribution for a new ultrasonic atomizer. Applied Thermal Engineering 31, 656–667. doi:10.1016/j.applthermaleng.2010.09.027

Wang, X., Wu, X., Liao, G., Wei, Y., Qin, J., 2002. Characterization of a water mist based on digital particle images. Experiments in Fluids 33, 587–593.

5.6 Experimental Analysis of Spatial Evolution of Mean Droplet Diameters in Effervescent Sprays

Abstract

Effervescent atomization has established itself in the past decade as a promising alternative to conventional spray formation mechanisms. A great effort is currently being put into understanding the involved phenomena and developing numerical models to predict outcomes of processes relying on effervescent atomizers (i.e. spray combustion, coating, drying). This still proves to be a formidable challenge as effervescent atomization is a complex process involving two phase flow.

The presented paper focuses on mean droplet sizes and how they vary throughout effervescent sprays at different operating conditions. The experiment was performed using Phase Doppler Anemometry (PDA) and the droplet data were collected in multiple locations varying both axially and radially. At each measurement location the Sauter Mean Diameter (SMD) was computed. The preliminary results show that closer to the spray nozzle the bigger droplets are concentrated in the spray core, while the small droplets are in the peripheral regions. However, this trend is slowly reversing with increasing distance from the spray nozzle. Finally, from a certain distance the initial trend is completely reversed with the small droplets being in the spray core, while larger droplets are found closer to the edge of the spray. Moreover, this phenomenon seems to be independent of operating conditions. Reasons for such behaviour are suggested and discussed. Furthermore, SMD sensitivity to operating conditions is analysed.

5.6.1 Introduction

In the field of spray combustion, especially in oil furnaces and combustors, effervescent atomizers (twin fluid atomizers with internal mixing) introduced by Lefebvre et al. (1988) are quickly gaining on popularity over more traditional forms of atomization (Kermes et al., 2012). The spray formation process in this type of atomizers does not rely solely on high liquid pressure and aerodynamic forces, instead a small amount of gas, usually air, is introduced in the liquid before it exits the atomizer and a two phase flow is formed (Jedelský et al., 2007). When the mixture exits through the nozzle, the pressure drop forces the gas bubbles to expand causing the liquid to break up. This breakup mechanism allows the use of lower injection pressures and larger nozzle diameters without compromising the drop-size distribution (Babinsky and Sojka, 2002). The only obvious drawback of this method, apart from the need to have a source of pressurized gas, is its complexity originating from the two-phase flow inside the nozzle. This complexity is the major challenge in finding accurate mathematical and numerical models that could be used as an aid to designers of burners and furnaces. Extensive experimental research is ongoing in the area of effervescent sprays aimed at providing validation data for numerical models in terms of Sauter mean diameter (SMD). The Sauter Mean Diameter is defined as a diameter of a representative droplet having the same volume/surface area ratio as the whole spray. As pointed out in (Broukal and Hájek, 2011a), this can be a very rough approach, since even if the global SMD of the spray in question is in good agreement with measurements, local SMD values may be significantly different and thus cause faulty numerical predictions. Moreover, as shown in (Broukal and Hájek, 2011b) and (Juslin et al.,1995), sprays often exhibit multimodal behaviour in drop size distributions, which further raises the question about legitimacy of using a single representative diameter. To remedy this, more detailed information is needed to make really sensible validations. Namely, data about radial distribution of droplet size and velocity would be

desirable (or equivalently depending on spray angle), especially for the case of large nozzles in industrial burners. In the last decade few papers can be found that address the issue of radial drop size distribution and radial SMD evolution sprays. Park et al. (2009) employed the wave breakup model to investigate biodiesel spray generated by two pneumatic nozzles. He takes into account various fuel and ambient conditions and focuses on SMD evolution. Along with axial SMD evolution, also radial SMD evolution was reported. Unfortunately, only three radial SMD were disclosed. In (Pougatch et al., 2009) an effervescent spray model is presented and applied to water-air atomization. Radial drop diameter evolution is predicted at various axial positions, but no comparison with experimental data has been made. Recently the situation has improved as more researchers focus in more detail on a complex effervescent spray measurement (Li et al., 2012). Lian-sheng et al. (2012) performs a detailed experimental measurement of effervescent spray combustion. The work reports various radial SMD and axial drop size distributions. Also, a swirl effervescent atomizer is employed and the influence of swirl on spray angle is demonstrated. However, the liquid mass flow rates are still in a lab-scale region with a maximum of only 10 kg/h.

The purpose of this study is to perform an experimental study with emphasis on SMD spatial evolution (both axial and radial) at various operating conditions that can be regarded as large-scale.

Table 1. Operating conditions

Measurement	Mass flow rate [kg/h]	GRL [%]	Liquid pressure [kPa]	Gas pressure [kPa]
#1	31.2	5	34.5	55.2
#2		10	89.6	144.1
#3		15	144.8	234.4
#4	42	5	72.4	103.4
#5		10	182.7	250.3
#6		15	289.6	386.1
#7	60	5	165.5	200
#8		10	310.3	399.9

Table 2. Measurement points overview

		Radial distance from spray axis [cm]					
Axial distance [cm]	5	0	0.5	1	1.5	2	2.5
	10	0	1	2	3	4	
	15	0	1	2	3	4	5

5.6.2 Experimental Setup

The experimental measurements where performed at Maurice J. Zucrow Laboratories at Purdue University, USA using a Dual PDA apparatus. The PDA is a non-intrusive optical technique, on-line and in-situ. Due to the nature of the technique, optical access to the measurement area is needed, which can be sometimes limiting for on-site industrial measurements. Since the method requires particles to be spherical (or only slightly deformed), measurements must be taken at a sufficient distance from the discharge orifice. Also, the method

is not suitable for very dense spray regions. The measurement device consists of a laser based optical transmitter, an optical receiver, a signal processor and a software for data analysis.

The spray was generated using vertically positioned effervescent atomizer described in (Jedelský et al., 2009) as E38 with nozzle diameter 2.5 mm. As seen in Table 1, eight various sprays have been measured varying in gas-liquid-ratio (GLR) and mass flow rate. At each operating condition data from 17 measurement points have been collected. The measurement points where divided among three planes perpendicular to the spray axis at distances 5, 10 and 15 cm from the nozzle tip. At each plane the points where distributed radially in an equidistant fashion starting from the spray axis (see Table 2). The working liquid was water and atomizing gas air, both at room temperature.

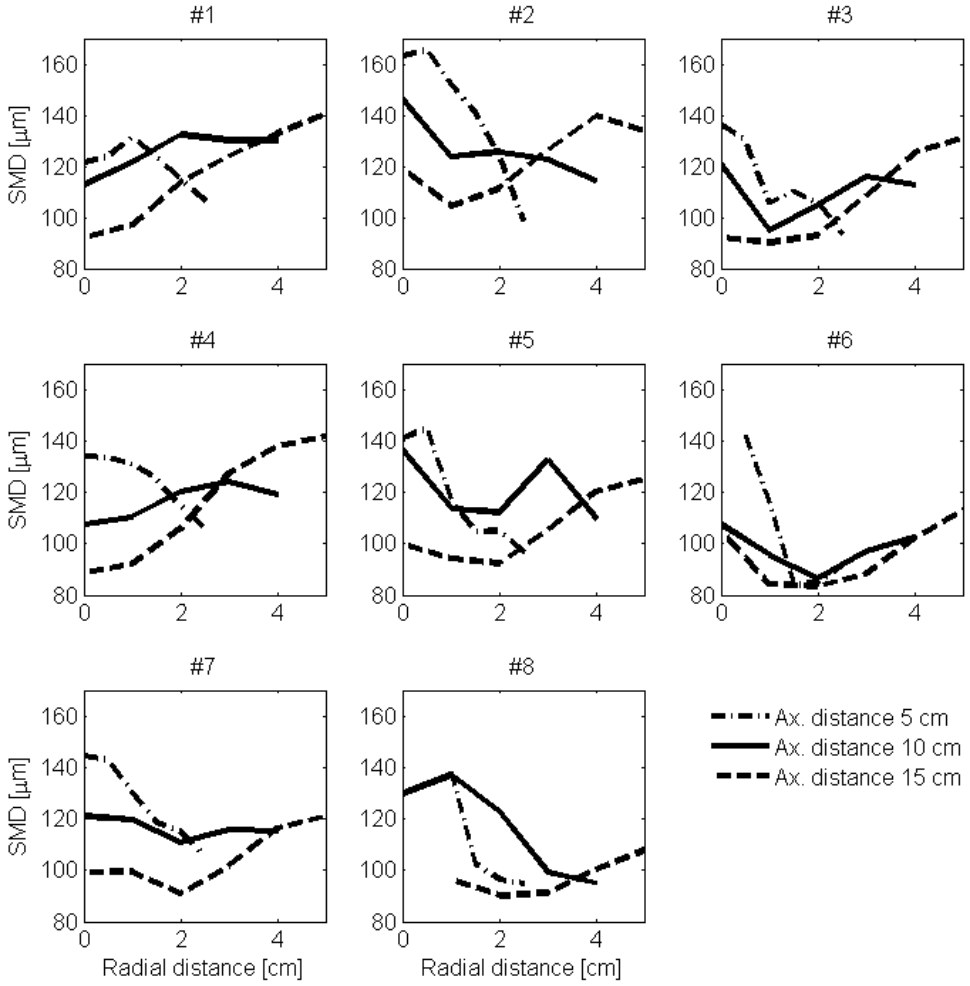

Figure 1. Radial SMD evolution at various axial distances for operating conditions #1 to #8

5.6.3 Results and Discussion

For combustion applications it is general practice to use SMD as a way of simplifying the spray in question. As shown in the previous paragraphs, a single value of SMD is not always suitable for global spray description. However, SMD can still be very useful to describe the spray locally. And in order to get a global spray description, multiple SMDs are needed.

The present work reports numerous measurements, in which drop size data were acquired at 17 locations for each of 8 different sprays. Four measurement points yielded no data due to the

local spray behaviour and experimental setup (one in #6 and three in #8). Figure 1 shows the radial evolution of SMD at various axial distances for operating conditions #1 to #8. In the region close to the spray nozzle (axial distance 5 cm) the SMD decreases monotonically with radial distance. This trend is valid for all operating conditions with only few exceptions (#1, #2, #3), which are exhibiting decreasing SMD nonetheless. On the other hand, SMD in the region further downstream (axial distance 15 cm) follows almost an opposite trend, when SMD increases with radial distance. The trend is fairly monotonous at low GLR (#1, #4 and #7) but with higher GLR local minima and maxima start to appear, although the overall increase in SMD between the spray core and rim is still obvious. Somewhere between these two axial distances must lie a region where the transition between the two aforementioned trends occurs. Again, at low GLR (#1, #4 and #7) the SMD evolution at axial distance 10 cm is quite flat, indicating the possible transition between the decreasing and increasing SMD trends, but more measurements would be needed to confirm this hypothesis.

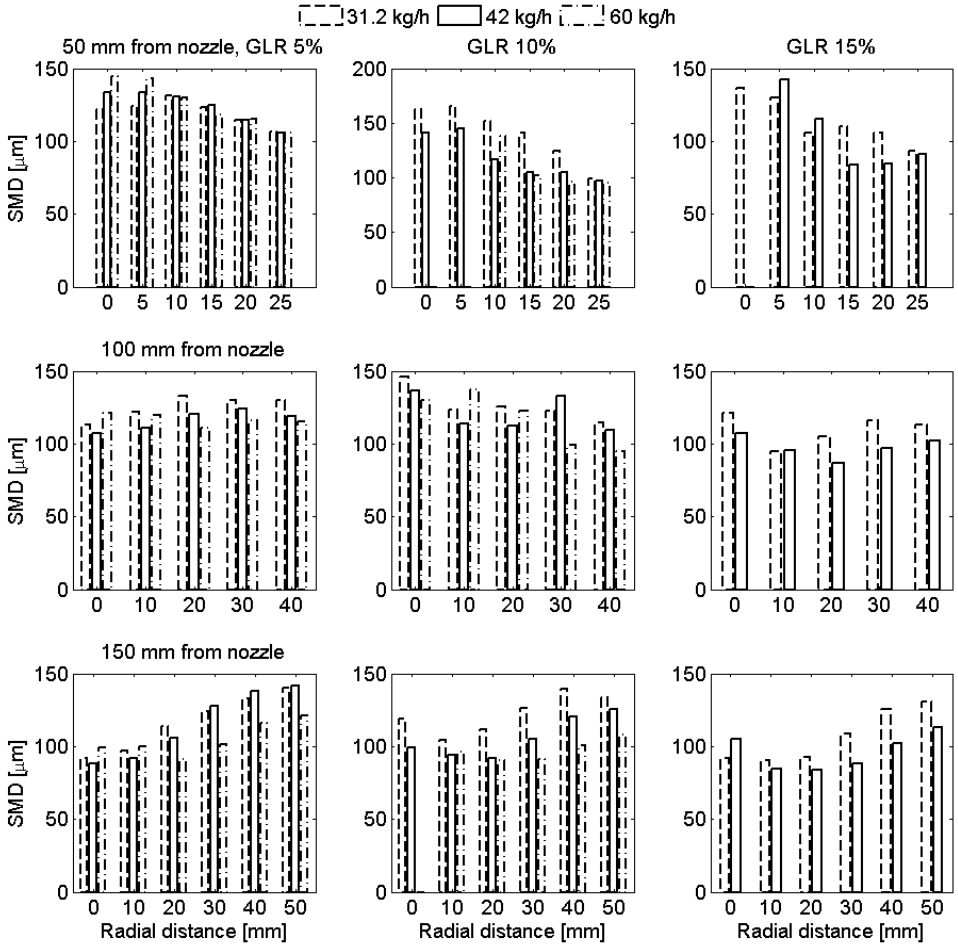

Figure 2. Effect of mass flow rate on SMD at various axial distances and GLRs

One of the possible explanations for the change of SMD radial evolution is that downstream in the spray rim region lower velocities favour drop coalescence. This could be supported by the fact that the SMD in the spray core decreases with axial distance, similarly to the radial SMD evolution trend in the close-to-nozzle regions. In both these cases relative velocities are still high preventing drop coalescence and promoting secondary breakup. On the other hand in the

peripheral regions further downstream the velocities decrease enough to allow droplets to coalesce increasing the local SMD.

Data represented in Figure 2 show the effect of mass flow rates on local SMD values. Rows represents axial distances and columns different GLRs. In general it can be said that outside of the spray core, increase in mass flow rate leads to decrease of SMD. The situation in the spray core is not as clear. In some cases (e.g. GLR 5% and axial distance 5 cm) the SMD in the core increases with mass flow rate. In few other cases there is no clear trend and it looks like mass flow rate has only little effect on SMD (cases with GLR 5% and 15%). One thing to note is that the SMD values in the spray core have a peak for GLR 10%. This points to a change in two-phase flow regime inside the atomizer and is also consistent with the findings of Ochowiak (et al., 2010), where a transition between the bubbly and annular regime was found to be at approximately GLR 7% for water-air mixture.

The effect of GLR on local SMD at various mass flow rates is displayed in Figure 3. No clear dependency can be inferred in the core region of the sprays. This is partly due to the fact pointed out in the previous paragraph, being that the core SMDs are highest for GLR 10%. In the spray rim regions however, the SMD gradually decreases with increasing GLR. This trend has only few exceptions, most notably in the case of 31.2 kg/h and axial distance 5 cm, where the SMD of GLR 10% is highest both in the core and outside of the core.

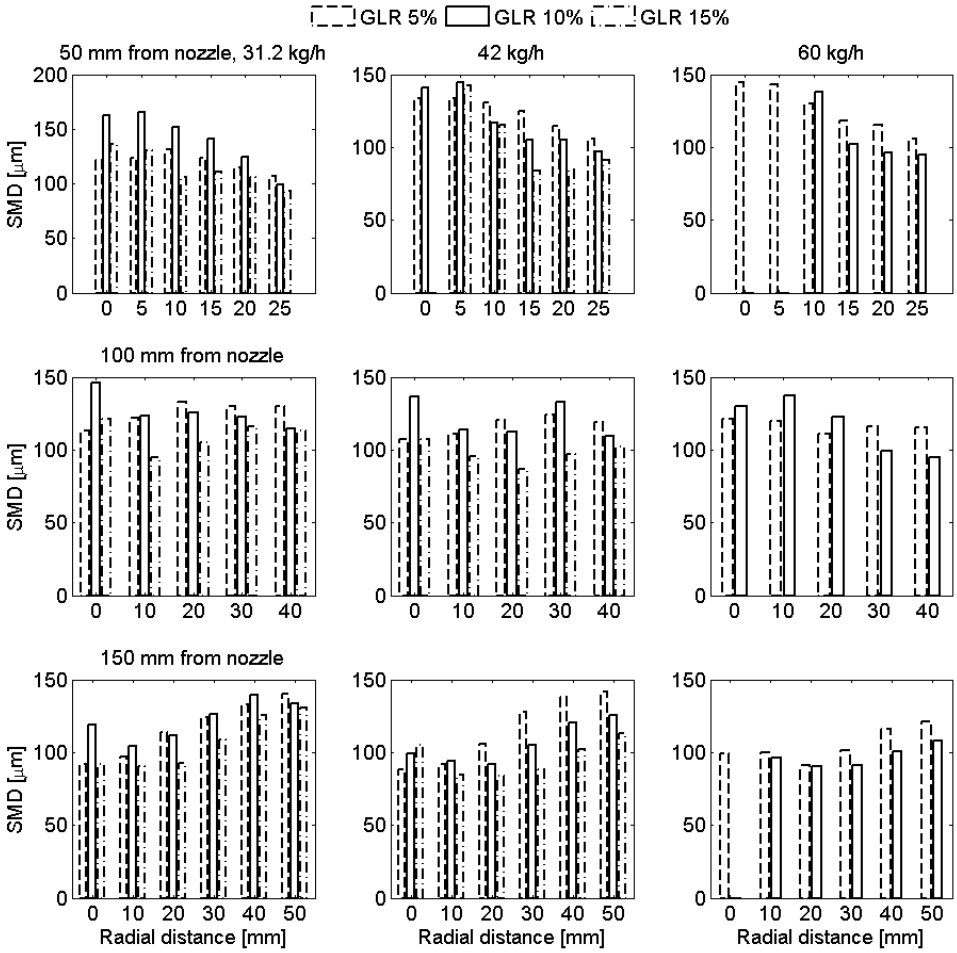

Figure 3. Effect of GLR on SMD at various axial distances and mass flow rates

More detailed analysis of particle drop size distributions instead of the local SMDs is required in order to enhance the understanding of the mechanisms that govern the behaviour of effervescent sprays. Previous results of a study performed on a smaller scale have already shown e.g. that multimodality of drop size distributions is quite common (Broukal and Hájek, 2011b). An adequate method to represent effervescent spray in numerical computations involving liquid fuel combustion should resolve these features in sufficient detail.

5.6.4 Conclusions

The present work discloses results of an experimental study focused on local SMD values in industry-scale effervescent sprays. The effect of mass flow rate and GLR on local SMD has been investigated based on numerous experimental data. Examining SMD values varying both axially and radially has shown that while in the regions closer to the spray nozzle SMD decreases toward the spray edge, in the regions further downstream this trend is completely opposite. This finding holds true regardless of the operating conditions. An explanation is proposed to explain this behaviour. The presented results furthermore accentuate the effervescent spray complexity and can be used as a solid foundation ground on which future numerical models for effervescent sprays can be validated.

Acknowledgement

This work is an output of research and scientific activities of NETME Centre, regional R&D centre built with the financial support from the Operational Programme Research and Development for Innovations within the project NETME Centre (New Technologies for Mechanical Engineering), Reg. No. CZ.1.05/2.1.00/01.0002 and, in the follow-up sustainability stage, supported through NETME CENTRE PLUS (LO1202) by financial means from the Ministry of Education, Youth and Sports under the „National Sustainability Programme I“.

References

Babinsky E., Sojka P. E., 2002, Modeling drop size distributions, Progress in Energy and Combustion Science, 28(4), 303-329.

Broukal J., Hájek J., 2011a, Validation of an effervescent spray model with secondary atomization and its application to modeling of a large-scale furnace, Applied Thermal Engineering, 31(13), 2153–2164, DOI: 10.1016/j.applthermaleng.2011.04.025.

Broukal J., Hájek J., 2011b, Effervescent Spray Modelling: Investigation of Drop Momentum Models and Validation by Measured Data, Chemical Engineering Transactions, 25(1), 797–802, DOI:10.3303/CET1125133.

Jedelský J., Jícha M., Otáhal J., Katolický J., Landsmann M., 2007, Velocity field in spray of twin-fluid atomizers, in 21st Sympozium on Anemometry, Proceedings, pp. 67-74, Prague, Czech Republic.

Jedelský J., Jícha M., Sláma J., Otáhal J., 2009, Development of an Effervescent Atomizer for Industrial Burners, Energy & Fuels, 23(12), 6121–6130.

Juslin L., Antikainen O., Merkku P., Yliruusi J., 1995, Droplet size measurement: I. Effect of three independent variables on droplet size distribution and spray angle from a pneumatic nozzle, International Journal of Pharmaceutics, 123(2), 247–256.

Kermes V., Skryja P., Nejezchleb R., 2012, Obstacles in the Utilization of Biodiesel as the Fuel in Small Stationary Combustion Units, Chemical Engineering Transactions, 29, 961–66, DOI:10.3303/CET1229161.

Lefebvre A. H., Wang X. F., Martin C. A., 1988, Spray Characteristics of Aerated-Liquid Pressure Atomizers, Journal of Propulsion and Power, 4(4), 293–298.

Li Z., Wu Y., Cai C., Zhang H., Gong Y., Takeno K., Hashiguchi K., Lu J., 2012, Mixing and atomization characteristics in an internal-mixing twin-fluid atomizer, Fuel, 97, 306–314.

Lian-sheng L., Hua Y., Xiang G., Runze D., Yan Y., 2012, Experimental Investigations on the Spray Combustion Produced by Effervescent Atomizers, in 2012 International Conference on Computer Distributed Control and Intelligent Environmental Monitoring (CDCIEM), pp. 305 – 311.

Ochowiak M., Broniarz-Press L., Rozanski J., 2010, The discharge coefficient of effervescent atomizers, Experimental Thermal and Fluid Science, 34(8), 1316–1323.

Park S. H., Kim H. J., Suh H. K., Lee C. S., 2009, Experimental and numerical analysis of spray-atomization characteristics of biodiesel fuel in various fuel and ambient temperatures conditions, International Journal of Heat and Fluid Flow, 30(5), 960–970.

Pougatch K., Salcudean M., Chan E., Knapper B., 2009, A two-fluid model of gas-assisted atomization including flow through the nozzle, phase inversion, and spray dispersion, International Journal of Multiphase Flow, 35(7), 661–675.

5.7 An Experimental Study of Effervescent Sprays: Axial Evolution of Mean Drop Diameter

5.7.1 Introduction

Effervescent atomization is a spray formation technique pioneered by Lefebvre and his colleagues in the late 1980s (Lefebvre et al, 1988). The idea behind this approach is to create a two phase flow inside the atomizer body by introducing the so-called atomizing gas to the liquid. Upon leaving the discharge orifice the atomizing gas in the two-phase mixture expands, thus aiding in the liquid breakup process. Such approach presents a very promising alternative to conventional techniques as it offers many advantages, including lower operating pressures, larger discharge orifices, lower sensitivity to viscosity and others (Babinsky and Sojka, 2002). It is therefore no surprise that effervescent atomization is becoming more and more frequently used in many industrial applications, ranging from pharmaceuticals, spray drying and coating to both internal and atmospheric combustion.

Such interest obviously necessitates development of predictive models that would help us gain insight into the complexities of effervescent atomization and also help industry-based engineers and designers with their decision-making. This is especially true in the area of liquid (or spray) combustion, where turbulence, chemistry and radiation play also a very important role and in order to obtain relevant numerical results reliable models are needed. Broukal and Hájek (2011) pointed out the need for effervescent spray models to take into account spatial drop size evolution and in order to validate such models experimental data is needed. Although a great deal of experimental research on effervescent sprays has been carried out, only a small portion of it reports radial evolution of drop sizes. Panchagnula and Sojka (1999) reported radial Sauter Mean Diameter (SMD) evolutions in their work. The reported data surprisingly show almost no influence of radial coordinate on SMD. This is probably due to the measurements being performed more than 30 cm from the spray nozzle. At such axial distance (considering the operating conditions used) the effervescent spray is already fully mixed due to its turbulent nature (Panchagnula and Sojka, 1999). A more interesting evolution of radial SMDs is presented in (Li et al., 2012). Radial measurement at three axial locations are performed and display a very similar trend of SMD increasing with radial distance. Similar measurements have been performed in (Broukal and Hájek, 2014) but with very different outcome, where closer to the spray nozzle the SMD would decrease with radial distance, while further downstream the trend was completely reversed. Radial SMD evolution is also investigated by Xu et al. (2012) for a case of multi-orifice effervescent atomizer, but measurements are performed at only one axial location. Axial SMD evolution is a more commonly used criterion to validate spray models and therefore experimental data are reported more frequently (Apte et al., 2003; Qian et al., 2010). In his work Apte develops an LES model for secondary atomization but the validation in terms of SMD occurs only using a single experimental value. Qian develops a fitting formula for axial SMD of effervescent sprays based both on the results of the previously proposed numerical model of Xiong et al (2009) and on multiple experimental axial values of SMD.

The purpose of this paper is to perform a deeper investigation of the axial evolution of SMD in effervescent sprays. The influence of liquid mass flow rate and gas-liquid ratio (GLR) will be taken into account both on cross-sectional SMDs and local SMDs.

5.7.2 Experimental Apparatus and Data Analysis

The experimental results presented in this paper are based on measurements performed at Maurice J. Zucrow Laboratories at Purdue University (West Lafayette, USA). The drop size data was collected using a Dual PDA apparatus, which is a non-intrusive laser based optical technique. Due to the nature of this technique the particles are assumed to be spherical (or only slightly deformed). The spray was generated using a vertically positioned effervescent atomizer described in (Jedelský et al., 2009) as E38 (see Figure 1). The measurement operating conditions are listed in Table 1. Measurements were taken at three axial locations 5, 10 and 15 cm from the nozzle. Moreover, at each axial location multiple radial measurements were performed. The working liquid was water and atomizing gas air, both at room temperature. More information about the measurement methodology and setup can be found in (Broukal and Hájek, 2014; Broukal et al., 2013).

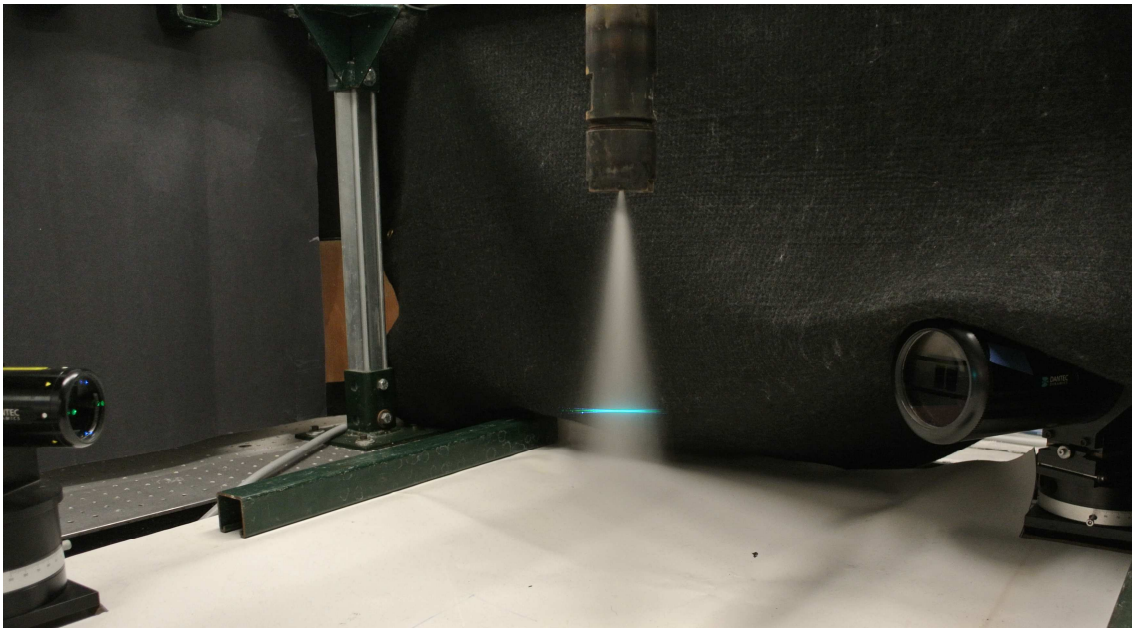

Figure 1. Experimental setup

Table 1. Operating conditions

Measurement	Mass flow rate [kg/h]	GRL [%]	Liquid pressure [kPa]	Gas pressure [kPa]
#1	31.2	5	34.5	55.2
#2		10	89.6	144.1
#3		15	144.8	234.4
#4	42	5	72.4	103.4
#5		10	182.7	250.3
#6		15	289.6	386.1
#7	60	5	165.5	200
#8		10	310.3	399.9

The drop size data were analysed using a custom made MATLAB code. Three different evolutions were examined - cross-sectional SMD, axial SMD (local SMD values on the spray axis) and boundary SMD (local SMD values on the spray edge) evolution. The last two evolutions are self-explanatory, but for the sake of clarity the cross-sectional SMD will be explained in more detail. In this work the cross-sectional SMD value is computed using the approach of Jedelský et al. (2009) as the Integral SMD (ID_{32}). The ID_{32} is calculated using data collected at various radial measurement locations. At each of these locations the local SMDs are computed and they contribute to the ID_{32} based on the ring area that they are representing and mass flow rate through these areas.

5.7.3 Results and Discussion

A quite common understanding of axial SMD evolution in effervescent sprays is that the drop size initially rapidly decreases as large droplets generated by the primary atomization process disintegrate into smaller droplets. Then as the droplets gradually lose their momentum due to the drag force, drop collisions begin to result in coalescence rather than further breakup and the droplet size slightly increases. A typical example of this predicament can be seen for example in Figure 2. However, in the experimental measurements performed in this work such behaviour has not been confirmed. Figure 3 shows the dependency of ID_{32} on axial distance for various GLRs and mass flow rates. According to the proposition mentioned in the beginning of this paragraph we should see slight increase of ID_{32}, but we only do so in the case of 31.2 kg/h and 15% GLR. In all other cases there is no obvious trend in the axial evolution, some cases even show a further decrease in ID_{32}. Overall, for each of the operating conditions the ID_{32} variability is less than 10%, which would indicate that the spray is not dense and particle interactions are scarce leading only to small fluctuations of ID_{32}. Figure 4 shows the influence of mass flow rate and GLR on ID_{32}. Each of the lines in a plot represents one of the three axial distances of the measurements. For GLRs up to 10% increase in mass flow rate results in decrease of ID_{32}. For GLR 15% however, mass flow rate seems to lead to larger ID_{32}. These findings agree with previously published experimental results, (Jedelský et al., 2009; Ghaffar et al., 2012) but some researchers claim there is no substantial effect of mass flow rate (or liquid pressure) on ID_{32} (Qian et al., 2010). The effect of GLR is similar. Its increase leads to smaller ID_{32}, which is in agreement with previously published results, e.g. (Ghaffar et al., 2012; Ochowiak, 2013).

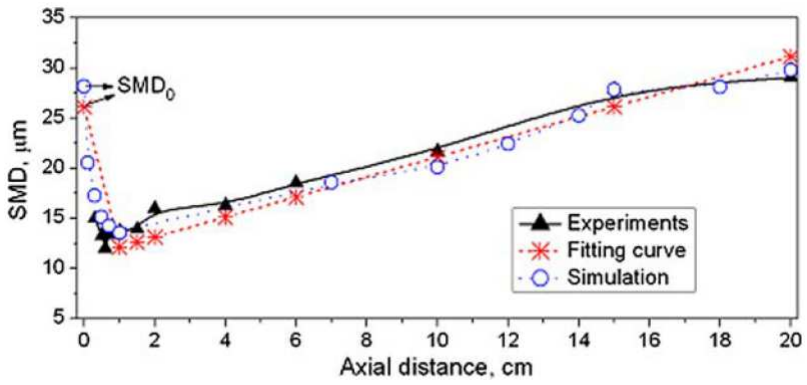

Figure 2. Axial SMD evolution, courtesy of (Qian et al., 2010)

Plots in Figure 5 represent the evolution of local SMDs on the spray axis. Some of the plots appear incomplete as only a single point is displayed. This is due to data unavailability caused be local spray behaviour and experimental setup. Data in Figure 5 display a clear trend, unlike the previous case of ID32. It is apparent, that on the spray axis the SMD decreases as we move further downstream regardless the operating conditions. This can be explained by the higher velocities in the spray core that support further breakup (either due to high relative velocity between droplets and surrounding air or as a result of drop collisions) rather than coalescence. It is probable that at a point further downstream the SMD would cease to decrease and start to increase. Figure 6 shows axial SMD as a function of liquid mass flow rate and GLR. For 5% GLR increase in liquid mass flow rate results in increase of axial SMD. In case of 10% and 15% GLR the trend is completely reversed. This might point to a transition in the two-phase flow regime from bubbly to annular flow inside the atomizer body. Ochowiak et al (2010) reports this transition occurs around 7% GLR, which would correspond to the data reported in the present work. The influence of GLR on axial SMD is non-trivial. The peak SMD values are often around 10% GLR which could again indicate towards a two-phase flow regime transition. Only for the highest liquid mass flow rate the dependence is monotonously decreasing.

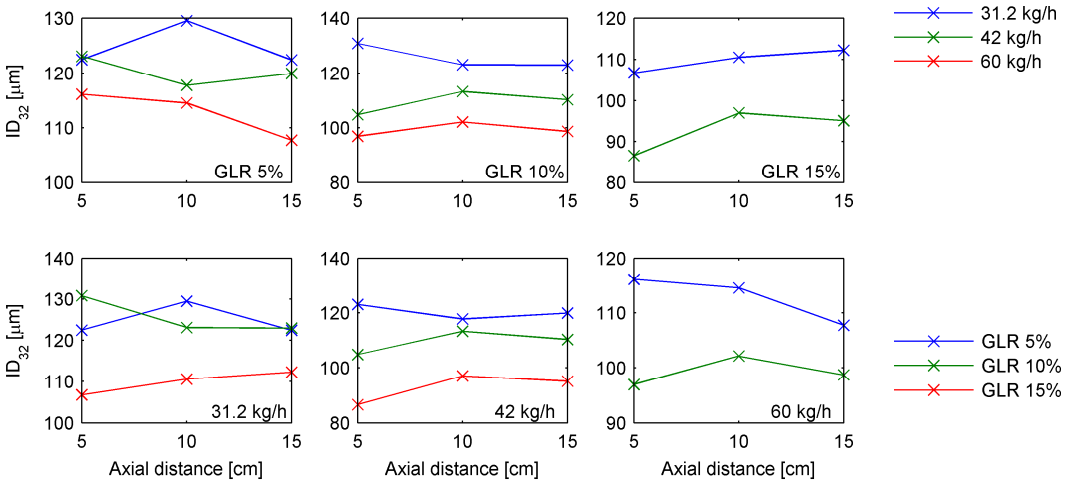

Figure 3. Plots of ID_{32} vs axial distance for different operating conditions

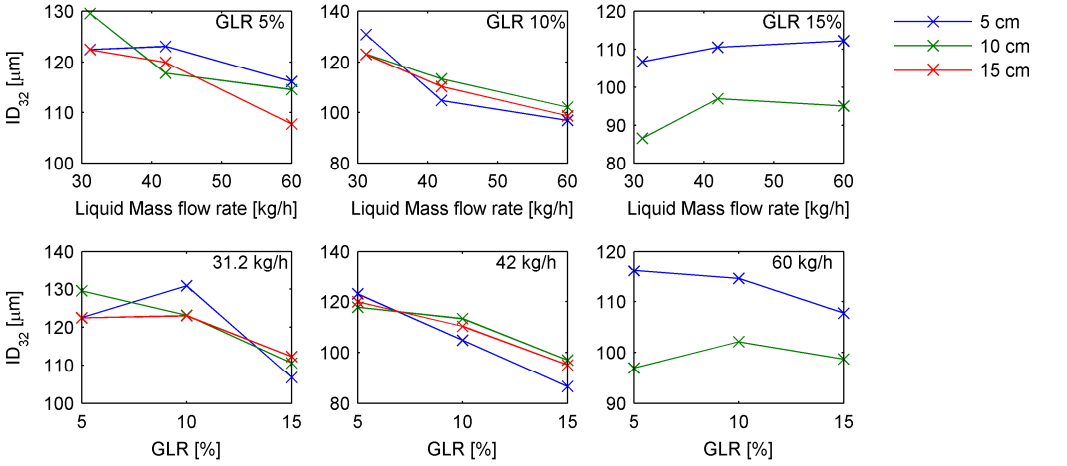

Figure 4. Plots of ID_{32} vs GLR and liquid mass flow rate at different axial distances

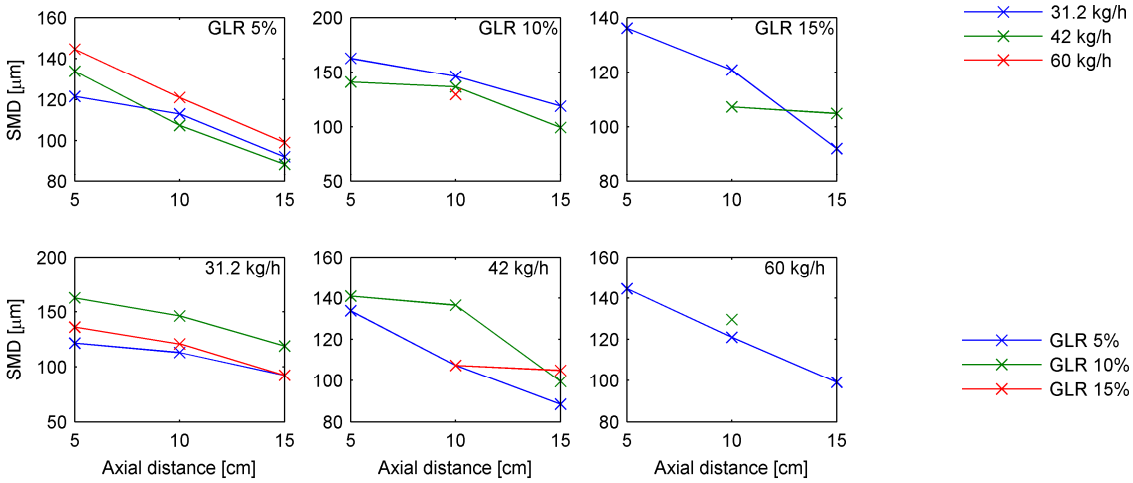

Figure 5. Plots of axial SMD vs axial distance for different operating conditions

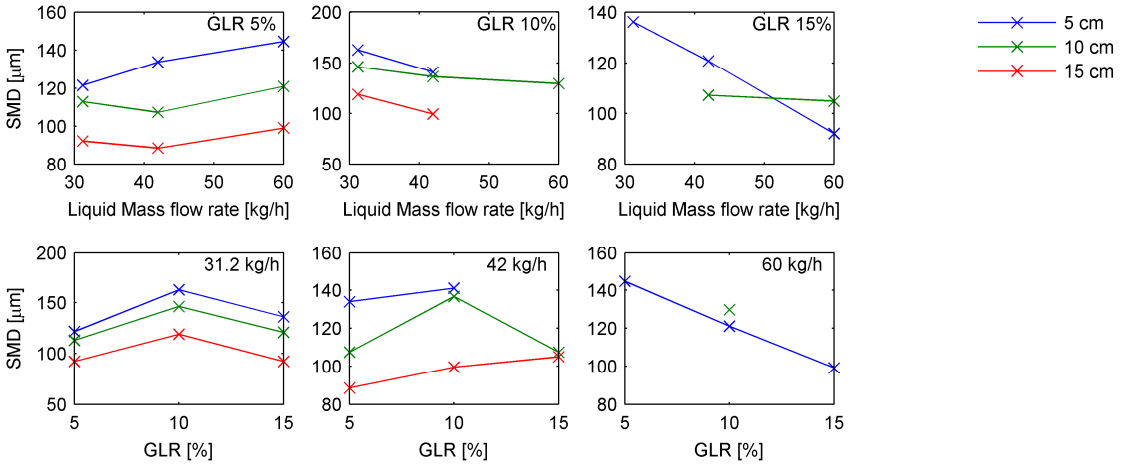

Figure 6. Plots of axial SMD vs GLR and liquid mass flow rate at different axial distances

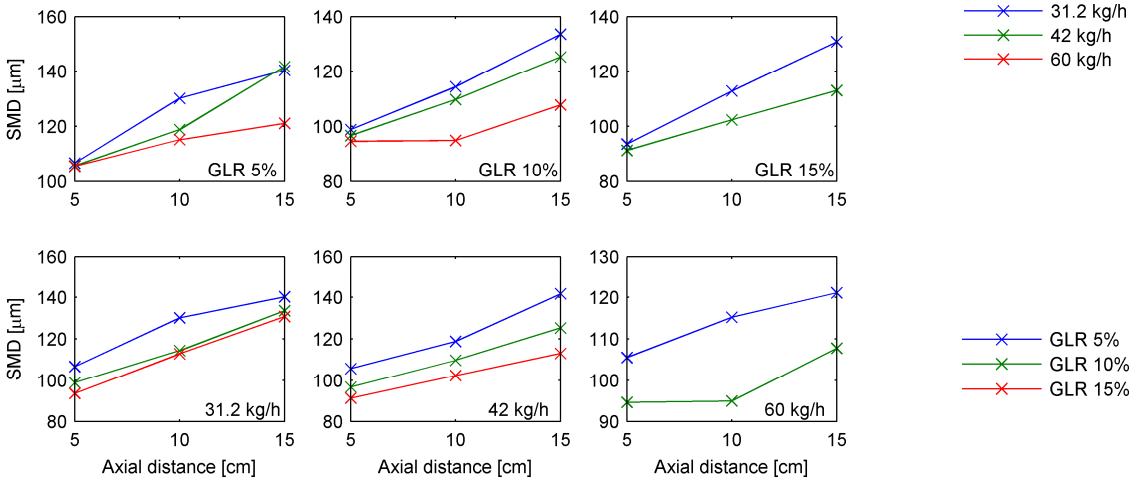

Figure 7. Plots of boundary SMD vs axial distance for different operating conditions

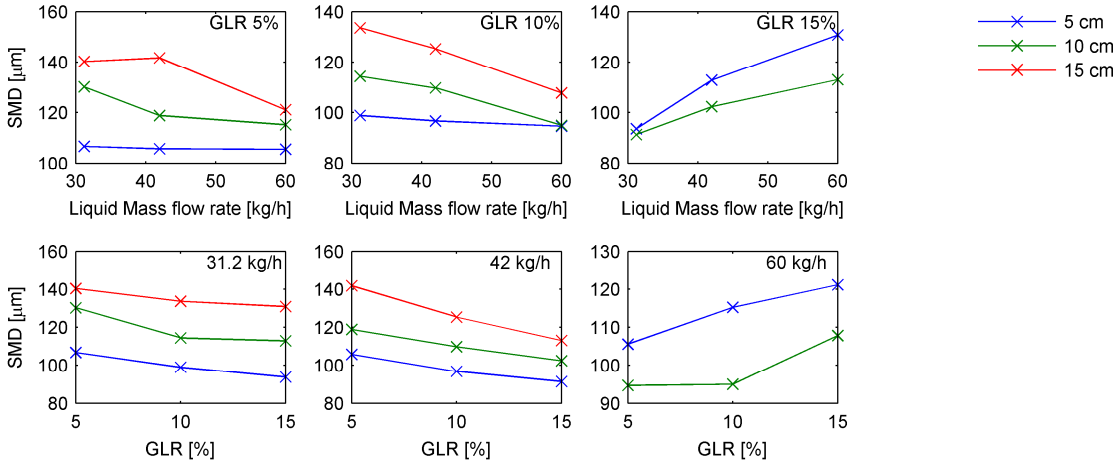

Figure 8. Plots of boundary SMD vs GLR and liquid mass flow rate at different axial distances

In plots in Figure 7 we introduce the boundary SMD evolution as the evolution of local SMDs at the edge of the spray. Similarly to the axial SMD evolution, the boundary SMD evolution also has a clear trend compared to the ID_{32} evolution, but also completely opposite compared to the axial SMD evolution. As seen in Figure 7, regardless of operating conditions, SMD at the edge of the spray increases with axial distance. This is probably caused by the rapid deceleration of the droplets on the spray edge and their subsequent coalescence. The effect of liquid mass flow rate and GLR is shown in Figure 8. Increase in liquid mass flow rate leads to smaller SMDs except for the case of 15% GLR, where the trend is reversed. This could again be caused by the two-phase flow regime transition. Interestingly, this trend is almost completely opposite to the analogous one in the case with axial SMD. The GLR effect is in this case very similar to the liquid mass flow rate effect as increase in GLR leads to small SMDs. Only for the highest liquid mass flow rate increase in GLR results in larger SMDs. Once again, two-phase flow regime transition might be the cause for this phenomenon.

5.7.4 Conclusions

The present work investigates SMD evolution along the spray axis. Three different SMDs are investigated - ID_{32} (or cross-sectional SMD), axial SMD (local SMD values along the spray axis) and boundary SMD (local SMD values along the spray edge). It has been shown, that each of these evolutions behave quite differently and also have different dependencies on liquid mass flow rate and GLR. In general it can be said that the ID_{32} seems to be rather constant at any given operating conditions. On the spray axis the SMD generally decreases, while on the edge of the spray SMD increases. The effects of liquid mass flow rate and GLR seem to be dominated by the transition in the two-phase flow regime inside the atomizer body, although further experiments would be needed to fully investigate this proposition. However, in the majority of cases increase of GLR leads to smaller SMD which is in agreement with previous studies (Ghaffar et al., 2012; Ochowiak, 2013). A similar, although less strong, dependency has been found also for the liquid mass flow rate.

Acknowledgment

This work is an output of research and scientific activities of NETME Centre, regional R&D centre built with the financial support from the Operational Programme Research and Development for Innovations within the project NETME Centre (New Technologies for

Mechanical Engineering), Reg. No. CZ.1.05/2.1.00/01.0002 and, in the follow-up sustainability stage, supported through NETME CENTRE PLUS (LO1202) by financial means from the Ministry of Education, Youth and Sports under the „National Sustainability Programme I“. This work was also supported by the project CZ.1.07/2.3.00/30.0039 of Brno University of Technology.

References

Apte, S.V., Gorokhovski, M., Moin, P., 2003. LES of atomizing spray with stochastic modeling of secondary breakup. International Journal of Multiphase Flow 29, 1503‑1522. doi:10.1016/S0301-9322(03)00111-3

Babinsky, E., Sojka, P.E., 2002. Modeling drop size distributions. Progress in Energy and Combustion Science 28, 303‑329. doi:10.1016/S0360-1285(02)00004-7

Broukal, J., Hájek, J., 2014. Experimental analysis of spatial evolution of mean droplet diameters in effervescent sprays. Chemical Engineering Transactions, Accepted, awaiting press

Broukal, J., Hájek, J., 2011. Validation of an effervescent spray model with secondary atomization and its application to modeling of a large-scale furnace. Applied Thermal Engineering 31, 2153‑2164. doi:16/j.applthermaleng.2011.04.025

Broukal, J., Hájek, J., Sojka, P.E., Juřena, T., 2013. Drop Size Distribution in Effervescent Sprays: An Experimental study Using PDA Technique, in: Proceedings of 6th European Combustion Meeting. Presented at the 6th European Combustion Meeting, Lund, Sweden, pp. 1‑6.

Ghaffar, Z.A., Hamid, A.H.A., Rashid, M.S.F.M., 2012. Spray Characteristics of Swirl Effervescent Injector in Rocket Application: A Review. Applied Mechanics and Materials 225, 423‑428. doi:10.4028/www.scientific.net/AMM.225.423

Jedelský, J., Jícha, M., Sláma, J., Otáhal, J., 2009. Development of an Effervescent Atomizer for Industrial Burners. Energy & Fuels 23, 6121‑6130. doi: 10.1021/ef900670g

Lefebvre, A.H., Wang, X.F., Martin, C.A., 1988. Spray Characteristics of Aerated-Liquid Pressure Atomizers. Journal of Propulsion and Power 4, 293‑298.

Li, Z., Wu, Y., Cai, C., Zhang, H., Gong, Y., Takeno, K., Hashiguchi, K., Lu, J., 2012. Mixing and atomization characteristics in an internal-mixing twin-fluid atomizer. Fuel 97, 306‑314. doi:10.1016/j.fuel.2012.03.006

Ochowiak, M., 2013. The experimental study on the viscosity effect on the discharge coefficient for effervescent atomizers. Experimental Thermal and Fluid Science 50, 187‑192. doi:10.1016/j.expthermflusci.2013.06.008

Ochowiak, M., Broniarz-Press, L., Rozanski, J., 2010. The discharge coefficient of effervescent atomizers. Experimental Thermal and Fluid Science 34, 1316‑1323. doi:10.1016/j.expthermflusci.2010.06.003

Panchagnula, M.V., Sojka, P.E., 1999. Spatial droplet velocity and size profiles in effervescent atomizer-produced sprays. Fuel 78, 729‑741. doi:10.1016/S0016-2361(98)00192-6

Qian, L., Lin, J., Xiong, H., 2010. A Fitting Formula for Predicting Droplet Mean Diameter for Various Liquid in Effervescent Atomization Spray. Journal of Thermal Spray Technology 19, 586‑601. doi:10.1007/s11666-009-9457-4

Xiong, H.-B., Lin, J.-Z., Zhu, Z.-F., 2009. Three-dimensional simulation of effervescent atomization spray. Atomization and Sprays 19, 75‑90.

Xu, F., Dong, W., Qiang, L., 2012. Experimental Study of Droplet Size Distribution Produced by a Multi-Orifice Effervescent Atomizer. Applied Mechanics and Materials 166-169, 3056‑3059.

5.8 Miscellaneous Unpublished Results

This section will disclose results that have not yet been published. It is however believed, that they may represent a meaningful addition to the published results as well to other researchers interested in the area of effervescent sprays.

5.8.1 Mean and Representative Diameters of Effervescent Sprays

An extensive drop size measurement has been performed using a PDA apparatus with emphasis on axial and radial mean drop size evolution. Sections 5.5 and 5.6 contain results of these measurements but only in terms of SMD (or D_{32}). This particular diameter was chosen as it is traditionally used in evaporating or combustion applications. For the sake of completeness, detailed data about other mean and representative diameters are listed in Appendix I.

5.8.2 Drop Size Distribution Functions

Atomizers used in industrial applications almost never produce monodisperse sprays, i.e. a spray with droplets of the same size. In fact, they produce a whole spectrum of drop sizes. Researchers therefore use various analytical functions to describe the drop size distributions. For effervescent atomizers the most commonly used is the Rosin-Rammler distribution (Rosin and Rammler, 1933) or the Log-normal distribution. The former is usually used to model the volume-based drop size distribution, while the latter to model the number-based (the number-based distribution is based on the number of droplets, while the volume-based distribution is based on the volume of droplets). Other distributions are also occasionally used, for a comprehensive overview see (Babinsky and Sojka, 2002).

A study has been performed using experimental data mentioned in the previous paragraph (5.7.1) with a goal to compare the Rosin-Rammler and Log-normal distributions. Both distributions were fitted to experimental data and the root square mean error (rmse) was used to judge the fit quality. Two separate cases have been evaluated for each distribution. First, the experimental number-based distribution was fitted. This fit was then converted to the volume-based distribution and was again compared to the volume-based distribution obtained experimentally. The second case is analogous, only the fitting procedure is applied to the volume-based distribution and the fit is then converted to the number-based distribution.

Table 1. Overview of root mean square errors for Log-normal and Rosin-Rammler fits

Fit	Distribution to fit	rmse (Number-based)	rmse (Volume-based)	rmse (Total)
Log-normal	Number-based	0.0021	0.0061	0.0082
	Volume-based	0.0065	0.0023	0.0088
Rosin-Rammler	Number-based	0.0044	0.0118	0.0162
	Volume-based	0.0399	0.0034	0.0433

A typical result of the comparison can be seen in the following two figures. Figure 1 displays Log-normal and Rosin-Rammler distributions fitted to the experimental number-based distribution. Both fits are quite close to the experimental data, but when we convert the fits to get the volume-based distributions, the Log-normal fit is clearly superior. In Figure 2 we start by fitting the volume-based distribution and then again convert the fits to the number-based

distribution. Similarly to the previous case, the Log-normal distribution gives more accurate fits. Very similar results were obtained at different spray locations and under various operating conditions. It might be noticed that the experimental volume-based distribution is not as smooth as the number-based distribution. It was concluded that this is a common occurrence since the tails of the volume-based distributions are very sensitive to diameter variations.

To get a more general idea of how the fits compare, they were applied to 132 experimental drop size distributions (various operating conditions and locations in the spray, see 5.5 and 5.6 for more details about the measurements) and the average root mean square errors were computed. The resulting errors can be seen in Table 1. It is clear that the Log-normal distribution is superior when compared to the Rosin-Rammler distribution. Also, best results were obtained when the Log-normal distribution was fitted to the number-based experimental distribution.

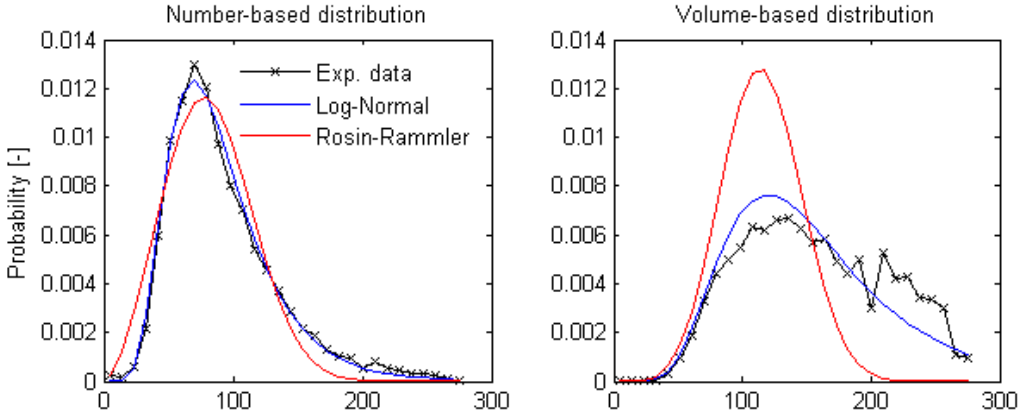

Figure 1. Drop size distribution and fits based on the number-based distribution, operating conditions: water mass flow rate 42 kg/h, 5% GLR, 5 cm from nozzle, on axis

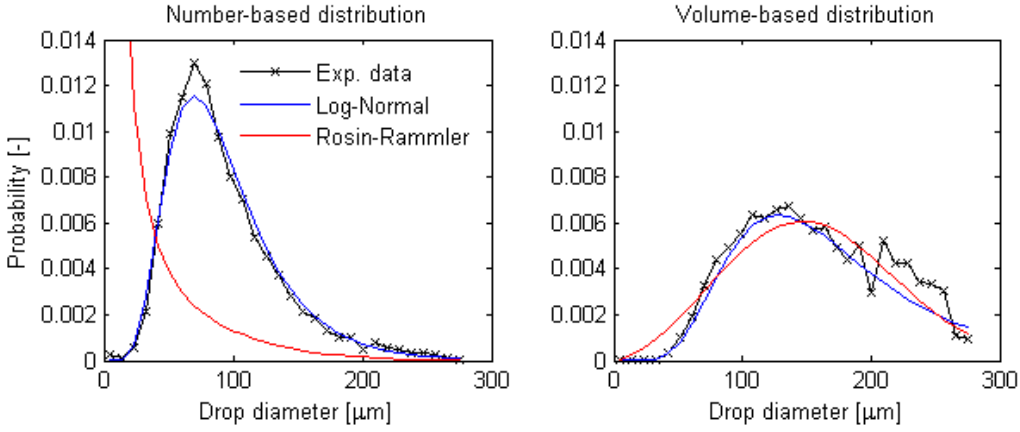

Figure 2. Drop size distribution and fits based on the volume-based distribution, operating conditions: water mass flow rate 42 kg/h, 5% GLR, 5 cm from nozzle, on axis

References

P Rosin, E.Rammler., 1933. Laws governing the fineness of powdered coal. J. Inst. Fuel 7, 29–36.

Babinsky, E., Sojka, P.E., 2002. Modeling drop size distributions. Progress in Energy and Combustion Science 28, 303–329. doi:10.1016/S0360-1285(02)00004-7

6 Summary and Conclusions

As stated in the first chapter, the long term goal to which this work tried to contribute, is the predictability of swirling spray combustion, with focus on the distribution of heat loading (wall heat fluxes) in the combustion chamber of a fired heater. In order to achieve this goal much ground needs to be covered and this work represents an effort in this direction. The thesis consists of a general theoretic introduction into the area of effervescent spray combustion and a collection of published articles disclosing the author's findings.

6.1 Results Summary

This section tries to summarize and mutually relate the results contained in individual papers from chapter 5.

The article in chapter 5.1 acts as a more rigorous introduction in the discussed area for the reader. As a matter of fact, at the time of its writing it was also an introduction to the doctoral research for the author. The main aim was to assess the suitability of simple (readily available) numerical spray models to represent effervescent atomization. Experimental data was used to set up the primary atomization model in terms of a Rosin-Rammler distribution of drop sizes. The question was whether the radial change in the drop size distribution found in the experimental data will emerge in the relatively simple numeric simulation. Only partial agreement was achieved. It was concluded, that more sophisticated models need to be used in order to represent adequately effervescent sprays.

A second attempt to model effervescent atomization is described in chapter 5.2. A spray model comprising a primary atomization model derived from first principles along with a secondary atomization model was applied to a large-scale swirling combustion simulation. First, the spray itself was analysed and compared to experimental data. Although the predicted mean drop sizes were in qualitative agreement, the spray model was not able to predict droplets smaller than 30 μm as well as the radial evolution of SMD observed in the experimental data. It was concluded, that these two deficiencies are responsible for the poor predictions of the wall heat fluxes. This further strengthened the opinion, that a single SMD is not a sufficient representation of an effervescent spray and spatial evolutions need to be accurately predicted in order to get acceptable wall heat fluxes predictions.

A small detour from effervescent atomization has been taken in chapter 5.3 where the goal was to try and confirm the conclusions from chapter 5.2, that the failure to predict the wall heat fluxes was indeed caused by the spray model. An analogous gas combustion simulation was performed with identical turbulence, chemistry and radiation models and good agreement with experimental measurements was found. The previous conclusion was therefore confirmed as well as the need of more complex effervescent spray models. Moreover, an extensive literature review on numerical approaches in swirling flow was performed (5.4).

In order to develop a new effervescent spray model validation data are needed. During an extensive literature review it was found that well documented experimental data are rarely available, especially in the case of drop size data of effervescent sprays. It was therefore essential to perform experimental measurements. Due to a fortunate turn of events a possibility arose to experiments and it was fully utilized. Chapter 5.5 presents an overview of experimental approaches and puts forward a measurement methodology that is believed to be appropriate for the present case, i.e. acquiring data suitable for validation of effervescent sprays.

The work presented in chapter 5.6 aims to investigate radial variations of experimental SMD at various axial distances and sensitivity to operating conditions. It was observed that closer to the spray nozzle the SMD decreases with radial distance, while further downstream the relationship is completely reversed. This phenomenon was preserved regardless of operating conditions. The effect of GLR and liquid mass flow rate is more unclear. In the spray core the relationship was difficult to determine, while in the outside spray region their increase led to smaller SMD. This investigation revealed complexities in the effervescent spray formation that have, to the author‘s knowledge, not yet been published.

The investigation of the experimental data continued in a follow up study (5.7) where both global and local axial evolutions of SMD were investigated. A technique for calculation of cross-sectional SMD was adopted (ID_{32}) and its axial evolution was compared to two axial evolutions of local SMDs – one consisting of local SMD computed on the spray axis and the other of local SMD computed on the spray edge. It has been shown that each of these three evolutions behave quite differently. Irregularities in the effect of GLR on individual SMD evolutions has been attributed to change in the two-phase flow regime inside the atomizer body. In general however, increase of GLR leads to smaller SMD and a similar, although less strong, dependency has been found also for the liquid mass flow rate.

The final chapter (5.8) contains unpublished research results. Mean and representative drop diameter data obtained from the experimental measurements are fully disclosed and a study on analytical drop size distribution is performed. It is concluded, that the Log-normal distribution surpasses the Rosin-Rammler distribution when fitting experimental data.

6.2 Conclusions and Future Work

The main conclusions of this thesis can be summarized as follows:

- Simple spray models contained in today’s commercial computational software products are not able to represent effervescent sprays in a sufficient manner.
- In order to predict wall heat fluxes in effervescent spray combustion simulations, the spray model needs to be able to predict radial drop size variations.
- Experimental validation data for new spray models must reflect the model’s purpose. Moreover, multiple radial and axial measurements provide valuable insight into the spray formation phenomena.
- A new phenomena was observed, where in the area close to the effervescent spray nozzle drop sizes decrease with radial distance, while further downstream the trend is completely opposite.
- The effect of GLR on drop sizes reported in numerous articles was confirmed.
- A new method in the investigation of axial drop size evolution was proposed based on a comparison of cross-sectional, axial and boundary SMDs evolutions.

During this research it has been recognized that a significantly more detailed effervescent spray model is needed instead of the commonly used ones. The results put forward in this thesis represent a solid foundation for development and validation of such models with emphasis on spray combustion applications. Implementation of the given guidelines and ideas into a numerical model is however a very challenging task that deserves a separate research of its own.

Nomenclature and Acronyms

Physical constants

g	standard gravity (9.80665 m-s^{-2})

Latin letters

C	Coefficient [-]
d	Diameter [m]
D	Drop diameter [m]
m	Mass [kg]
Oh	Ohnesorge number [-]
p	Pressure [Pa]
r	Drop radius [m]
Re	Reynolds number [-]
t	Time [s]
u	Velocity [m-s^{-1}]
We	Weber number [-]

Greek letters

μ	Viscosity [Pa-s]
ρ	Density [kg-m^{-3}]
σ	Surface tension [N-m]

Subscripts

A	Aerodynamic
D	Drag
g	Gaseous phase
I	Internal
l	Liquid phase
o	Orifice
p	Particle
r	Relative
σ	Surface tension

Acronyms

CFD	Computational Fluid Dynamics
DNS	Direct Numerical Simulation
LES	Large Eddy Simulation
RANS	Reynolds-Averaged Navier-Stokes
SMD	Sauter Mean Diameter

Appendix I - List of Author's Publications

[1] J. Broukal, J. Hájek, J. Vondál, An experimental study of effervescent sprays: axial evolution of mean drop diameter, in: Proceedings of 26th European Conference on Liquid Atomization and Spray Systems, (2014) To be published.

[2] J. Broukal, J. Hájek, Experimental analysis of spatial evolution of mean droplet diameters in effervescent sprays. Chemical Engineering Transactions, (2014) Accepted, awaiting press.

[3] T. Juřena, J. Broukal, Review on validation of CFD models of swirling flows by experimental data, in: Sborník 60. konference chemického a procesního inženýrství, Srní, Czech Republic, (2013) 1–8.

[4] J. Broukal, J. Hájek, P.E. Sojka, Experimental Investigations of Effervescent Atomization Using Non-intrusive Techniques. Chemical Engineering Transactions, 35 (2013), 1135-1140

[5] J. Broukal, J. Hájek, P.E. Sojka, T. Juřena, Drop Size Distribution in Effervescent Sprays: An Experimental study Using PDA Technique, in: Proceedings of 6th European Combustion Meeting, Lund, Sweden, (2013) 1–6.

[6] J. Broukal, J. Vondál, J. Hájek, Experimental and numerical investigation of wall heat fluxes in a gas fired furnace: practicable models for swirling non- premixed combustion. Chemical Engineering Transactions, 29 (2012) 1399-1404.

[7] J. Broukal, J. Hájek, Validation of an effervescent spray model with secondary atomization and its application to modeling of a large-scale furnace, Applied Thermal Engineering, 31 (2011) 2153–2164.

[8] J. Broukal, J. Hájek, Development of an effervescent spray model for combustion simulations and its application to modelling of a large-scale furnace, in: Proceedings of 9th European Conference on Industrial Furnaces and Boilers, Estoril, Portugal, (2011) 1–10.

[9] J. Broukal, J. Hájek, Effervescent Spray Modelling: Investigation of Drop Momentum Models and Validation by Measured Data, Chemical Engineering Transactions, 25 (2011) 797–802.

[10] J. Broukal, J. Hájek, J. Jedelský, Effervescent atomization of extra-light fuel-oil: Experiment and statistical evaluation of spray characteristics, in: Proceedings of 23rd European Conference on Liquid Atomization and Spray Systems, Brno, Czech Republic, (2010) 1–10.

[11] J. Broukal, J. Hájek, Wall heat fluxes in swirling combustion of extra-light fuel-oil in large-scale test combustor: Experiment and modelling using Eddy Dissipation Model, Chemical Engineering Transactions, 21 (2010) 1111–1116.

Appendix II – Experimental Drop Diameters

This appendix contains experimental data from measurement of effervescent sprays in terms of mean diameters $D_{a\,b}$ and representative diameters D_X [µm].

$$D_{a\,b} = \left[\frac{\sum N_i D_i^a}{\sum N_i D_i^b}\right]^{1/(a-b)}$$

D_X is a drop diameter, such that X×100 % of total liquid volume is in drops of smaller diameter. D_{peak} is then drop diameter containing most volume. MRF stands for water mass flow rate, GLR is gas-liquid-ratio of atomizing air and r is the radial distance of the measurement point in cm.

MFR = 31,2 kg/h 5% GLR
axial distance = 5 cm

r	D_{10}	D_{20}	D_{30}	D_{21}	D_{31}	D_{32}	D_{43}	$D_{0.1}$	$D_{0.5}$	$D_{0.632}$	$D_{0.9}$	$D_{0,99}$	D_{peak}
0	79,49	88,29	98,22	98,06	109,2	121,5	147,1	67,39	136,4	161,8	227,6	265,3	88,62
0,5	81,28	90,36	100,3	100,5	111,5	123,7	147,8	69,69	140	163,8	223,2	259	95,98
1	82,88	93,13	104,4	104,7	117,1	131,1	157,6	72,5	152	175,5	236,6	267,4	164,5
1,5	79,53	88,71	99,08	98,94	110,6	123,6	149,5	67,69	141,7	166,9	227,2	264,7	147,9
2	76,26	84,13	93,26	92,81	103,1	114,6	138,7	62,2	129,1	152,5	216,8	259,4	125,3
2,5	73,11	79,83	87,92	87,16	96,42	106,7	130,2	58,1	117,1	139,5	207,7	260,5	70,48

MFR = 31,2 kg/h 5% GLR
axial distance = 10 cm

r	D_{10}	D_{20}	D_{30}	D_{21}	D_{31}	D_{32}	D_{43}	$D_{0.1}$	$D_{0.5}$	$D_{0.632}$	$D_{0.9}$	$D_{0,99}$	D_{peak}
0	74,52	82,02	91,25	90,27	101	112,9	140,3	60,14	127,8	156,2	225,4	267,1	71,22
1	81,64	89,65	99,29	98,45	109,5	121,8	148,8	66	137,4	168,8	231,6	264,1	89,71
2	91,26	99,89	109,7	109,3	120,3	132,5	157,2	73,57	150,8	177,4	234,3	262,6	135,6
3	94,75	102,2	110,8	110,3	119,8	130,1	152	74,58	144,2	168,5	226,4	263,6	81,49
4	97,55	104,3	112,3	111,6	120,5	130,2	151,6	76,35	140,9	168,6	228,9	265,8	97,84

MFR = 31,2 kg/h 5% GLR
axial distance = 15 cm

r	D_{10}	D_{20}	D_{30}	D_{21}	D_{31}	D_{32}	D_{43}	$D_{0.1}$	$D_{0.5}$	$D_{0.632}$	$D_{0.9}$	$D_{0,99}$	D_{peak}
0	62,38	67,79	75,1	73,68	82,41	92,16	119,7	49,85	94,9	124,7	215,1	260,9	61,38
1	65,8	71,64	79,26	78,01	86,99	97,01	123,9	53,14	101,7	128,8	218,7	260,8	71,58
2	77,93	85,13	93,84	92,99	103	114	139,7	63,34	124,8	153,5	226,2	262,5	81,25
3	86,19	93,99	103,1	102,5	112,8	124,1	149,2	71,02	137,9	164,1	234,2	263,5	89,16
4	96,42	104,2	113	112,5	122,3	132,9	155,7	78,34	144,8	172,1	237,2	268,3	94,91
5	110,4	117	124,3	124	131,9	140,3	158,2	88,18	147,3	173,3	231	259,1	97,9

MFR = 31,2 kg/h 10% GLR
axial distance = 5 cm

r	D_{10}	D_{20}	D_{30}	D_{21}	D_{31}	D_{32}	D_{43}	$D_{0.1}$	$D_{0.5}$	$D_{0.632}$	$D_{0.9}$	$D_{0,99}$	D_{peak}
0	128,9	137,2	145,3	146,2	154,3	162,8	178,4	108,1	172,1	193,4	243,8	270,7	164,8
0,5	131,2	139,7	147,8	148,7	156,9	165,5	180,9	109,7	176,8	197,8	241,1	269,5	224,1
1	118	125,9	134	134,3	142,7	151,7	168,8	96,33	162,2	183,6	234,5	266,4	163,2
1,5	105,8	113,8	122,2	122,3	131,3	140,9	159,8	86,13	152	173,2	230,6	262,6	154,7
2	92,94	99,76	107,3	107,1	115,3	124,2	143,1	74,38	132,7	153,4	212,7	264,3	99,4
2,5	70,73	76,54	83,35	82,81	90,47	98,84	118,3	55,75	105,8	123,1	184,7	242,2	117,1

MFR = 31,2 kg/h 10% GLR
axial distance = 10 cm

r	D_{10}	D_{20}	D_{30}	D_{21}	D_{31}	D_{32}	D_{43}	$D_{0.1}$	$D_{0.5}$	$D_{0.632}$	$D_{0.9}$	$D_{0,99}$	D_{peak}
0	100,3	111,3	121,9	123,4	134,3	146,3	166,9	90,74	161,3	183,3	236,3	267,4	144,5
1	86,01	93,84	102,9	102,4	112,5	123,6	147,6	69,8	136,6	162	227,7	263,9	109,6
2	89,94	97,58	106,2	105,9	115,4	125,8	147,8	72,41	137,5	160,3	226,4	263,2	145,2
3	91,89	98,45	105,9	105,5	113,7	122,6	142	72,62	130,4	153,1	215,7	251,9	108,6
4	87,89	93,51	100	99,5	106,7	114,4	131,8	68,91	120,7	139,9	202,1	242,4	82,33

MFR = 31,2 kg/h 10% GLR
axial distance = 15 cm

r	D_{10}	D_{20}	D_{30}	D_{21}	D_{31}	D_{32}	D_{43}	$D_{0.1}$	$D_{0.5}$	$D_{0.632}$	$D_{0.9}$	$D_{0,99}$	D_{peak}
0	83,58	90,69	99,27	98,4	108,2	118,9	144	67,69	127,9	158,8	229,8	264,5	83,89
1	78,17	83,54	89,97	89,27	96,52	104,4	123,7	62,03	106,5	126,7	197,8	253,8	81,86
2	81,09	87,41	94,75	94,23	102,4	111,3	131,9	65,41	116,8	138,9	209	255,2	89,66
3	92,18	99,63	107,8	107,7	116,6	126,3	146,7	75,22	135,3	158,2	221,9	261,6	108,1
4	106,6	114,2	122,1	122,3	130,6	139,5	157,3	86,42	148,6	171,2	224,6	257,9	127,1
5	105,9	112,4	119	119,2	126,2	133,6	148,6	85,05	139,4	159,5	210,1	249,9	113,4

MFR = 31,2 kg/h 15% GLR
axial distance = 5 cm

r	D_{10}	D_{20}	D_{30}	D_{21}	D_{31}	D_{32}	D_{43}	$D_{0.1}$	$D_{0.5}$	$D_{0.632}$	$D_{0.9}$	$D_{0,99}$	D_{peak}
0	96,2	105,1	114,6	114,8	125	136,1	158,6	81,31	147	173,8	236,9	271,3	127,7
0,5	92,76	101	109,9	110,1	119,7	130,1	151,7	78,25	137,7	162,4	231,8	264,6	141,4
1	76,94	82,83	89,87	89,18	97,14	105,8	127,3	61,7	108,6	128,8	210,8	267,9	82,19
1,5	77,39	84,17	92,09	91,55	100,5	110,2	133	62,78	117,4	138,5	220	266,7	98,42
2	74,54	80,99	88,49	88,01	96,43	105,6	126,7	59,84	113	132,6	204,8	251,7	101
2,5	69,28	74,4	80,32	79,9	86,49	93,63	110,5	54,2	97,5	113,5	174,2	233,4	90,32

MFR = 31,2 kg/h 15% GLR
axial distance = 10 cm

r	D_{10}	D_{20}	D_{30}	D_{21}	D_{31}	D_{32}	D_{43}	$D_{0.1}$	$D_{0.5}$	$D_{0.632}$	$D_{0.9}$	$D_{0,99}$	D_{peak}
0	86,99	94,46	102,5	102,6	111,3	120,8	140,7	72,87	127,5	150,1	217,3	256,3	128,2
1	75,66	79,63	84,41	83,82	89,16	94,83	109,8	59,64	92,11	107,8	176,4	245,5	86,68
2	81,58	86,5	92,27	91,73	98,13	105	121,8	64,34	105,6	123,2	191,6	254	86,75
3	88,59	94,59	101,2	101	108,2	115,9	132,5	69,96	121,8	139,3	196,7	247,6	109,3
4	87,83	93,3	99,4	99,11	105,7	112,8	128,9	69,02	116,9	133,9	192,6	250,4	101,1

MFR = 31,2 kg/h 15% GLR
axial distance = 15 cm

r	D_{10}	D_{20}	D_{30}	D_{21}	D_{31}	D_{32}	D_{43}	$D_{0.1}$	$D_{0.5}$	$D_{0.632}$	$D_{0.9}$	$D_{0,99}$	D_{peak}
0	69,99	74,47	79,94	79,23	85,43	92,12	110	55,62	91,37	108,2	180,3	244,2	75,03
1	71,73	75,6	80,18	79,68	84,76	90,18	104,3	56,92	88,28	101,9	162,8	233,4	74,82
2	76,45	80,05	84,1	83,84	88,21	92,82	104,1	60,53	90,73	102,3	149,8	236,9	87,43
3	86,06	90,96	96,44	96,14	102,1	108,4	123,3	68,92	108,3	124,2	188,4	246,8	89,16
4	97,72	104,1	110,8	110,8	118	125,6	141,6	79,89	130,4	150,1	204,4	254	98,84
5	105,6	111,4	117,5	117,4	123,9	130,8	145,6	84,45	132,9	152,6	211,8	250,8	121

MFR = 42 kg/h 5% GLR

axial distance = 5 cm

r	D_{10}	D_{20}	D_{30}	D_{21}	D_{31}	D_{32}	D_{43}	$D_{0.1}$	$D_{0.5}$	$D_{0.632}$	$D_{0.9}$	$D_{0,99}$	D_{peak}
0	92,71	102	111,7	112,2	122,5	133,9	155,9	79,4	145,7	169,6	231,6	264,7	135,6
0,5	91,43	100,7	110,6	110,9	121,6	133,4	156,2	77,71	148,8	173,1	230,4	266	174,5
1	88,27	97,57	107,6	107,8	118,8	130,8	154,3	75,44	146,1	169,8	232,6	266,5	129,2
1,5	85,14	93,7	103,2	103,1	113,5	125	148,2	71,24	138,9	162,5	224,8	259,8	118
2	81,44	88,53	96,53	96,23	105,1	114,8	135,4	65,8	124,3	146,5	205	257,2	114,5
2,5	74,46	80,91	88,45	87,93	96,4	105,7	126,7	59,29	113,9	135,1	199,9	260,7	89,3

MFR = 42 kg/h 5% GLR

axial distance = 10 cm

r	D_{10}	D_{20}	D_{30}	D_{21}	D_{31}	D_{32}	D_{43}	$D_{0.1}$	$D_{0.5}$	$D_{0.632}$	$D_{0.9}$	$D_{0,99}$	D_{peak}
0	69,3	76,7	85,79	84,89	95,45	107,3	135	57,62	120,8	149,6	223,1	256,6	67
1	73,35	80,69	89,63	88,76	99,08	110,6	137,3	59,7	123,2	148,9	226,6	260,7	70,76
2	83,39	91,04	99,93	99,39	109,4	120,4	144	66,61	135	159	219,2	262,3	71,64
3	91,67	98,58	106,5	106	114,7	124,1	144,6	72,25	134,2	156,4	222,2	261,1	96,66
4	92,1	97,85	104,4	104	111,1	118,8	136,4	72,28	124,5	143,2	206,8	257,8	87,51

MFR = 42 kg/h 5% GLR

axial distance = 15 cm

r	D_{10}	D_{20}	D_{30}	D_{21}	D_{31}	D_{32}	D_{43}	$D_{0.1}$	$D_{0.5}$	$D_{0.632}$	$D_{0.9}$	$D_{0,99}$	D_{peak}
0	61,53	66,61	73,23	72,11	79,89	88,5	112,3	49,25	90,61	114,8	199,7	246,2	64,57
1	68,97	73,57	79,24	78,49	84,94	91,92	110,5	54,33	90,95	108,8	182,2	255,4	77,36
2	78,31	83,96	90,69	90,01	97,6	105,8	126,1	62,51	108,2	130,3	202,2	262,7	82,45
3	93,35	100,8	108,9	108,8	117,7	127,3	147,7	75,85	136,6	161,7	222,1	260,6	91,48
4	107,5	114,4	121,8	121,9	129,7	138,1	155,3	86,23	145,5	167,9	224	260,5	107,3
5	112,8	119,4	126,4	126,3	133,8	141,7	158,2	89,83	149,1	171,5	227,2	265	125,6

MFR = 42 kg/h 10% GLR

axial distance = 5 cm

r	D_{10}	D_{20}	D_{30}	D_{21}	D_{31}	D_{32}	D_{43}	$D_{0.1}$	$D_{0.5}$	$D_{0.632}$	$D_{0.9}$	$D_{0,99}$	D_{peak}
0	108,8	116,4	124,1	124,6	132,5	141	157,5	90,79	147,5	167	227	259,1	130
0,5	111,5	119,4	127,3	127,8	136	144,7	161,6	92,45	152,6	173,1	227,4	267,2	148
1	85,02	92	99,63	99,55	107,8	116,8	136,2	70,23	124,3	142,7	210,1	257	98,25
1,5	74,84	81,1	88,32	87,87	95,95	104,8	125,2	60	110,8	129,9	199	260,9	97,57
2	73,73	80,14	87,72	87,11	95,67	105,1	127	58,87	112,7	134	204	258,3	90,82
2,5	70,75	76,13	82,44	81,92	88,99	96,68	115,1	55,65	100,7	118,2	180,1	254,9	93,57

MFR = 42 kg/h 10% GLR

axial distance = 10 cm

r	D_{10}	D_{20}	D_{30}	D_{21}	D_{31}	D_{32}	D_{43}	$D_{0.1}$	$D_{0.5}$	$D_{0.632}$	$D_{0.9}$	$D_{0,99}$	D_{peak}
0	103,4	111	119	119,2	127,6	136,6	154,4	86,81	145,4	170,2	225,4	251,5	116,4
1	85,74	91,63	98,46	97,93	105,5	113,7	133,2	68,49	115,7	136,7	213	269	99,52
2	87,82	92,99	98,97	98,47	105,1	112,1	128,8	69,02	113,9	131,9	199,3	258,5	98,82
3	94,77	103,2	112,2	112,5	122,1	132,5	153,2	79,71	143,1	165,8	227,3	263,5	116,6
4	85,14	90,48	96,49	96,15	102,7	109,7	125,5	67,06	114	131,2	186,2	237,5	95,2

MFR = 42 kg/h 10% GLR

axial distance = 15 cm

r	D_{10}	D_{20}	D_{30}	D_{21}	D_{31}	D_{32}	D_{43}	$D_{0.1}$	$D_{0.5}$	$D_{0.632}$	$D_{0.9}$	$D_{0,99}$	D_{peak}
0	75,22	80,26	86,21	85,63	92,29	99,47	117,6	59,7	100,8	118,3	183,5	264,3	87,63
1	76,55	80,29	84,65	84,21	89,01	94,09	107,1	60,6	91,73	104,7	163,3	238,9	79,11
2	80,13	82,79	85,81	85,54	88,8	92,19	100,8	63,91	88,67	97,85	139,6	221,8	82,06
3	88,74	92,29	96,38	95,99	100,4	105,1	116,7	70,66	101,8	114,9	171,8	240,6	85,71
4	99,1	103,7	108,9	108,5	114,2	120,1	134,4	78,34	120,2	137,6	199,1	257,5	97,91
5	101,7	107,1	112,8	112,8	118,8	125,2	139,6	81,32	126	144,2	207,2	254,5	114,1

MFR = 42 kg/h 15% GLR

axial distance = 5 cm

r	D_{10}	D_{20}	D_{30}	D_{21}	D_{31}	D_{32}	D_{43}	$D_{0.1}$	$D_{0.5}$	$D_{0.632}$	$D_{0.9}$	$D_{0,99}$	D_{peak}
0	-	-	-	-	-	-	-	-	-	-	-	-	-
0,5	109,2	116,8	124,7	125	133,2	142	159,3	90,15	150,2	169,6	226,8	268,2	136,1
1	81,68	88,75	96,81	96,44	105,4	115,2	137,2	67,42	121,7	144,2	216,6	267,3	113,9
1,5	63,96	67,95	72,89	72,18	77,82	83,89	100,8	49,97	83,15	97,38	167,8	244,2	66,53
2	63,58	67,84	73,02	72,38	78,26	84,62	101,4	49,29	85,12	100,7	162	248,4	68,28
2,5	67,31	72,18	78,06	77,39	84,06	91,31	109,6	52,34	94,93	111,8	173,5	249,5	65,4

MFR = 42 kg/h 15% GLR

axial distance = 10 cm

r	D_{10}	D_{20}	D_{30}	D_{21}	D_{31}	D_{32}	D_{43}	$D_{0.1}$	$D_{0.5}$	$D_{0.632}$	$D_{0.9}$	$D_{0,99}$	D_{peak}
0	71,6	79,71	88,01	88,75	97,58	107,3	124,3	63,34	126,6	138,1	183	188,6	155,5
1	75,93	80,01	84,89	84,3	89,76	95,57	110,9	60,04	94,75	109,6	176,7	255,1	75,96
2	71,74	74,87	78,58	78,14	82,24	86,56	97,68	55,96	84,05	95,8	146,5	225	68,13
3	79,67	83,35	87,64	87,2	91,92	96,9	109,2	61,56	95,94	110,4	162	230,4	75,96
4	79,09	83,8	89,57	88,8	95,32	102,3	120,3	61,31	103,9	123,9	191,3	257,3	69,3

MFR = 42 kg/h 15% GLR

axial distance = 15 cm

r	D_{10}	D_{20}	D_{30}	D_{21}	D_{31}	D_{32}	D_{43}	$D_{0.1}$	$D_{0.5}$	$D_{0.632}$	$D_{0.9}$	$D_{0,99}$	D_{peak}
0	77,44	83,23	89,9	89,44	96,86	104,9	123,5	62,52	109,2	130,1	193,5	250,8	102
1	72,09	74,76	77,81	77,54	80,84	84,29	93,26	57,24	81,01	90	129,6	224	72,71
2	72,62	75,04	77,77	77,54	80,47	83,51	91,21	58	80,31	88,3	124,8	210,6	76,08
3	75,8	78,56	81,62	81,42	84,69	88,1	96,52	61,62	84,5	94	137	209,2	78,88
4	85,07	88,73	92,94	92,55	97,14	102	114,3	68,49	98,13	112,3	169,9	253,3	86,37
5	92,18	96,69	101,9	101,4	107,1	113	128	73,59	110,6	127,8	199,3	248,9	86,49

MFR = 60 kg/h 5% GLR

axial distance = 5 cm

r	D_{10}	D_{20}	D_{30}	D_{21}	D_{31}	D_{32}	D_{43}	$D_{0.1}$	$D_{0.5}$	$D_{0.632}$	$D_{0.9}$	$D_{0,99}$	D_{peak}
0	108	116,5	125,2	125,6	134,8	144,6	163,6	90,44	154,6	176	236,1	268,7	154,8
0,5	109,4	117,2	125,1	125,5	133,8	142,7	160,4	90,84	149,4	171,7	235,5	263	125,4
1	94,57	102,5	110,9	111,1	120,2	130	150,2	78,66	137,2	160,4	226,2	265,9	128,2
1,5	82,51	90,04	98,69	98,27	107,9	118,5	141,7	67,56	128,8	151,7	224,1	260,8	106
2	81,7	88,74	96,76	96,39	105,3	115	136,4	65,89	123,8	145,2	213,4	261,4	125,9
2,5	77,72	83,59	90,35	89,91	97,41	105,5	124	61,53	111,9	130,4	191,6	237,3	117,7

MFR = 60 kg/h 5% GLR
axial distance = 10 cm

r	D_{10}	D_{20}	D_{30}	D_{21}	D_{31}	D_{32}	D_{43}	$D_{0.1}$	$D_{0.5}$	$D_{0.632}$	$D_{0.9}$	$D_{0,99}$	D_{peak}
0	82,27	90,64	99,79	99,87	109,9	121	143,8	70,42	132,1	154,9	222,3	262,6	99,04
1	84,08	91,77	100,2	100,2	109,4	119,5	141	70,29	127,7	149,7	221,7	260,2	116,3
2	79,89	86,26	93,79	93,14	101,6	110,9	132,7	63,89	116,5	138,9	213,7	262	89,13
3	84,97	91,38	98,86	98,28	106,6	115,7	136,4	66,92	123,4	143,8	213,7	260,5	89,03
4	85,93	92,06	99,21	98,62	106,6	115,2	135,1	67,1	121,7	143,7	209,8	255,4	97,89

MFR = 60 kg/h 5% GLR
axial distance = 15 cm

r	D_{10}	D_{20}	D_{30}	D_{21}	D_{31}	D_{32}	D_{43}	$D_{0.1}$	$D_{0.5}$	$D_{0.632}$	$D_{0.9}$	$D_{0,99}$	D_{peak}
0	70,4	76,11	83,11	82,29	90,29	99,07	120,8	56,12	104,4	128,2	195,8	253,4	79,38
1	72,12	77,53	84,26	83,34	91,07	99,53	121,7	57,05	100,6	123,7	202,7	265,5	80,89
2	71,62	75,58	80,44	79,76	85,24	91,1	107,3	56,47	88,27	103,4	176	251,3	75,34
3	77,8	82,71	88,57	87,93	94,5	101,6	119,3	61,41	102,7	120,5	190,2	254,1	77,11
4	88,11	94,03	100,9	100,3	108	116,3	135,6	69,8	121	143,4	211,3	255,3	78,25
5	94,57	100,3	106,8	106,3	113,5	121,1	139	74,31	124,8	145	212,9	267,9	88,55

MFR = 60 kg/h 10% GLR
axial distance = 5 cm

r	D_{10}	D_{20}	D_{30}	D_{21}	D_{31}	D_{32}	D_{43}	$D_{0.1}$	$D_{0.5}$	$D_{0.632}$	$D_{0.9}$	$D_{0,99}$	D_{peak}
0	-	-	-	-	-	-	-	-	-	-	-	-	-
0,5	-	-	-	-	-	-	-	-	-	-	-	-	-
1	103,6	111,6	119,8	120,2	128,8	138	156,1	87,34	146,8	167,6	227	262,1	124,4
1,5	76,98	82,29	88,49	87,97	94,87	102,3	120,4	62,16	103,3	121,4	192,7	249,4	86,87
2	72,72	77,69	83,51	83,01	89,49	96,48	113,5	57,27	98,75	115,6	177,6	248,1	82,05
2,5	71,88	76,69	82,26	81,83	88	94,64	110,2	55,72	97,67	113,3	167,8	239,5	85,25

MFR = 60 kg/h 10% GLR
axial distance = 10 cm

r	D_{10}	D_{20}	D_{30}	D_{21}	D_{31}	D_{32}	D_{43}	$D_{0.1}$	$D_{0.5}$	$D_{0.632}$	$D_{0.9}$	$D_{0,99}$	D_{peak}
0	95,26	103,1	111,2	111,5	120,2	129,6	148,6	80,15	139,3	158,5	221,2	258,9	105,1
1	105,7	113	120,5	120,8	128,7	137	153,5	87,67	143,3	157,8	220,6	257,1	214,1
2	92,32	98,78	106,2	105,7	113,8	122,6	142,5	74,24	126,3	148,1	223	266,9	105,1
3	83,4	86,88	90,83	90,52	94,79	99,27	110,3	65,4	97,15	109,2	154,2	239,9	91,59
4	78,22	81,73	85,92	85,41	90,05	94,94	107,5	60,46	93,69	106,8	162,7	242,9	74,97

MFR = 60 kg/h 10% GLR
axial distance = 15 cm

r	D_{10}	D_{20}	D_{30}	D_{21}	D_{31}	D_{32}	D_{43}	$D_{0.1}$	$D_{0.5}$	$D_{0.632}$	$D_{0.9}$	$D_{0,99}$	D_{peak}
0	-	-	-	-	-	-	-	-	-	-	-	-	-
1	76,03	80,32	85,36	84,85	90,45	96,43	111,4	59,92	95,06	111,3	172,8	239	82,01
2	75,71	78,8	82,43	82,02	86,01	90,19	101,2	60,33	87,07	97,59	150,5	218,6	76,69
3	76,25	79,41	83,14	82,69	86,82	91,15	103	60,22	87,33	98,06	151,7	250,9	70,79
4	82,87	86,58	90,94	90,45	95,26	100,3	113,4	65,14	97,91	112,2	168,6	242,7	79,64
5	88,34	92,48	97,32	96,81	102,1	107,8	122,2	69,44	105,7	122,7	184,3	270,3	80,07

Appendix III – Experimental Drop Data

All data obtained from the PDA spray measurements are available on the enclosed CD.